INVESTIGATION OF HALON 1301 INTERACTIONS IN METHANE COMBUSTION

Thesis

Submitted to

The School of Engineering of the

UNIVERSITY OF DAYTON

In Partial Fulfillment of the Requirements for

The Degree

Master of Science in Chemical Engineering

by

Matthew G. Getz

UNIVERSITY OF DAYTON

Dayton, Ohio

August 1997

INVESTIGATION OF HALON 1301 INTERACTIONS IN METHANE COMBUSTION

Approved by:

Jamie S. Ervin, Ph.D.
Associate Professor
Mechanical and Aerospace Engineering
Thesis Advisor

Steven S. Zabarnick, Ph.D.
Research Chemist
University of Dayton Research Institute
Research Advisor

Kevin J. Myers, D. Sc.
Professor
Chemical & Materials Engineering
Academic Advisor

Tony E. Saliba, Ph.D.
Professor, Chairman
Chemical & Materials Engineering
Committee Member

Donald L. Moon, Ph.D.
Associate Dean
Graduate Engineering & Research
School of Engineering

Joseph F. Lestingi, D. Eng.
Dean
School of Engineering

ABSTRACT

INVESTIGATION OF HALON 1301 INTERACTIONS IN METHANE COMBUSTION

Name: Matthew G. Getz
University of Dayton, 1997

Thesis Advisor: Dr. Jamie Ervin
Research Advisor: Dr. Steven Zabarnick
Academic Advisor: Dr. Kevin J. Myers

An understanding of the interactions of halon 1301 in methane combustion will aid in the search for a replacement fire inhibitor. First, improvements are made to the experimental sampling system of the well stirred reactor (WSR). A new modeling scheme using Chemkin (Kee et al., 1989a) simulates the sampling probe as a series of isothermal perfectly stirred reactor (PSR) elements and predicts the consumption of CO and THC (total hydrocarbons) occurring within a probe design. An optimal probe is designed to recover more than 90% of the CO and to prevent complete consumption of THC. More importantly, the measurements taken with any probe are now predicted accurately with this new modeling scheme. This allows for the correlation of WSR measurements to the modeling predictions of the PSR code (Glarborg et al., 1988). Therefore, modeling of halon 1301 (CF_3Br) interactions is performed with the Battin-Leclerc et al. (1994) mechanism. Methane combustion is modeled at equivalence ratios of 0.7 and 1.2 with the Miller and Bowman mechanism (1989), and a 2 molar percent addition of halon 1301 is used for inhibition studies. Halon 1301 is found to both initiate and prolong the consumption of methane. The initiation is caused by the dissociation of halon 1301 into the CF_3 and Br radicals, which abstract a hydrogen atom from methane to form CHF_3 and HBr. Prolongation of methane consumption occurs as a result of the delay in the accumulation of the radical pool (O, H, and OH radicals). This delay is caused by the consumption of the H radical by HBr to produce H_2.

ACKNOWLEDGMENTS

I would like to thank the many people that helped guide me in my pursuit of this degree. I thank Kevin Myers for helping me with the decision to pursue a Masters degree and for continued advice on my class selection. I thank Jamie Ervin for hiring me and giving me the opportunity to work for the University of Dayton Research Institute. Jamie provided me with guidance throughout the past year. I thank Steve Zabarnick for giving me guidance in my thesis work when I needed it the most. His suggestions and comments always led to a greater understanding of the material and project.

There are fellow workers who deserve many thanks. The first is Jim Blust, a Ph.D. student who was a constant help in all aspects of the WSR experiments. Thanks also to Jim for allowing me to work with him on the probe design problem. I would like to thank Rich Striebich for his help in the halon 1301 pulse experiments last summer, and his continued insights into the project. I thank Joe Calo at Brown University for his inputs on the project via E-mail. And lastly, but not least, Tom Miller and John Ballenthin from Phillips Lab at Hanscom AFB for providing the mass spectrometer for the experiments of last summer.

I would also like to recognize the U. S. Air Force for the financial support of this project. This thesis was conducted under contract number F33615-92-C-2207 in the Aero Propulsion & Power Directorate, Combustion Division at Wright Labs at the Wright Patterson Air Force Base. I thank Chuck Frayne, our technical monitor, for making it possible for me to have access to the building when necessary.

TABLE OF CONTENTS

LIST OF FIGURES

LIST OF TABLES

NOMENCLATURE

SYMBOLS

a_1 through a_7	coefficients for the NASA polynomials
A	cross sectional area (m^2)
A_i	pre-exponential Arrhenius factor (mol, s, m)
AE PSR	Allied-Signal Engines PSR code
AIAA	American Institute of Aeronautics and Astronautics, Inc.
C_p	heat capacity (cal/g K)
C^o_{pk}	standard heat capacity (cal/mol K)
CFC	chlorofluorocarbon
CSTR	continuous stirred tank reactor
D	diameter (m)
E	activation energy (J/mol)
F	fuel (moles)
h	enthalpy (cal/g)
H°	standard enthalpy (cal/mol)
I	total number of reactions
ID	inside diameter (m)
JEMS	jet exhaust mass spectrometer
k	reaction rate constant (mol, s, m)
K	total number of species
K_c	equilibrium constant calculated with concentrations
K_p	equilibrium constant calculated with partial pressures
$\dot{m}$	mass flow rate (g/sec)
O	oxidant (moles)
OD	outside diameter (m)

P	pressure (atm)
PFR	plug-flow reactor
PSR	perfectly stirred reactor
q	rate-of-progress variable (mol/m^3 s)
Q	volumetric flow rate (m^3/s)
Q_{loss}	heat loss rate (cal/s)
R	universal gas constant (8.314 J/mol K)
Re	Reynolds number
ROP	rate-of-production
S°	standard entropy (cal/mol K)
SS	stainless steel
T	temperature (K)
THC	total hydrocarbons
u	velocity (m/s)
V	volume of the reactor (m^3)
W	molecular weight (g/mol)
WSR	well stirred reactor
x	distance (m)
[X]	concentration of species X (mol/m^3)
Y	mass fraction
ϕ	equivalence ratio
μ	viscosity (g/m s)
ν	stoichiometric coefficient
ρ	density (g/m^3)
τ	residence time (s)
$\dot{\omega}$	molar production rate (mol/m^3/s)

SUBSCRIPTS

atm	atmospheric
avg	average
f	forward
i	one of the I reactions
k	one of the K species
meas	measured
n	defines end of PSR element
n-1	defines beginning of PSR element
r	reverse
stoich	stoichiometric

SUPERSCRIPTS

*	incoming property
′	reactant property
″	product property
β	modified Arrhenius exponent for temperature

CHAPTER I

INTRODUCTION

Halogenated hydrocarbons are collectively called halons, and are classified as halon abcde according to the formula $C_aF_bCl_cBr_dI_e$ (Gann, 1975a). They have been used for fire suppression purposes since the late 1800's when CCl_4 (halon 104) was used world-wide (Ford, 1975). In the 1920's, methyl bromide (halon 1001) was found to be more effective, but was never used extensively in the U. S. because of its toxicity (Pitts, 1990). During World War II, Germany discovered that a less toxic chlorobromomethane (halon 1011) was as effective as halon 1001 in suppressing flames. The U. S. Air Force adopted halon 1011 as an aircraft fire inhibitor after the war ended, but recognized that significant toxicological problems remained. Thus, the Air Force and the U. S. Army Corps of Engineers began an extensive search for new fire-fighting agents (Ford, 1975). Trifluorobromomethane (halon 1301) and bromochlorodifluoromethane (halon 1211) were found to be the most effective inhibitors, and have been utilized extensively (Pitts, 1990). However, by the late 1980's there was sufficient evidence to conclude that ozone depletion was occurring as a result of reactions involving Cl and Br atoms introduced into the stratosphere by man-made chlorofluorocarbons (CFCs) and fire suppressing halons (Pitts, 1990). It was also discovered that halons accounted for up to 19% of the depletion despite the fact that CFC production was nearly 50 times greater than that of halons 1301 and 1211 (Battin-Leclerc, 1994).

In 1987, the U. S., Canada, members of the European Economic Community, and 23 other countries signed the Montreal Protocol (Anderson, 1995). This legislation limited the production of halons and CFCs. An amendment to the protocol required commercial halon production to cease in 1994 (Grosshandler, 1994). As a consequence, industry and government agencies were forced to find a replacement for the halons.

Unfortunately, the Air Force has relied on halon 1301 for fire suppression on aircraft for decades (Grosshandler, 1994). It has an inherent ability to inhibit flames at low concentrations with a low toxicity and low cost. Other advantages of halon 1301 are a high level of stability to aid in its production, a high liquid density for storage, and a low boiling point to assist in gaseous use. Other advantages include low electrical conductivity for use in electrical fires and low corrosion potential to its container and the fire area. Replacements with comparable characteristics have not been found (Freemantle, 1995). Replacement candidates often do not inhibit a flame at relatively low concentrations as found with halon 1301. As a consequence, a larger quantity of the potential replacement is added to inhibit the flame; thus, the inhibitor has a greater tendency to deplete the ozone. The search for a suitable replacement for halon 1301 must begin with a fundamental understanding of how halon 1301 inhibits a flame.

The objectives of this thesis are to first explain the difference between species concentration measurements from the WSR and the model predictions of Chemkin II and the PSR code. This objective will be followed by a computational study of halon 1301 inhibition of methane combustion using the PSR code. The future of the project includes the analysis of experimental data from pulse experiments with fire inhibitors and the comparison of the data to the computational study provided here. First, however, a number of the previous studies that consider the chemical inhibition process of halon 1301 are described in the next section.

CHAPTER II

BACKGROUND

Biordi et al. (1974, 1975a, 1977, 1978) conducted a series of experiments with a low-pressure flat flame burner. Using a molecular-beam sampling system coupled to a modulated-beam mass spectrometer, Biordi et al. (1974) determined concentration profiles of various species (CF_3Br, HF, Br, HBr, COF_2, H_2CO, OH, H_2O, CO_2, CO and H_2) within a CH_4-O_2-Ar flame, both with and without 0.3% CF_3Br. The concentration profiles were used to propose elementary reactions that characterized the production and consumption of the species. The reaction rates were later reported (Biordi et al., 1975a). However, the interactions resulting from the decomposition of halon 1301 were not well understood because the CF_3 radical was difficult to detect with the addition of 0.3% halon 1301. Thus, Biordi et al. (1977) increased the concentration of CF_3Br to 1.1%. The more pronounced effects of the inhibitor were used to clarify the mechanisms in the complex reaction system, and the rates for the reactions involving the CF_3 radical were reported (Biordi et al., 1978).

Westbrook (1983) performed a computational study of halon 1301 inhibition of methane laminar flame propagation. His model consisted of a one-dimensional system of mass and energy conservation equations solved simultaneously in finite difference form. The time-dependent system of equations used the steady state propagation of a laminar flame as the time-asymptote. The inhibition mechanism was based upon the set of elementary reactions proposed by Biordi et al. (1975a, 1978). Verification of the computations was accomplished by comparing the results to the species and temperature profiles measured by Biordi et al. (1974, 1977). Westbrook extended his study of inhibited flames into otherwise difficult experimental regimes and considered the effects of equivalence ratio, pressure, and temperature. Burgess (1995) labeled the Westbrook mechanism as the first comprehensive chemical kinetics mechanism to describe the

detailed reaction chemistry of CF_3Br for the modeling of inhibition in hydrocarbon flames. The Westbrook mechanism was used to model inhibition in other experimental systems, such as coflow and counterflow diffusion flames (Masri, 1994, Trees et al., 1995, and Hamins et al., 1994). Different fuels were combusted and simulated with this mechanism, including propane (Masri, 1994), hydrogen, methanol, ethylene (Trees et al., 1995), and liquid hydrocarbons (Hamins et al., 1994).

Modeling with the Westbrook mechanism requires the solution of a system of simultaneous ordinary differential equations, which is conveniently handled by Chemkin (Kee et al., 1989a). Additional Fortran code is used to define the governing equations for the experimental systems and to designate a method of solution. Babushok et al. (1996) used Chemkin to study high temperature methane combustion in a plug-flow reactor (PFR). The PFR was modeled as a homogeneous gas mixture in a closed system at constant pressure with a time-varying temperature (Lutz et al., 1988). They compared the results of these calculations to those obtained for a steady laminar one-dimensional premixed flame (Kee et al., 1989b). Babushok et al. (1996) defined a measurement technique to evaluate the suppression power of an inhibitor, yielded insight into flame inhibition by CF_3I, and examined ignition delay.

Battin-Leclerc et al. (1994) also used Chemkin and the Westbrook inhibition mechanism. However, new thermochemical data was used to modify the mechanism. Studies were performed using a continuous stirred tank reactor (CSTR) and modeled as a perfectly stirred reactor (PSR) (Glarborg et al., 1988). The CSTR was operated at a constant temperature of 1070 K maintained by an external heat source. Thus, the experiment is described as an oxidation study of methane in the presence of helium. (Combustion environments self-regulate the temperature with their exothermic reactions.) The oxidation was conducted at a pressure of 1 bar, with residence times varying from 1 to 7 seconds. Battin-Leclerc et al. (1994) concluded that the inhibiting effects of halon 1301 are attributed to the presence of Br radicals, which leads to additional termination reactions for the CH_3 and H radicals.

One objective of this thesis is to study the inhibition mechanism of Battin-Leclerc et al. (1994) at combustion conditions. These conditions are characterized by higher temperatures (~1600 K) and shorter residence times (~6 milliseconds) than those of the

past oxidation study. Modeling of halon 1301 interactions is performed with Chemkin (Kee et al., 1989a) and the PSR code (Glarborg et al., 1988). Another objective is to improve the experimental measurements of the well stirred reactor (WSR), which is used to perform combustion studies. Presently, a large discrepancy exists between model predictions and experimental data for methane combustion (Zelina, 1996a). The WSR will be used to perform an experimental study of halon 1301 and several replacement fire suppressants, thus these errors must be corrected. A description of the WSR facility is found in the next section.

CHAPTER III

EXPERIMENTAL

The experiments were performed using the WSR facility (Figure 1). The flow and thermal characteristics of the WSR approximate those of a PSR, which has a uniform temperature and species concentration. This spatial uniformity allows chemical kinetics to control the overall reaction rates because it eliminates the influence of mass transfer. Thus, the WSR provides a nearly ideal environment in which to study the chemical kinetics of combustion (Zabarnick and Zelina, 1994), and is used in this work to study the chemical inhibition mechanism of halon 1301. The reactor is contained within a steel housing that directs the effluent gases upward into a fume hood. Volumetric flow rates of methane and air are measured with rotameters before entering the reactor as a premixed feed. The temperature of the combustion environment is measured using a thermocouple, and the combustion gases are drawn through a probe to the emissions analyzers using a pump. The various components of the WSR facility are described in more detail in the following paragraphs.

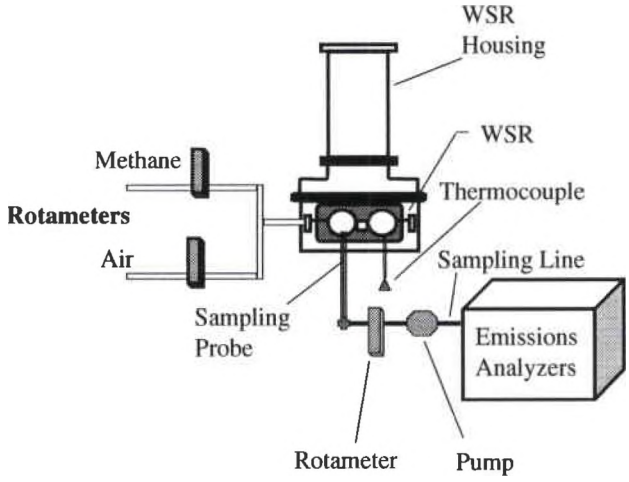

Fig. 1: WSR test facility and associated instrumentation.

The WSR is a modified version (Zelina and Ballal, 1994) of the original reactor (Nenniger et al., 1984). The fuel and air are supplied to the WSR by a stainless steel jet ring (Figure 2), which has 32-1 mm ID alumina jets angled 20 degrees from a radial line of the jet ring. The alumina jets are sealed between the two halves of the reactor with alumina paste, and both the WSR and the jet ring are secured within steel housing with alumina packing. The heat loss to the alumina packing has been estimated at 100 calories per second (Zelina, 1996a). The 250-ml toroidal reactor (Figure 3) is comprised of two alumina halves. The bottom half has three ports that provide access to the combustion environment. With the two halves placed together, the inner wall of the toroid contains eight flow passages leading to the flow straightener. This flow straightener causes the exhaust to flow axially upward.

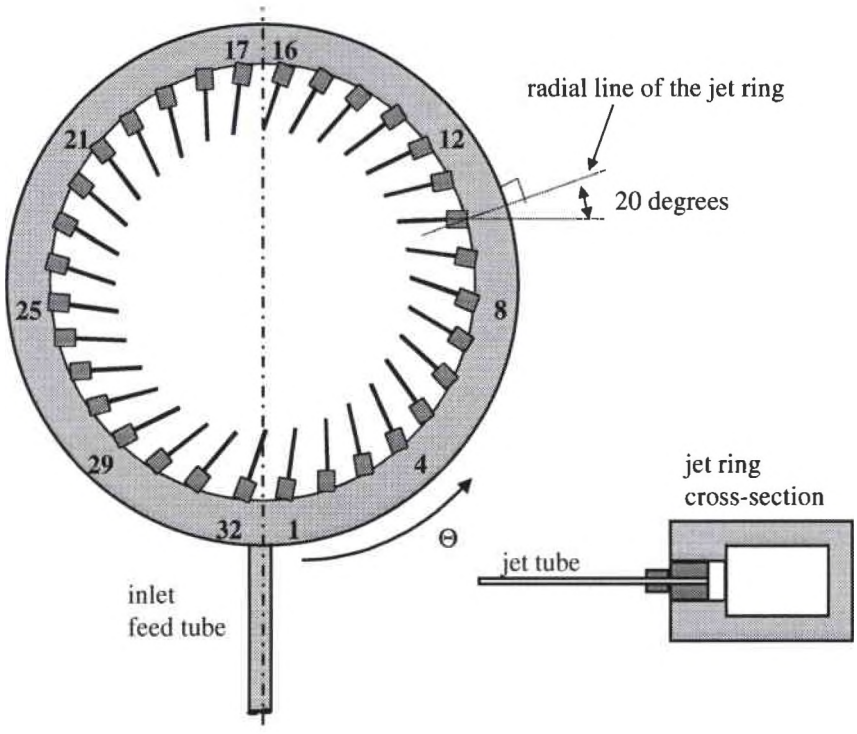

Fig. 2: Jet ring for the WSR.

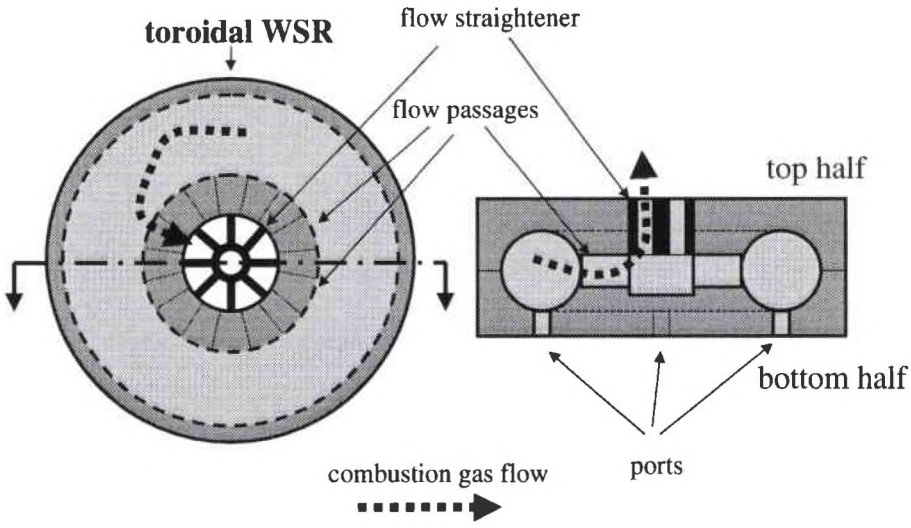

Fig. 3: 250-ml toroidal WSR.

Volumetric flow rates for air and methane are measured with rotameters (Gilmont) (up to 600 slpm and 58 slpm, respectively). The uncertainty in the flow rate measurement is ±2 percent. The equivalence ratio (ϕ) (equation 1) is varied from 0.4 to 2.2, and is calculated within ±3.5 percent. The residence time (τ) (equation 9, p. 13) is varied from 5 to 18 milliseconds, and is maintained with an accuracy of ±0.6 milliseconds. The air is preheated by a 3 kW air heater (Hotwatt), and is premixed with the fuel in a chamber. This chamber also serves as a vaporizer for liquid fuels (Blust et al., 1997b). A fast-pulse solenoid valve (General Valve) is attached just prior to the jet ring feed tube (Ballenthin et al., 1997), and is used to pulse fire suppressants into the WSR.

$$\phi = \frac{\left(\frac{F}{O}\right)}{\left(\frac{F}{O}\right)_{stoich}} \qquad (1)$$

$$\left(\frac{F}{O}\right) = \frac{\text{moles of fuel}}{\text{moles of oxidant}} \qquad (2)$$

The WSR ports provide access to the combustion environment for a sampling probe, thermocouple, and ignitor. The combustion gases are drawn through a quartz air-cooled probe (Blust et al., 1997a), which despite being fragile prevents catalytic reactions that would otherwise occur in the stainless steel design. The temperature of the WSR is measured with a type B thermocouple (platinum-6% rhodium, platinum-30% rhodium) coated with alumina ceramic paste. Radiative heat loss corrections are made to the temperature measurements (Blust et al., 1997b). Temperatures range from 1300 K to 2000 K, and are measured with a ±50 K accuracy. A spark ignitor is removed immediately after igniting the methane-air mixture.

Sample analysis is performed with a jet exhaust mass spectrometer (JEMS) (Ballenthin et al., 1997). The JEMS requires a corrosion resistant pump (Air Dimensions Inc.) to direct WSR combustion gas past the JEMS sampling cup at a rate of 8 slpm. The sampling line is heated prior to the mass spectrometer to prevent water condensation. However, prior to the sampling pump, an impinger condenses the water and soluble acids to prevent damage to the pump. The acidic water is collected, neutralized with NaOH, and stabilized with $CaCl_2$. The pump exhaust is directed into a fume hood.

The temperature profile of the sampling probe is measured using a 0.02-inch OD type K thermocouple, which is placed in the probe through a ¼-inch tube tee attached directly to the probe (Figure 4). The tube tee is sealed with a rubber septum. The sampling pump is used to draw combustion gas through the perpendicular port at a flow rate of 8 slpm. The thermocouple wire is bent into an "S" shape to keep the bead from touching the walls of the probe (Figure 5), and to ensure a measurement of the sample gas temperature. The bead is placed at the tip of the probe as it enters the WSR combustion environment, and is retracted down the probe to record the temperature profile. The measurements are taken with a hand-held digital thermometer (Omega model HH82) with an accuracy of ±2 percent of the reading.

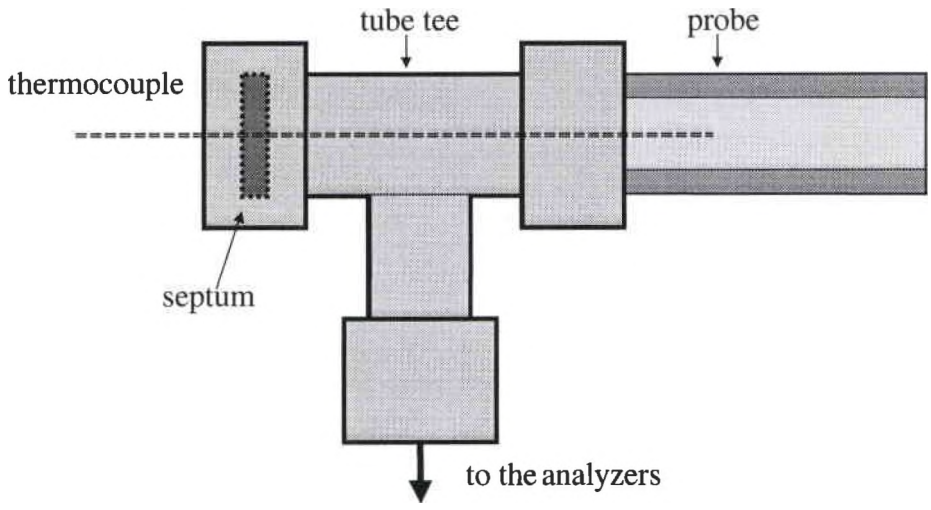

Fig. 4: ¼-inch tube tee used to measure probe temperature profile.

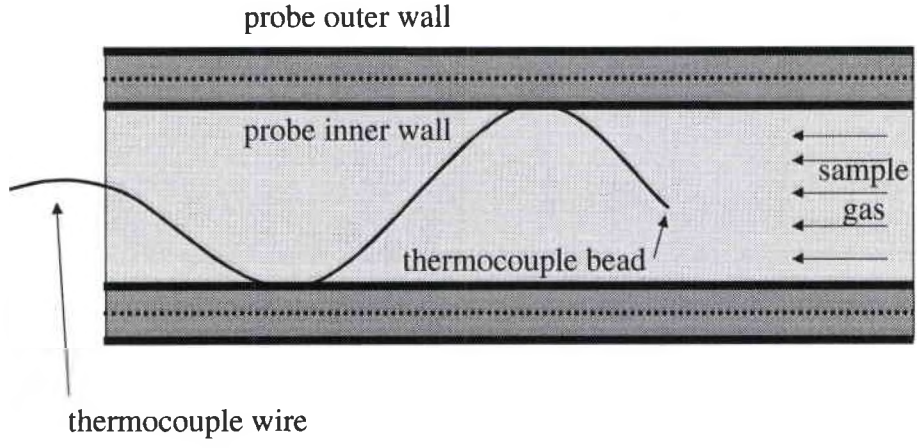

Fig. 5: Placement of the thermocouple bead in the sample gas.

The axial flow from the flow straightener is directed through a scrubber by an additional airflow (Figure 6). The carrier air passes the WSR effluent over water spraybars that collect the acids produced by the fire inhibitors. A screen prevents the acidic water from leaving the scrubber, and the water is drained into a plastic tank for neutralization (NaOH) and stabilization ($CaCl_2$). The scrubbed gases pass through the screen and enter a fume hood.

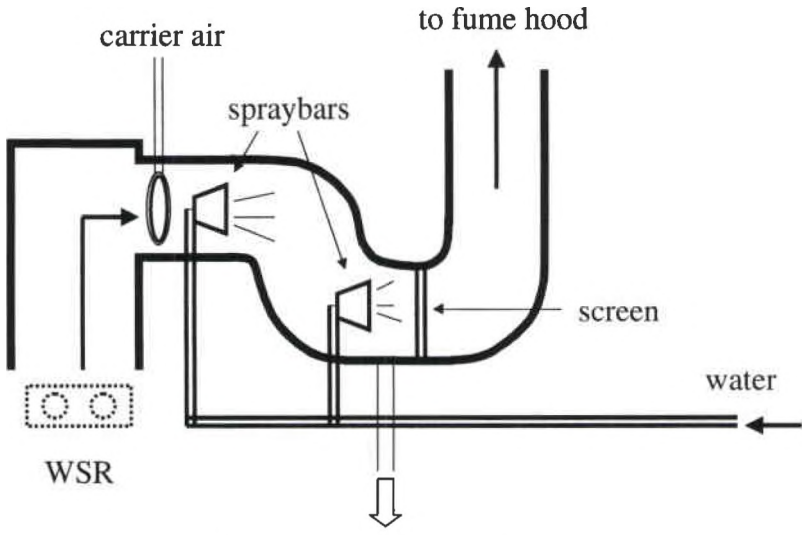

Fig. 6: Water scrubber used for the acidic effluent gas of the WSR.

CHAPTER IV

SIMULATION

Chemkin II (Kee et al., 1989a) is used to simulate methane combustion in the WSR. Because of the spatial uniformity of the temperature and species concentrations in the WSR, the PSR code (Glarborg et al., 1988) is used to model the effluent conditions. The steady-state mass conservation for each species (equation 3) and the conservation of energy (equation 4) are solved simultaneously. (Kinetic and potential energy are neglected.)

$$\dot{m}\left(Y_k - Y_k^*\right) - \dot{\omega}_k W_k V = 0 \tag{3}$$

$$\dot{m}\sum_{k=1}^{K}\left(Y_k h_k - Y_k^* h_k^*\right) + Q_{\text{loss}} = 0 \tag{4}$$

The subscript k represents a particular species, with K representing the total number of species in the system. The superscript * indicates an inlet condition. Mass flow rates are represented with a total mass flow rate ($\dot{m}$) and the species mass fractions (Y_k). The accumulation of mass is defined with a molar production rate per unit volume ($\dot{\omega}_k$), and is converted into a mass production rate with the species molecular weight (W_k) and the reactor volume (V). The energy flow rates are expressed with the species enthalpies (h_k), and a characteristic heat loss (Q_{loss}) is assigned to the reactor. The conservation equations form a set of K+1 nonlinear algebraic equations and are solved with a Newton-Raphson method (Glarborg et al., 1988). This method requires an initial guess for the temperature and species mole fractions, which can be supplied by an equilibrium calculation. If the guess is inadequate, the transient conservation equations are solved with a finite number of time steps to better approximate the steady-state solution. The transient conservation

of mass (equation 5) and transient reactor energy balance (equation 6) are combined with the definition of transient energy in terms of temperature (equation 7) to form equation 8, which is solved with the finite number of time steps. (The reactor pressure and volume are assumed to be constant, and the gas mixture is assumed to behave as an ideal gas.)

$$\frac{dY_k}{dt} = -\frac{1}{\tau}\left(Y_k - Y_k^*\right) + \frac{\dot{\omega}_k W_k}{\rho} \tag{5}$$

$$\frac{dh}{dt} = -\frac{1}{\tau}\sum_{k=1}^{K}\left(Y_k h_k - Y_k^* h_k^*\right) - \frac{Q_{loss}}{\rho V} \tag{6}$$

$$\frac{dh}{dt} = C_p \frac{dT}{dt} + \sum_{k=1}^{K} h_k \frac{dY_k}{dt} \tag{7}$$

$$C_p \frac{dT}{dt} = \frac{1}{\tau}\sum_{k=1}^{K} Y_k^*\left(h_k^* - h_k\right) - \sum_{k=1}^{K}\frac{h_k \dot{\omega}_k W_k}{\rho} - \frac{Q_{loss}}{\rho V} \tag{8}$$

The residence time of the reactor (τ) is defined by equation 9. This definition requires the mass-averaged density and molecular weight of the combustion gas to be calculated by equations 10 and 11. The specific heat represents a mass-averaged value defined in equation 12.

$$\tau = \frac{\rho V}{\dot{m}} \tag{9}$$

$$\rho = \frac{PW}{RT} \tag{10}$$

$$W = \sum_{k=1}^{K} W_k Y_k \tag{11}$$

$$C_p = \frac{\sum_{k=1}^{K} C_{pk}^{o} Y_k}{W} \tag{12}$$

The evaluation of the conservation equations requires both thermodynamic and kinetic rate data. The thermodynamic properties for all species can be determined by correlations developed by a least-squares fit of measured data (equations 13, 14, and 15).

Gordon and McBride (1976) defined the format of these polynomials in their NASA Chemical Equilibrium and Transport Properties Calculations code.

$$\frac{C_{pk}^{o}}{R} = a_{1k} + a_{2k}T + a_{3k}T^2 + a_{4k}T^3 + a_{5k}T^4 \tag{13}$$

$$\frac{H_k^{o}}{RT} = a_{1k} + \frac{a_{2k}}{2}T + \frac{a_{3k}}{3}T^2 + \frac{a_{4k}}{4}T^3 + \frac{a_{5k}}{5}T^4 + \frac{a_{6k}}{T} \tag{14}$$

$$\frac{S_k^{o}}{R} = a_{1k}\ln T + a_{2k}T + \frac{a_{3k}}{2}T^2 + \frac{a_{4k}}{3}T^3 + \frac{a_{5k}}{4}T^4 + a_{7k} \tag{15}$$

The temperatures are given in Kelvin, and the reference temperature is 298 K. Seven coefficients (a_{1k} – a_{7k}) are used as input to define temperature relationships of the standard heat capacity (C_{pk}^{o}), enthalpy (H_k^{o}), and entropy (S_k^{o}) for each species.

The rate of production of a species is expressed as the sum of the rate-of-progress variables (q_i) (equation 16), where the subscript i is used to indicate a particular reaction in the set of I reactions. The symbol ν_{ki} is defined as the difference in product (″) and reactant (′) stoichiometric coefficients (equation 17). This variable selects the reactions that involve the production or consumption of species k. Rate-of-progress variables (q_i) are defined as the difference of the forward and reverse reaction rates (equation 18), which are the product of their respective rate constants (k_{fi} and k_{ri}) and reactant molar concentrations ([X_k]) raised to the power of their stoichiometric coefficients (ν_{ki}').

$$\dot{\omega}_k = \sum_{i=1}^{I} \nu_{k_i} q_i \tag{16}$$

$$\nu_{ki} = \left(\nu_{ki}'' - \nu_{ki}'\right) \tag{17}$$

$$q_i = k_{f_i} \prod_{k=1}^{K} [X_k]^{\nu_{ki}'} - k_{r_i} \prod_{k=1}^{K} [X_k]^{\nu_{ki}''} \tag{18}$$

Chemkin assumes a modified Arrhenius form for the forward rate constants (k_f) of each elementary reaction (equation 19).

$$k_{fi} = A_i T^{\beta_i} \exp\left(-\frac{E_i}{RT}\right) \tag{19}$$

The Arrhenius parameters include a pre-exponential factor (A_i), an exponent for the temperature dependence (β_i), and an activation energy for the reaction (E_i). The reverse reaction rates (k_r) are calculated using the molar concentration equilibrium constant (K_c) (equation 20), which is related to the partial pressure equilibrium constant (K_p) by equation 21.

$$k_{ri} = \frac{k_{fi}}{K_{ci}} \tag{20}$$

$$K_{ci} = K_{pi}\left(\frac{P_{atm}}{RT}\right)^{\sum_{k=1}^{K} \nu_{ki}} \tag{21}$$

The pressure is estimated as atmospheric (P_{atm}). The partial pressure equilibrium constant is calculated using thermodynamic properties and equation 22.

$$K_{pi} = \exp\left[\left(\sum_{k=1}^{K} \nu_{ki} \frac{S_k^o}{R}\right) - \left(\sum_{k=1}^{K} \nu_{ki} \frac{H_k^o}{RT}\right)\right] \tag{22}$$

The kinetic rate data for methane combustion in air is represented by the Miller and Bowman mechanism (1989), which accounts for C_1 and C_2 species. Additional rate data describes the formation of NO_x in methane combustion (Zabarnick, 1991). Warnatz (1983) provides reactions that involve C_3 species for future approximation of propane combustion. The interactions of halon 1301 are represented with the Battin-Leclerc mechanism (1994). The compilation of these mechanisms is found in Appendix A. The input for a simulation of a PSR includes a temperature, pressure, reactor volume, residence time, and inlet mole fractions. Sample input data are recorded in output files provided in Appendices B and C.

CHAPTER V

RESULTS OF PROBE INVESTIGATION

DISCREPANCIES IN WSR MEASUREMENT

Past WSR modeling attempts reveal a discrepancy between model predictions and experimental measurements (Zelina, 1996b). These discrepancies must be corrected prior to the study of halon 1301 interactions. Therefore, methane combustion is simulated for various equivalence ratios and compared to the simulations of an established Allied-Signal Engines PSR model (AE PSR) and the experimental measurements of the WSR. The calculated results from both models are comparable, but the experimental results do not agree with model predictions. Specifically, the measured mole fraction of CO is an order of magnitude lower than the model predictions (Figure 7). The experimental sampling system includes a quartz air-cooled sampling probe, which is designed to terminate combustion reactions of the WSR by cooling the combustion gas. However, the termination of the consumption of CO and reduction of THC (total hydrocarbons) requires a relatively low temperature. Thus, the cooling rate of a sampling probe determines the recovery of CO and THC. Therefore, a study of probe designs is conducted to understand the limitations of the quartz probe.

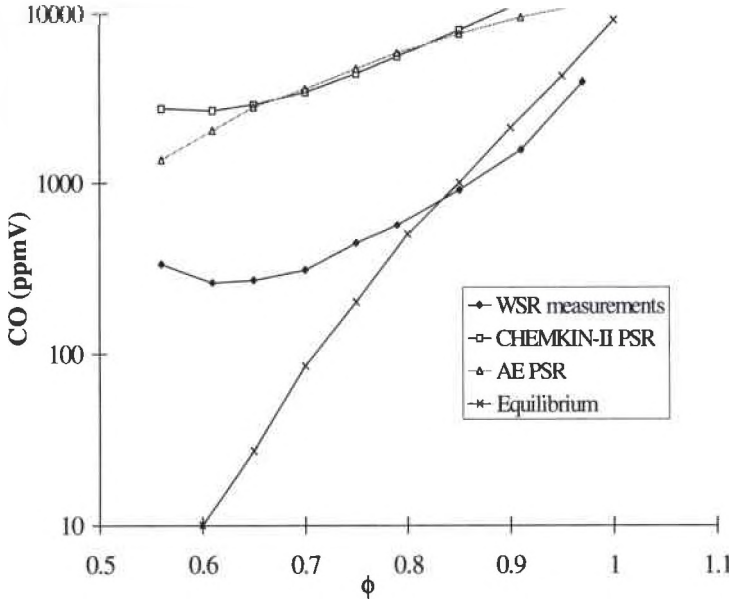

Fig. 7: CO versus equivalence ratio for methane combustion with τ=6 ms.

MODELING PROCEDURE FOR PROBE DESIGNS

The investigation of sampling probe designs is reported in "Probe Design Optimization for the Well Stirred Reactor" (Blust et al., 1997a, Appendix D). The result of the investigation is a rationalization of the differences between modeling predictions and experimental measurements with different probe designs. In addition, an optimal probe is designed to deliver a sample gas that best represents the WSR effluent gas. The correlation of experimental measurements to model calculations uses a new modeling scheme.

To predict the consumption of CO and THC prior to their measurement, the probe is modeled as a series of isothermal PSR elements. The probe's quenching ability is studied while maintaining its PFR characteristic. The combustion gas (~1600 K) is cooled to as low as 400 K within the probe, and the temperature profile is measured and plotted as a function of distance down the probe (x). This profile is approximated as a series of isothermal elements (Figure 8). Calculations are performed using an Excel spreadsheet (Appendix E), and the procedure for defining these probe elements follows.

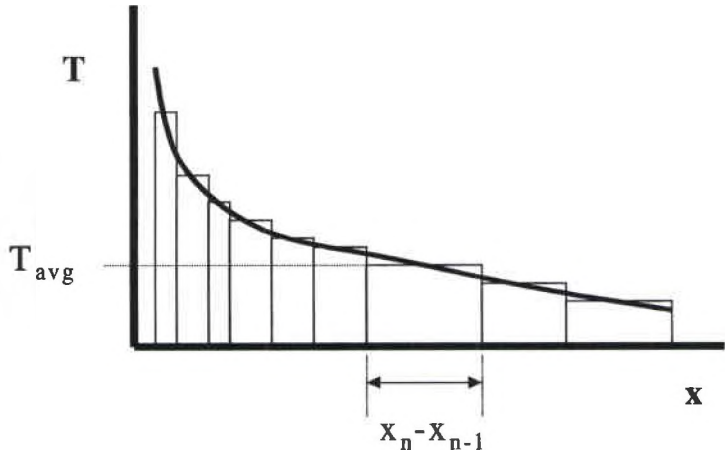

Fig. 8: Approximation of isothermal PSR elements.

Temperatures are arithmetically averaged to define an isothermal element, and densities are calculated at these average temperatures using the ideal gas law (equation 23). The pressure (P) is 1 atmosphere, and the molecular weight (W) is estimated as 28.168 g/mole (representative of combustion frozen at ϕ=0.7).

$$\rho_{avg} = \frac{PW}{RT_{avg}} \tag{23}$$

The average velocity (u_{avg}) (equation 24) is tabulated for each bin using a volumetric flow rate (Q_{meas}) measured with a flowmeter in the slpm units and adjusted for T_{avg}.

$$u_{avg} = \frac{Q_{meas}}{A} \tag{24}$$

This average velocity (u_{avg}) is then used to define the residence time (τ) of each individual PSR element, identified by a subscript n (equation 25).

$$\tau_n = \frac{x_n - x_{n-1}}{\left(\frac{(u_{avg})_n + (u_{avg})_{n-1}}{2}\right)} \quad (25)$$

The input for each PSR element includes a volume (V) and volumetric flow rate (Q) (equations 26 and 27, respectively).

$$V_n = (x_n - x_{n-1})A \quad (26)$$

$$Q_n = \frac{V_n}{\tau_n} \quad (27)$$

The average of the individual volumetric flow rates is used as the flow rate for every PSR element to simplify the modeling effort. The Reynolds number (Re) is calculated for each PSR element (equation 28), and the viscosity of air at the average temperature is used as an estimate (Incropera and DeWitt, 1990).

$$\mathrm{Re}_{avg} = \frac{\rho_{avg} u_{avg} D}{\mu} \quad (28)$$

The probe designs are qualitatively compared by plotting their temperature profiles versus both the distance down the probe and the cumulative residence time (Figures 9 and 10). The probe designs compared in the plots are outlined in Appendix D (Blust et al., 1997a). The former plot is used to define a length of the probe used to cool the combustion gas, and the latter is used to estimate the length of time that the combustion gas is reacting at higher temperatures. The plots indicate that the water-cooled probe designs made of stainless steel (SS) cool the combustion gas to approximately the same temperature (~450 K), but the quartz air-cooled probe cools only to ~750 K (liquids generally have better heat transfer characteristics than gases). The plot of temperature versus residence time illustrates that the small-bore stainless steel probe achieves the highest cooling rate, which is therefore the optimal design.

A more quantitative comparison is achieved by simulating the PSR elements in series as illustrated in Figure 11. The WSR is first simulated, and its products are used as input for the first probe PSR element. This element is simulated to compute input for the

next probe PSR element, and this is repeated for each probe PSR element. The output from the last PSR element simulation represents the analyzer readings.

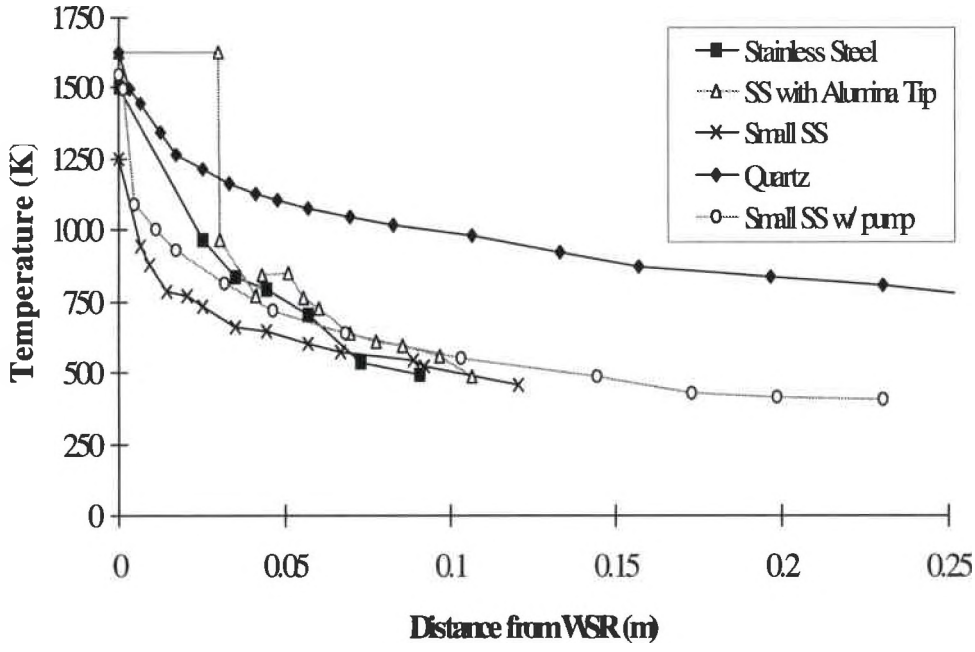

Fig. 9: Temperature profile in probe versus distance from WSR.

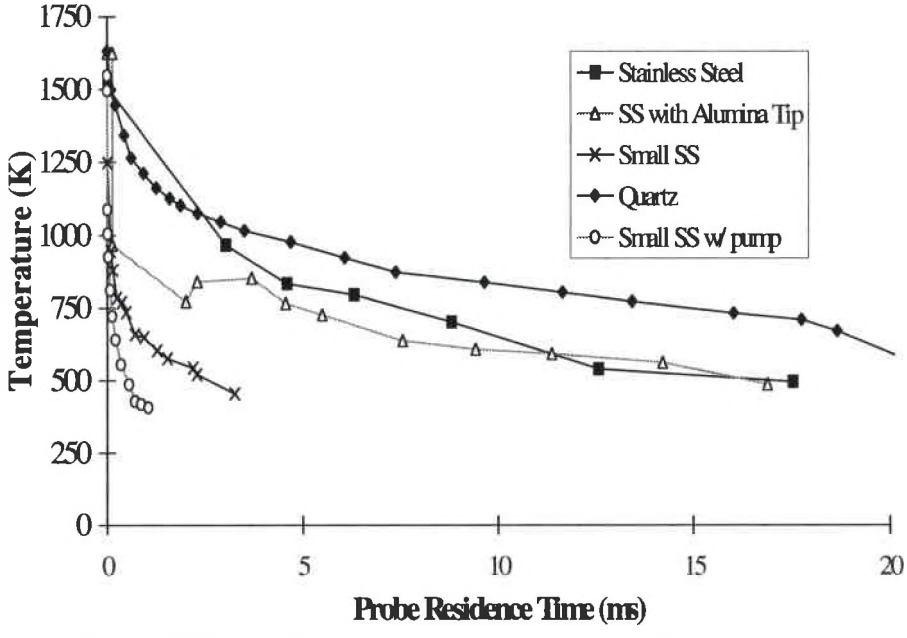

Fig. 10: Temperature profile in probe versus cumulative probe residence time.

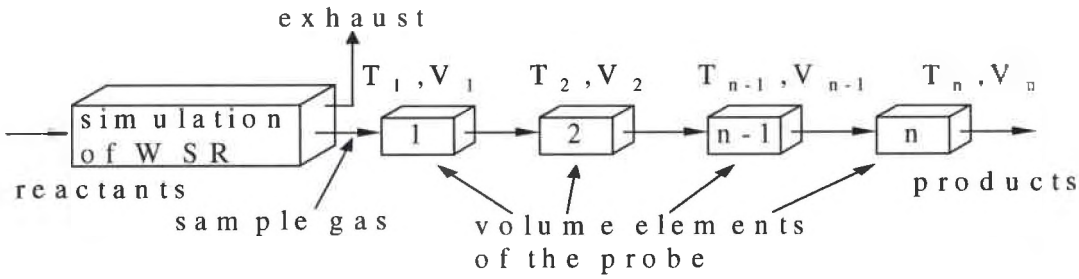

Fig. 11: PSR tanks-in-series simulation of a probe design.

However, the repeated simulation of PSR elements requires some additional programming because the PSR code only simulates a single PSR. The code is modified to perform this repetitive modeling with a single input file for the WSR and probe PSR elements. A description of the modified code is presented in Appendix F.

PROBE DESIGN MODELING

The simulated probe profiles of CO and THC are presented as a function of distance and residence time in Figures 12-15. The profiles illustrate that the probe designs cannot completely prevent the consumption of CO and THC. The highest recovery of both species is achieved with the water-cooled, small-bore stainless steel probe, which requires a sampling pump to overcome the pressure drop of its inner diameter of 0.152 centimeters. The recovery of CO improves to greater than 90%, and THC is no longer completely consumed within the probe. The use of this new probe design allows the experimental measurements for CO to be plotted on the same scale as the modeling predictions (Figure 16).

The PSR tanks-in-series modeling scheme can be used to deduce the WSR effluent species concentrations from the quartz probe measurements. These approximate effluent concentrations are used to make observations about the kinetics of the combustion environment, which lead to the proposal of new mechanisms or reactions.

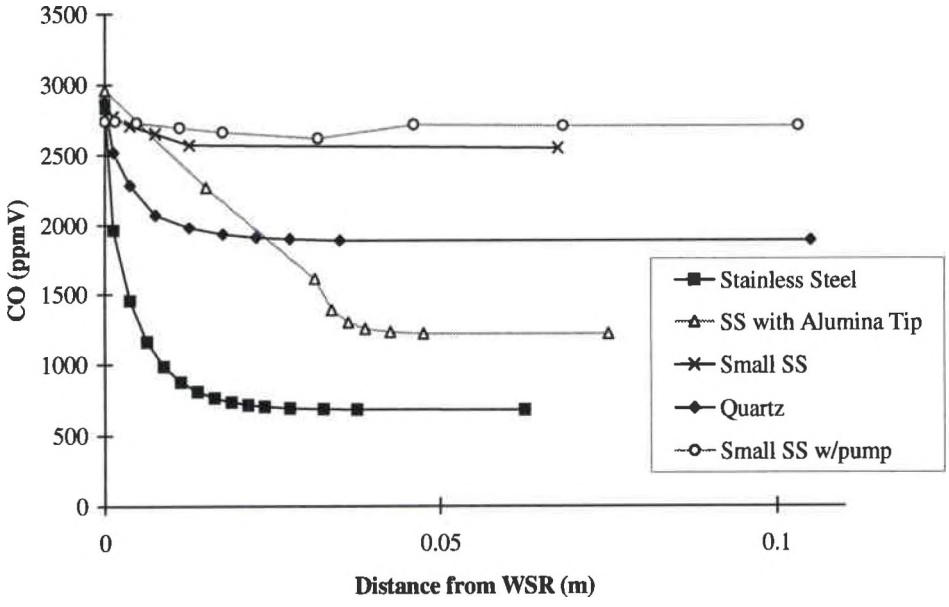

Fig. 12: Simulated CO versus distance from WSR.

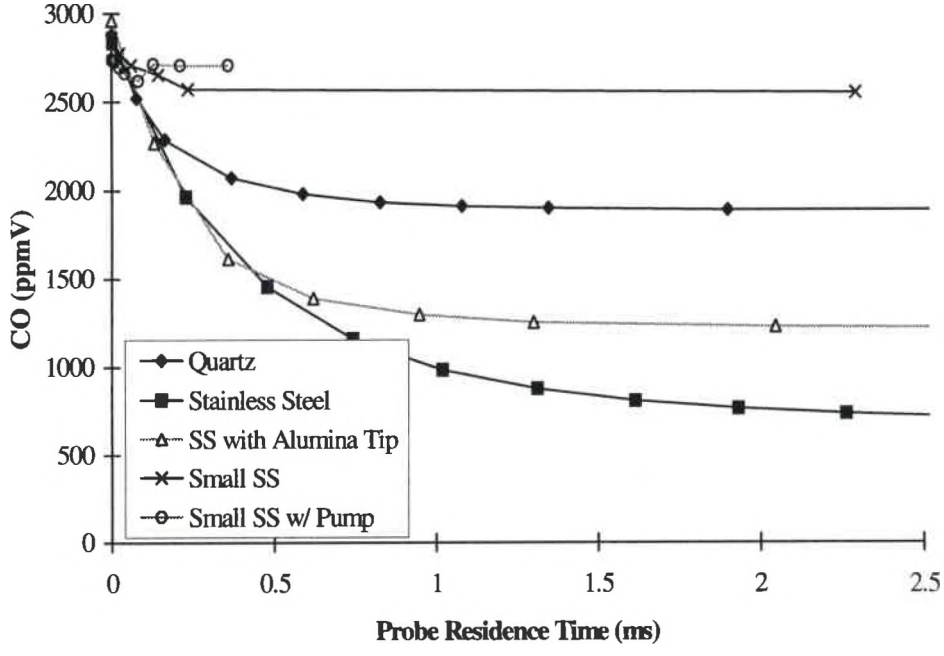

Fig. 13: Simulated CO versus cumulative probe residence time.

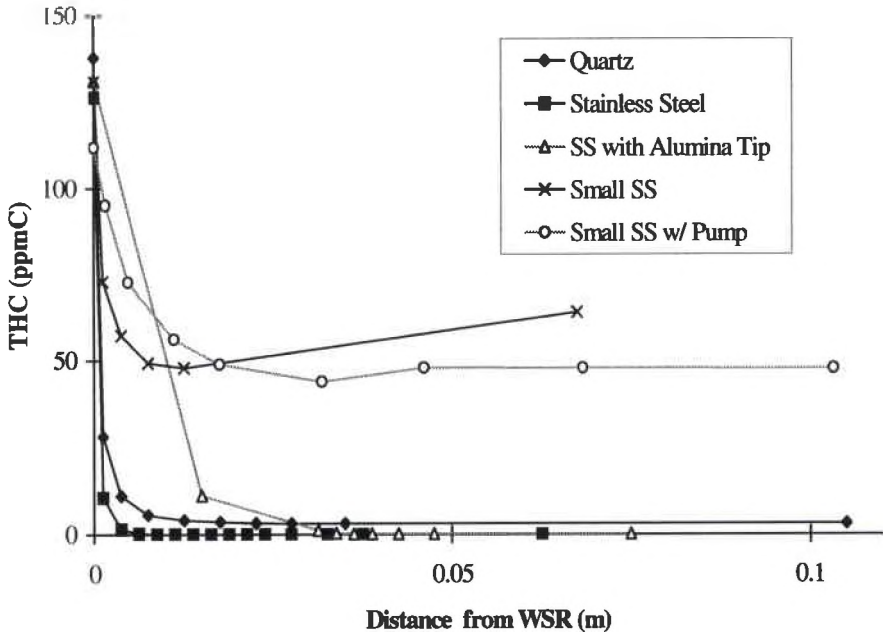

Fig. 14: Simulated THC versus distance from WSR.

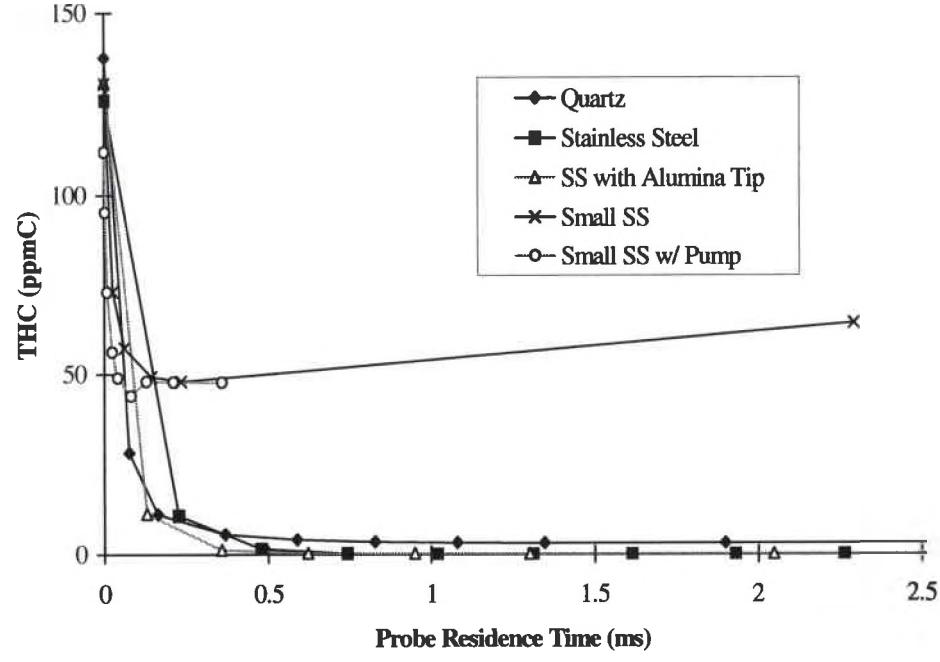

Fig. 15: Simulated THC versus cumulative probe residence time.

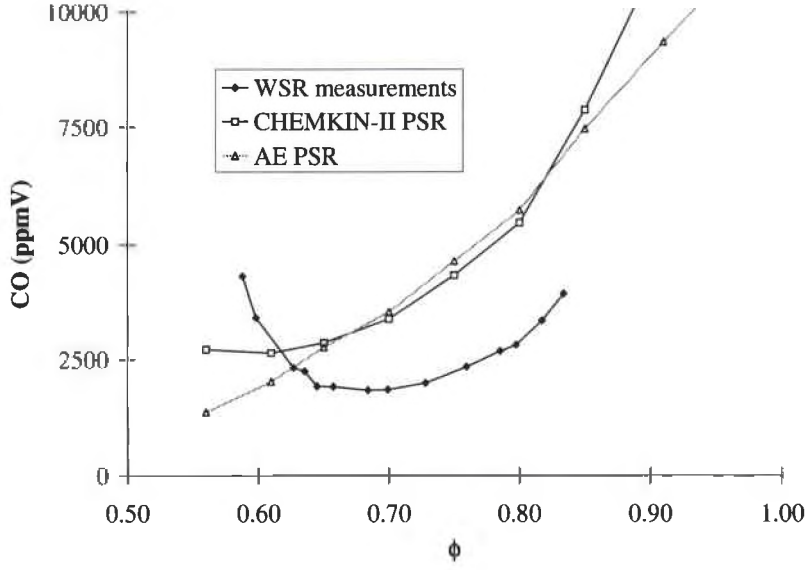

Fig. 16: Measured CO versus equivalence ratio for methane using small-bore stainless steel probe with pump.

CHAPTER VI

RESULTS OF HALON 1301 MODELING

CHOICE OF METHANE CONSUMPTION MECHANISM

The modeling study of halon 1301 inhibition of methane combustion is performed with the Miller and Bowman (1989) mechanism. The mechanism is intended for modeling the short residence times and high temperatures of methane combustion. This mechanism differs from the one used by Battin-Leclerc et al. (1994) because of the differences in experimental systems. They studied the interactions of halon 1301 in a CH_4-O_2-He mixture at 1070 K in a quartz flow reactor. The temperature was maintained by an external heat source, thus the conditions represent an oxidation of methane. (The term oxidation is used when an environment's temperature is maintained by an external heat source, as opposed to the self-sustained temperature of a combustion environment due to its exothermic reactions.) Consequently, Battin-Leclerc et al. used a methane consumption mechanism presented by Tsang et al. (1986), which is intended to apply to the initial stages of C_1 and C_2 hydrocarbon combustion similar to the conditions of oxidation. Since the intention of this study is to model halon 1301 interactions in a combustion environment, the Miller and Bowman mechanism (1989) is the proper choice.

INITIAL OBSERVATIONS OF HALON 1301 INHIBITION

The investigation of halon 1301 interactions in a combustion environment includes the simulation of lean and rich methane combustion in air, represented by equivalence ratios (ϕ) of 0.7 and 1.2. A 2 molar percent addition of halon 1301 is used, which was the concentration studied by Battin-Leclerc et al. (1994). The modeling

procedure begins with the solution of the steady-state energy and mass conservation equations for a residence time of 6 milliseconds and a heat loss of 100 calories per second to represent the WSR environment (Zelina, 1996a). The solution temperature is then used to solve the steady-state mass conservation equations at different residence times. The simulated species concentrations are plotted versus residence time and represent the species concentration profiles.

The profiles of methane, oxygen, and the major combustion products (H_2O, CO, and CO_2) are plotted for each simulated condition and used to define a time interval in which these species are being produced or consumed. Reactions of methane combustion at ϕ=0.7 occur within the first 50 μsec (Figure 17), but the addition of halon 1301 extends this time interval to 100 μsec (Figure 18). The same extension of the reaction time interval occurs at ϕ=1.2 (Figures 19 and 20). The higher temperatures of combustion at ϕ=1.2 cause the reactions to occur faster, but the addition of halon 1301 still extends the reaction time interval from 20 to 50 μsec. Comparison between the uninhibited and inhibited methane profiles provides more specific observations about the inhibition phenomena.

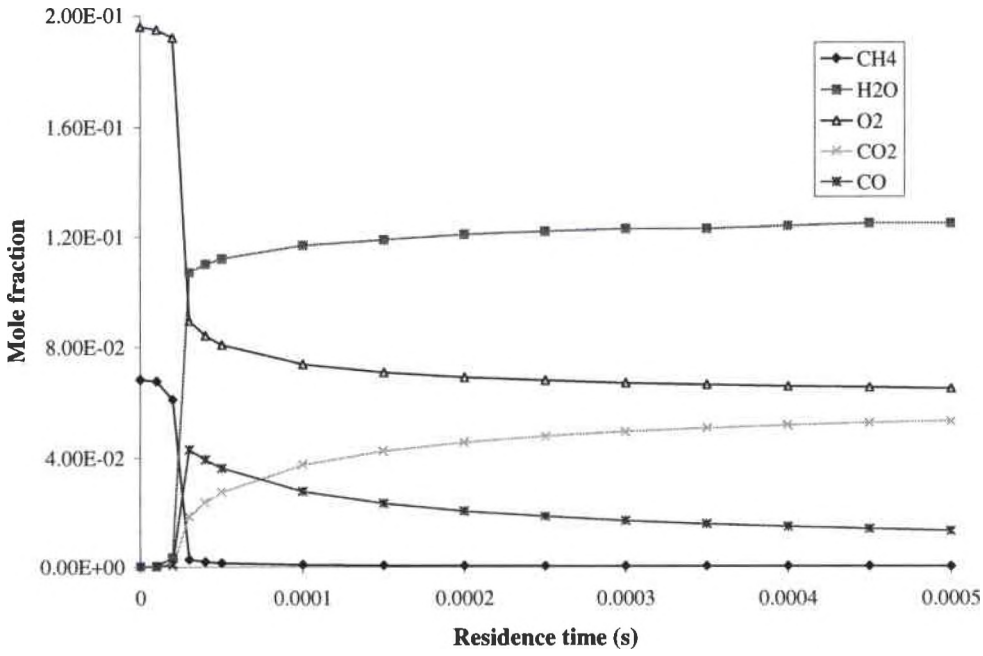

Fig. 17: Profiles for methane combustion at ϕ=0.7.

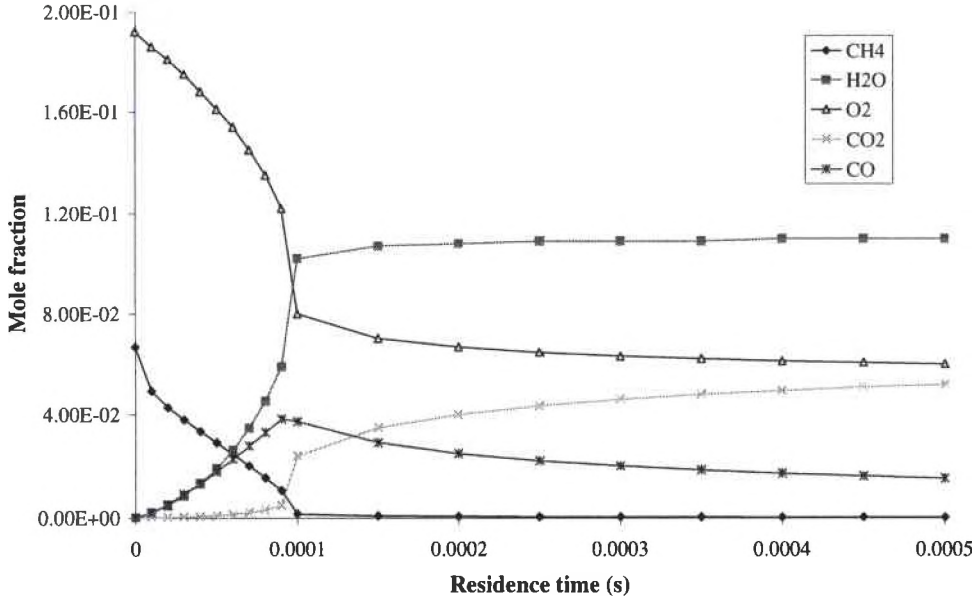

Fig. 18: Profiles for methane combustion at ϕ=0.7 with halon 1301.

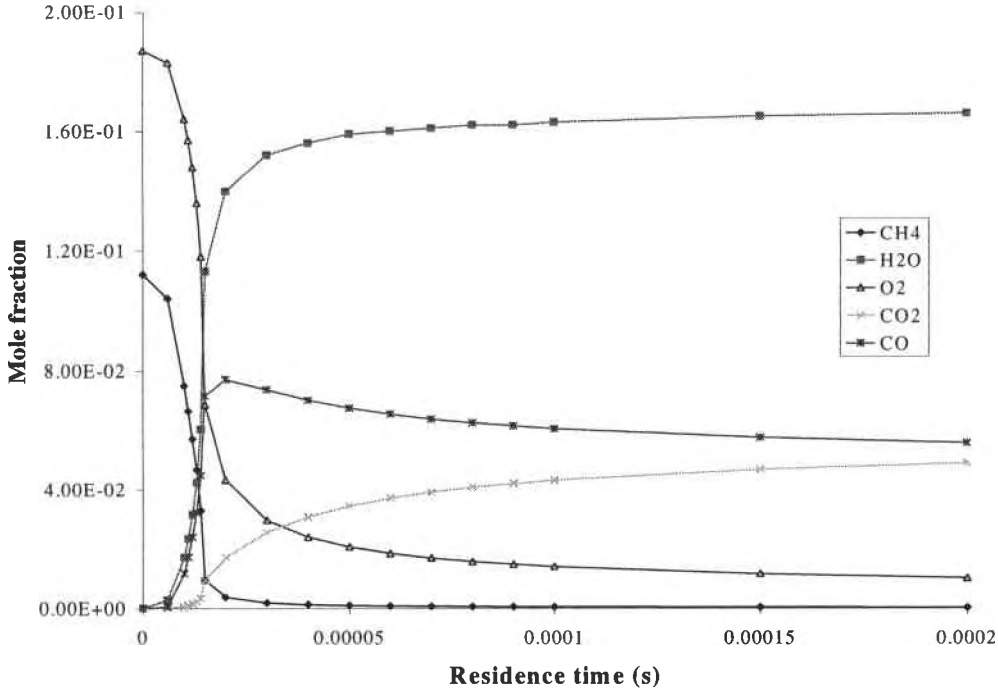

Fig. 19: Profiles for methane combustion at ϕ=1.2.

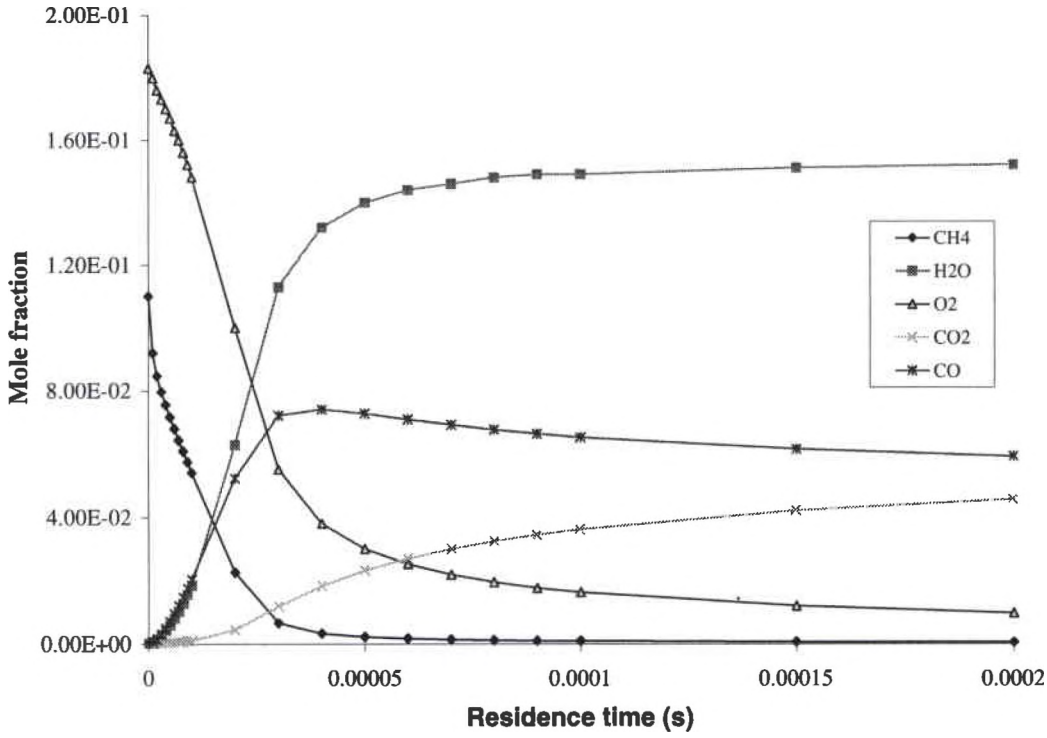

Fig. 20: Profiles for methane combustion at ϕ=1.2 with halon 1301.

Figures 21 and 22 illustrate methane consumption profiles with and without halon 1301 for equivalence ratios of 0.7 and 1.2, respectively. The temperature of combustion decreases with the addition of halon 1301, qualitatively indicating that inhibition is occurring. Methane consumption is initially accelerated before it is slowed down by halon 1301. Once again, the higher combustion temperatures at ϕ=1.2 cause the consumption of methane to occur faster than at ϕ=0.7. The initiation of methane consumption was experimentally observed by Babushok et al. (1996) in a plug flow reactor and by Battin-Leclerc et al. (1994) in a quartz flow reactor.

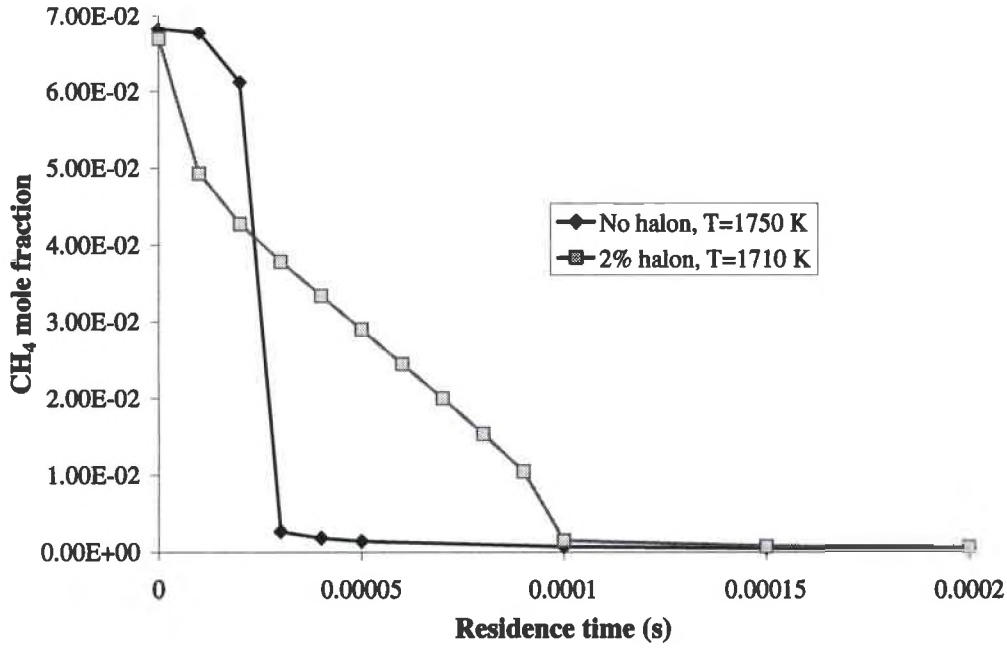

Fig. 21: Methane profiles for methane combustion at ϕ=0.7.

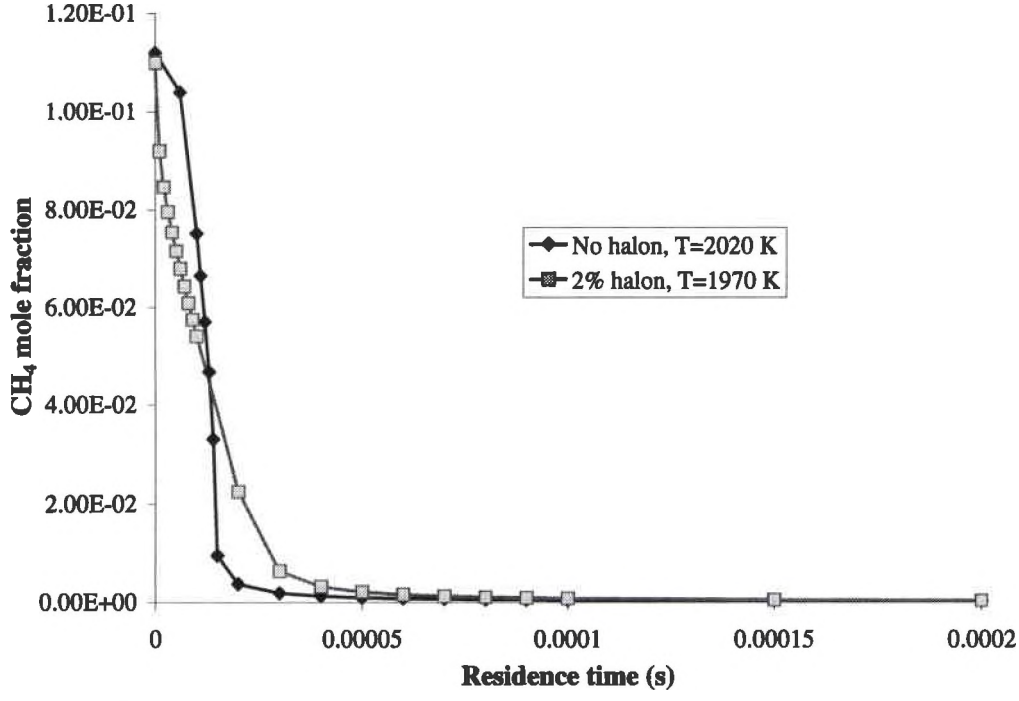

Fig. 22: Methane profiles for methane combustion at ϕ=1.2.

To simplify the analysis of the data, the following discussions present data from modeling combustion at ϕ=0.7. A comparison of the bond strengths in the reactant species results in a possible explanation for the initiation of methane consumption. The C-Br bond of halon 1301 has the weakest bond strength at 70.6 kcal per mole (Lide, 1991). The next lowest bond strengths are found in the C-H bond of methane [104 kcal per mole (Benson, 1976)] and the C-F bond of halon 1301 [107 kcal per mole (Glassman, 1987)]. This comparison suggests that halon 1301 dissociates faster than methane is consumed, and the plot of the consumption of both species supports this suggestion (Figure 23). Further, Gann (1975b) reported that CF_3Br decomposition can be expected to occur within periods of the order of a microsecond at temperatures higher than 1500 K. The accelerated methane consumption is apparently caused by the accumulation of the CF_3 and Br radicals. The concentration profiles of CHF_3 and HBr (Figures 24 and 25), which are products of hydrogen abstraction reactions with methane, illustrate that both species behave as intermediates that are accumulated at the time of initiated methane consumption. The bond strengths and profiles suggest that the CF_3 and Br are most likely responsible for the accelerated consumption of methane.

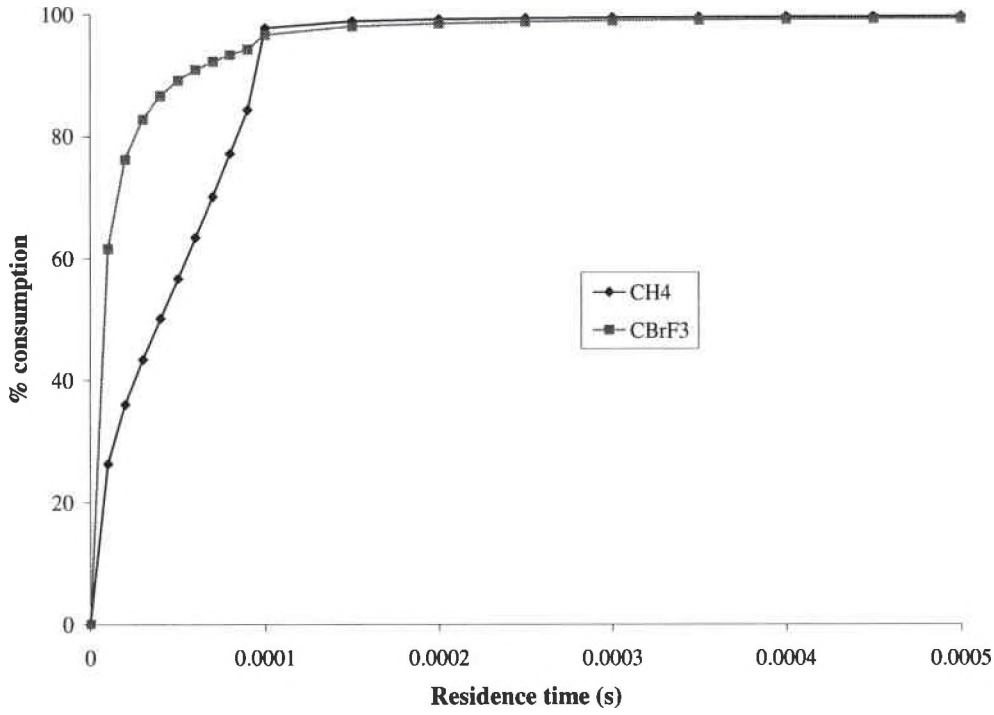

Fig. 23: Consumption of methane and halon 1301 for ϕ=0.7.

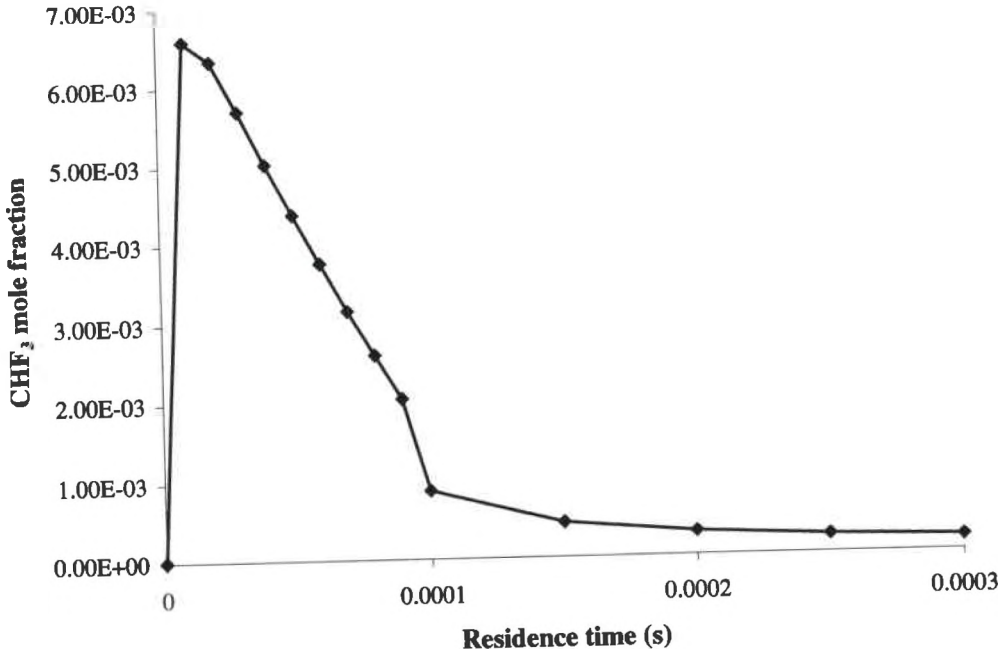

Fig. 24: Profile of CHF_3 at ϕ=0.7.

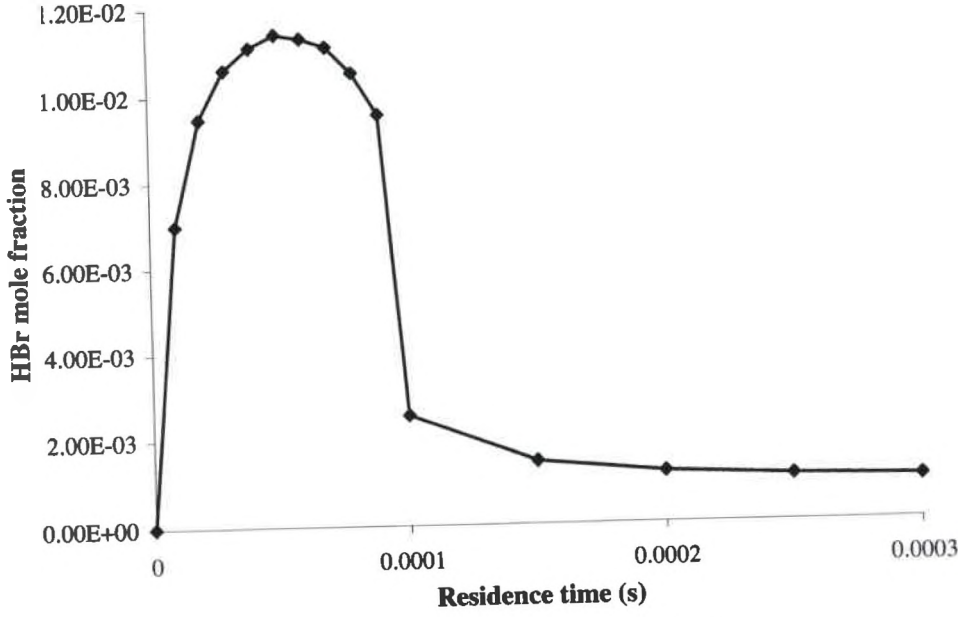

Fig. 25: Profile of HBr at ϕ=0.7.

An investigation of radical concentration profiles assists in an understanding of the prolonged consumption of methane. The radicals of most importance in a combustion system are O, H, and OH radicals which abstract a hydrogen atom from methane at high rates (Glassman, 1987). Thus, the rate of methane consumption is determined by the abundance of O, H, and OH radicals, which will be collectively referred to as the radical pool. Figures 26, 27, and 28 illustrate that the addition of halon 1301 prevents the accumulation of these radicals for 90 μsec, by which time methane is consumed. A delay in the accumulation of the radical pool was experimentally observed by Biordi et al. (1975b). The prevention of radical accumulation is responsible for the slower consumption of methane.

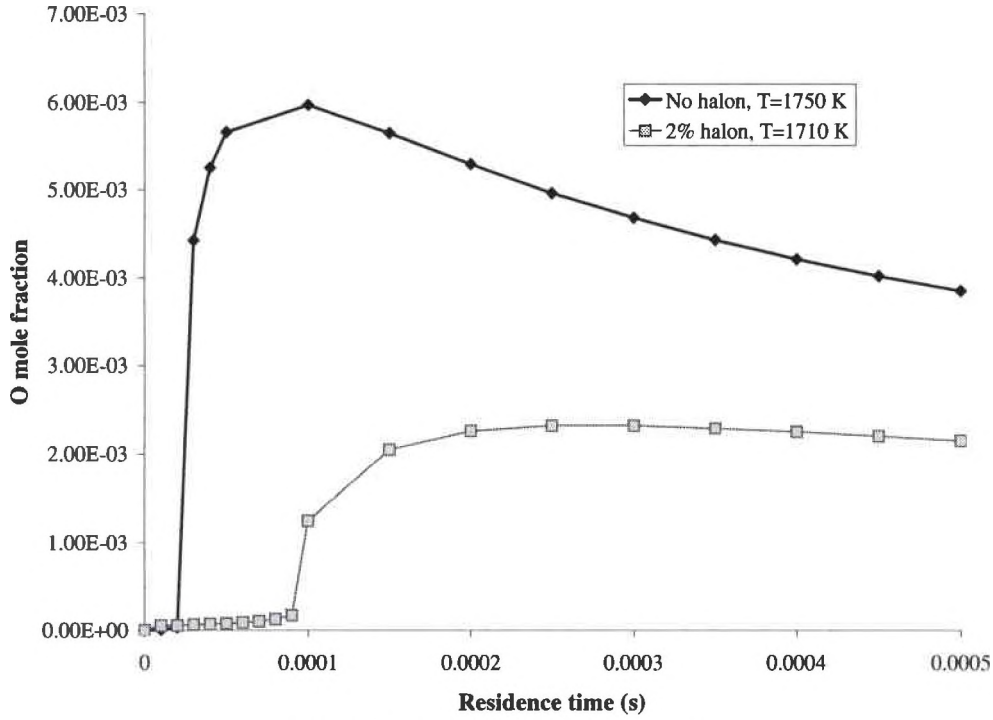

Fig. 26: Profiles of the O radical.

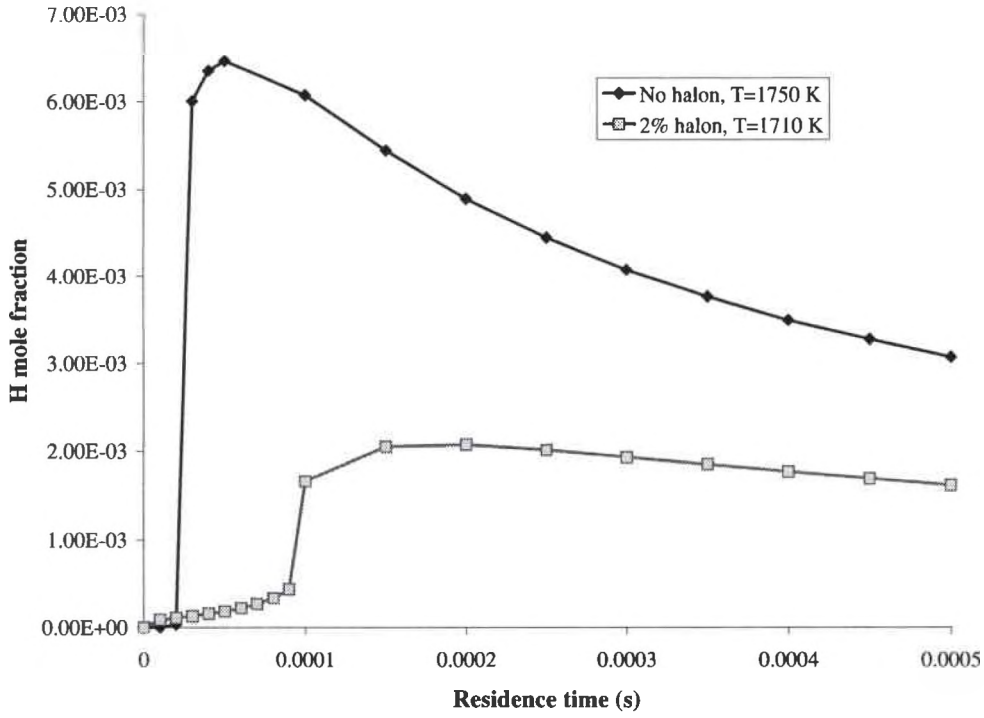

Fig. 27: Profiles of the H radical.

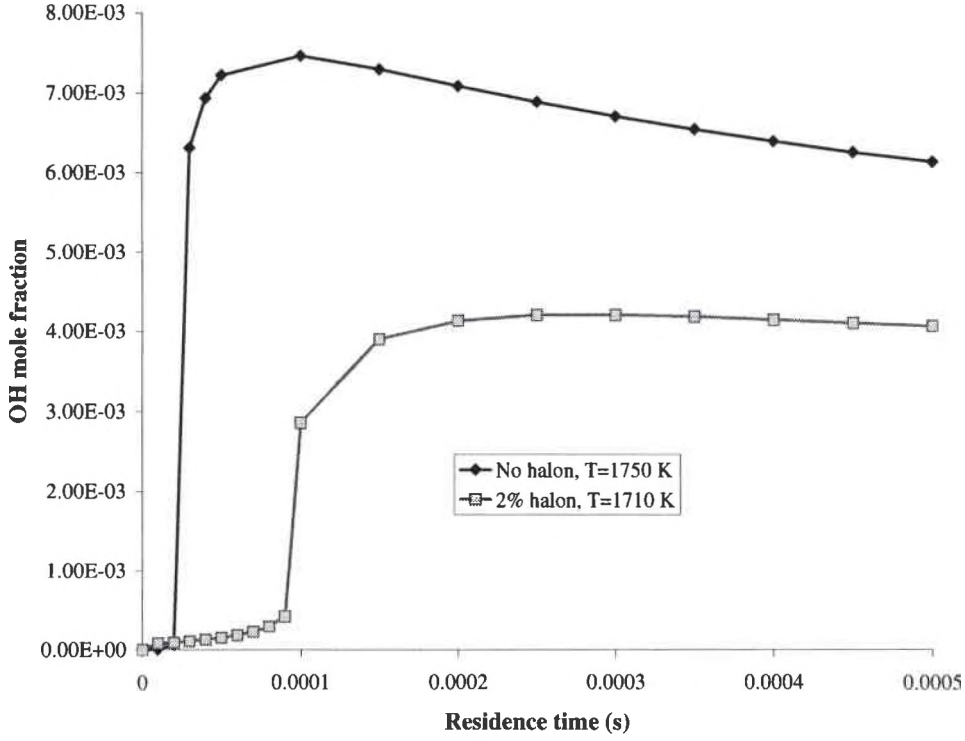

Fig. 28: Profiles for the OH radical.

A rate-of-progress (ROP) analysis is used to identify the reactions responsible for the initiation and prolongation periods of methane consumption (Glarborg et al., 1988). (This analysis is included in the Chemkin PSR code, and a sample output is provided in Appendix G.) The uninhibited combustion of methane is analyzed at τ=25 μsec, the initiation period of inhibited combustion is analyzed at τ=5 μsec, and the prolongation period is analyzed at τ=80 μsec. Each analysis is used to create a reaction path diagram for methane consumption and the activity of the radical pool. A solid arrow is used to indicate a major reaction pathway, a dotted arrow represents a minor reaction pathway, and a large dashed arrow represents a reaction resulting in the net consumption of a radical.

The reaction path diagram for uninhibited combustion of methane is illustrated in Figure 29. The consumption of methane is attributed to the radicals OH and H, and the propagation of all major reactions involves the radical pool. The OH and H radical concentrations peak at a residence time of 20 μsec (Figures 26-28), thus the methane consumption begins to occur rapidly at this time. The reactions responsible for the accumulation of radicals (τ<20 μsec) are illustrated in Figure 30. The combustion sources for radicals are indicated by the species not in bold, such as HCO and CH_3O thermally decomposing to produce the H radical and CH_3 reacting with O_2 to produce the O radical. The consumption of the H and OH radicals occurs as they react with methane. The radical pool activity during methane consumption (τ=25 μsec) is illustrated in Figure 31. The reactions do not involve the net consumption of radicals, and this stability in the radical pool is responsible for the high rate of methane consumption.

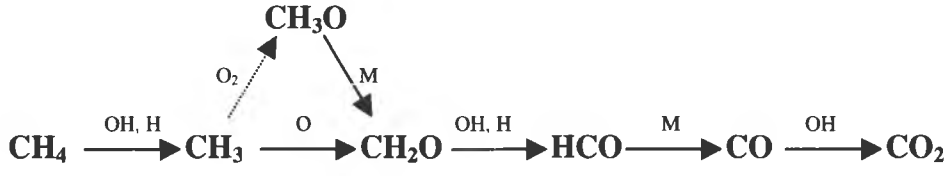

Fig. 29: Reaction path diagram for uninhibited methane combustion.

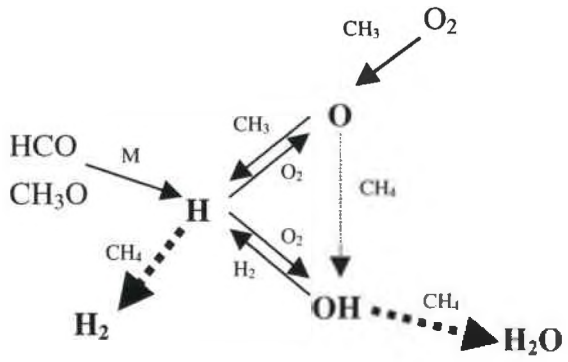

Fig. 30: Radical pool activity for uninhibited methane combustion (τ<20 μsec).

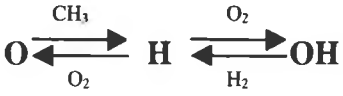

Fig. 31: Radical pool activity during uninhibited methane combustion (τ=25 μsec).

Inhibited methane consumption at τ=5 μsec is represented by the reaction path diagram in Figure 32. Reactions with the CF_3 and Br radical are responsible for the initial consumption of methane, as was proposed earlier. Further, the consumption of the CH_3 radical is altered from the uninhibited case. Due to an extended delay in accumulation of the radical pool, the CH_3 radical reacts with itself to produce the species C_2H_6, and with the CF_3 radical to produce $C_2H_3F_3$. Both reactions represent new pathways introduced during the initial stages of halon 1301 inhibition.

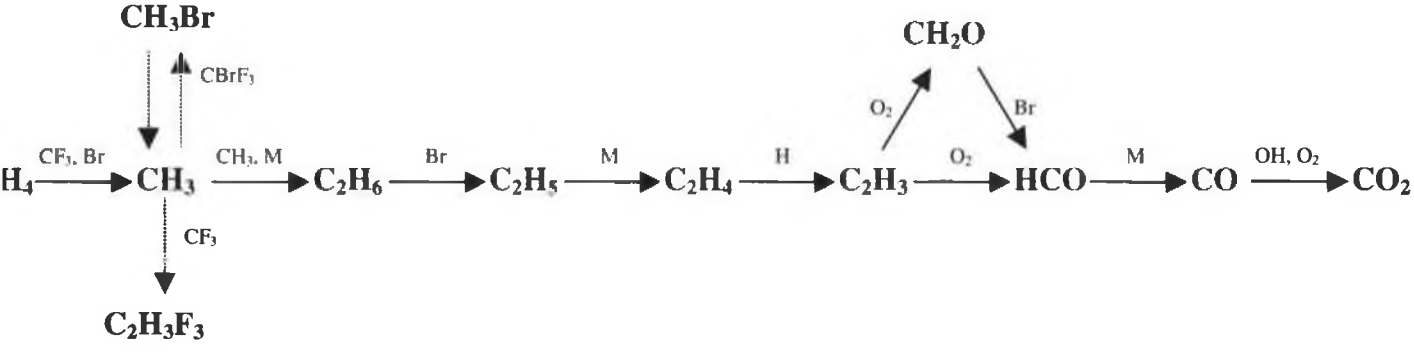

Fig. 32: Reaction path diagram for inhibited methane combustion at τ=5 μsec.

Inhibited methane consumption at τ=80 μsec is represented by the reaction path diagram in Figure 33. The Br radical still abstracts a hydrogen atom from methane, but the H and OH radicals are comparably responsible for this consumption. The CH_3 radical still reacts with itself, but it also reacts with the O radical. This latter reaction would proceed slowly because the O radical is not very abundant (Figure 26), thus the formation of C_2H_6 is once again observed in the inhibited system. The activity of the radical pool affects both the initiation and prolongation of methane combustion, thus the activity of these radicals is discussed next.

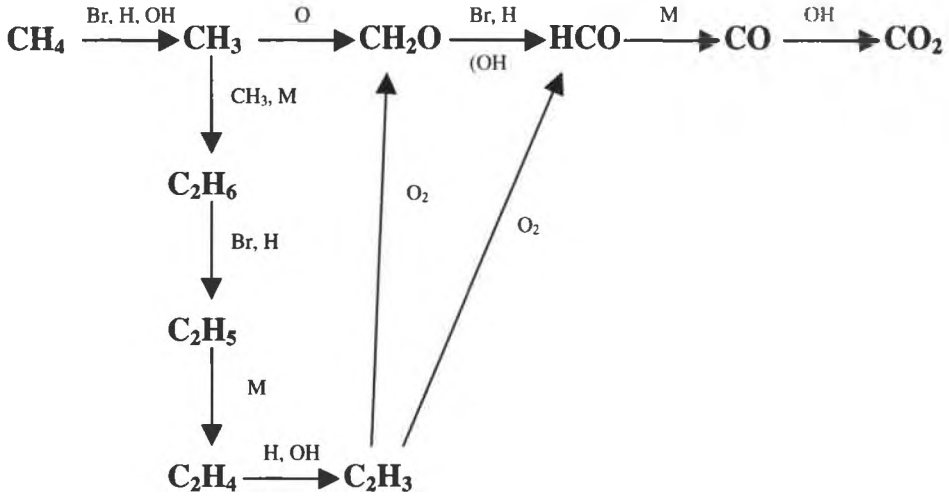

Fig. 33: Reaction path diagram for inhibited methane combustion at τ=80 μsec.

The reactions that prevent the accumulation of the radical pool at τ=5 μsec are illustrated in Figure 34. An additional radical consumption reaction is introduced with the addition of halon 1301, and this is the reaction of HBr with the H radical. As in Figure 30, the combustion sources for the H radical are represented by the species not in bold. The analysis is also performed at 80 μsec to determine the activity of the radical pool during the prolonged consumption of methane. The reactions are illustrated in Figure 35, and HBr still consumes the H radical. Thus, this reaction is responsible for the delay of radical pool accumulation and the prolongation of methane combustion.

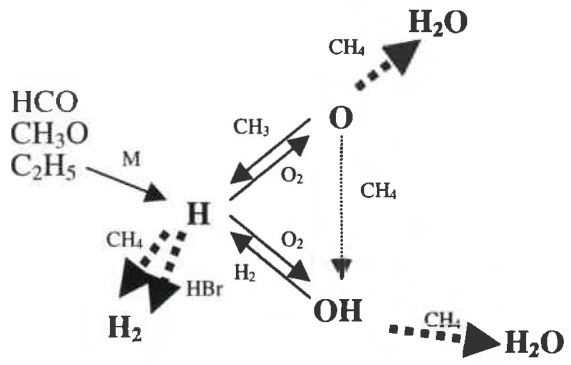

Fig. 34: Initial radical pool activity for inhibited methane combustion at τ=5 μsec.

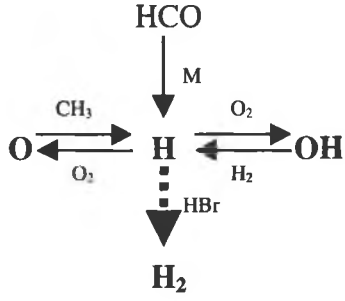

Fig. 35: Radical pool activity during the inhibited methane combustion (τ=80 μsec).

ADDITIONAL OBSERVATIONS OF HALON 1301 INHIBITION

In anticipation of experimental data from the WSR, the effects of halon 1301 on the species concentrations for a residence time of 6 milliseconds are studied. The accumulation of C_2 species increases with the addition of halon 1301. The species of C_2H_6, C_2H_4, and C_2H_2 are produced to a concentration of parts-per-thousand as opposed to the part-per-million level observed without the inhibitor. The formation of these C_2 species is accounted for by the reaction of CH_3 with itself, therefore the concentration profile of the CH_3 radical (Figure 36) is studied to provide insight into this formation process. The CH_3 radical concentration decreases rapidly at the time of O radical accumulation (Figure 26), both with and without the addition of halon 1301. With the addition of halon 1301, however, the CH_3 radical is consumed prior to this time as it

reacts with itself (Figures 32 and 33). The rate of consumption of CH_3 during this time, indicated by the slope of the concentration profile, and despite the consumption of two CH_3 radicals in a single reaction, is slower than at the time of high concentrations of the O radical. This indicates that the formation of C_2H_6 is slower than the reaction of CH_3 with the O radical.

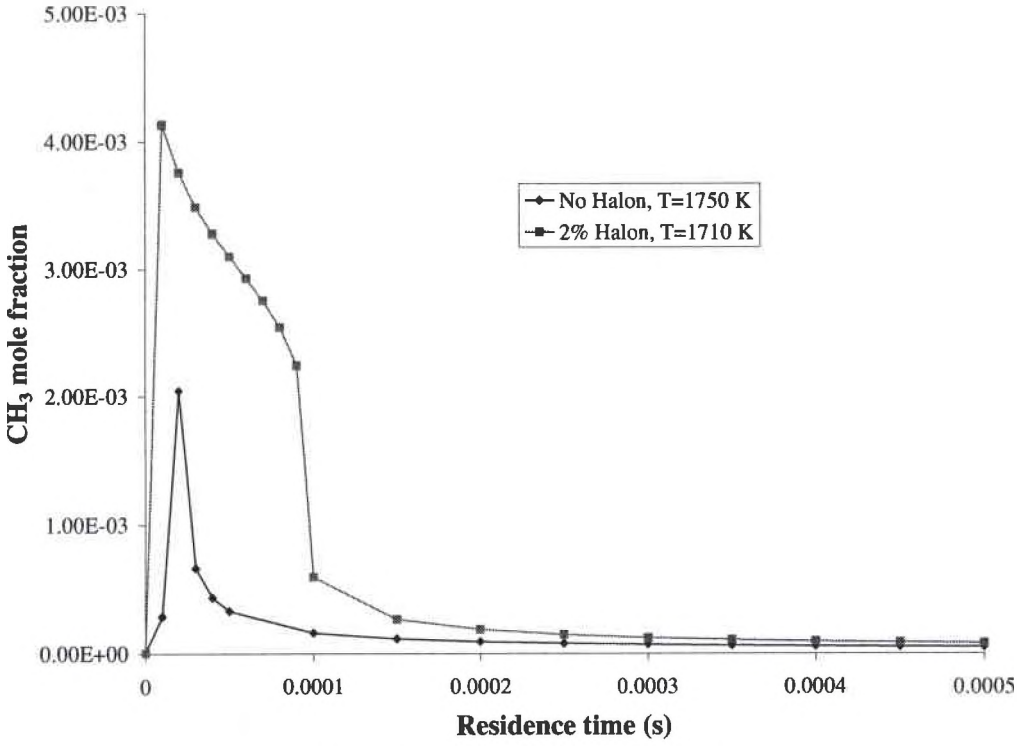

Fig. 36: Profiles of CH_3 radical.

Inhibition changes the profiles of the combustion products CO, CO_2, and H_2 (Figures 17 and 18). Initially, the absence of the OH radical accelerates the accumulation of CO by preventing the formation of CO_2. As a result, both CO and CO_2 are maintained at a higher concentration with the addition of halon 1301 (Table 1). The profile of the hydrogen molecule (Figure 37) reflects an increase in production as the H radical reacts with HBr, but the concentration after 6 milliseconds decreases with the addition of the inhibitor (Table 1).

Table 1: Combustion products at τ=6 milliseconds.

	CO mole fraction	CO_2 mole fraction	H_2 mole fraction
Uninhibited	3.41E-3	6.44E-2	1.16E-3
Inhibited	3.69E-3	6.69E-2	8.44E-4

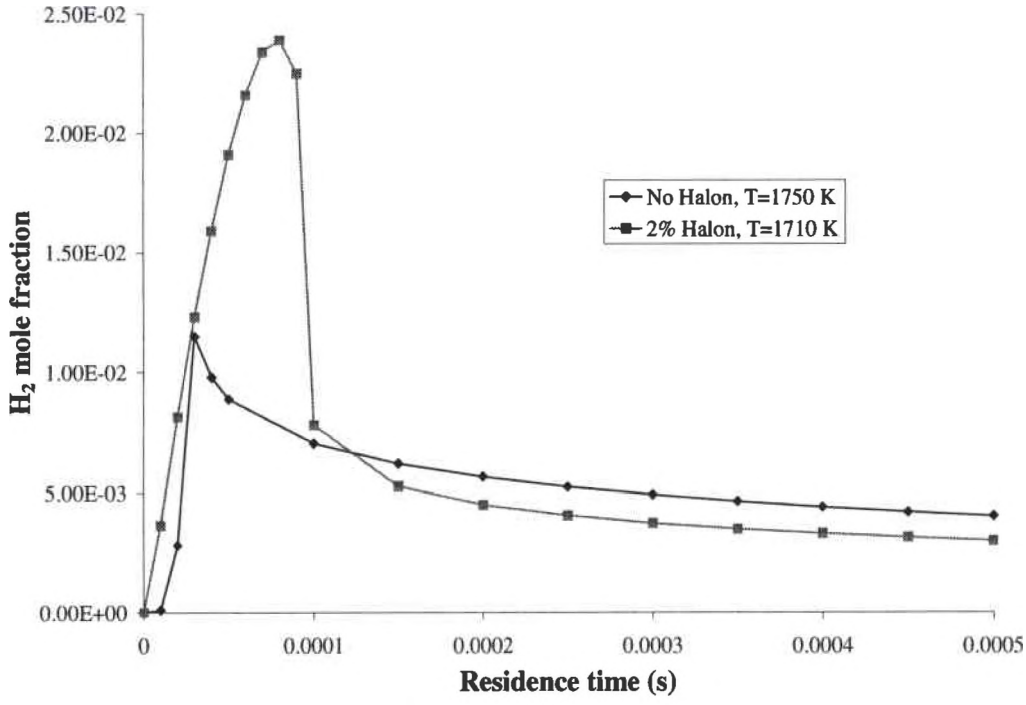

Fig. 37: Profiles of H_2.

Major products (mole fraction > 1E-3 at a residence time of 6 milliseconds) of the interactions of halon 1301 include HF, COF_2, Br, and HBr (Table 2). Minor products (mole fraction > 1E-5) include CF_3Br, Br_2, CH_3Br, and FO (Table 2). Products such as HOF, F, CF_3 and CHF_3 are detectable in the range of 1E-6 to 1E-5 (Table 2). The profile of $C_2H_3F_3$ indicates that it behaves as a post-consumption (τ>100 μsec) intermediate (Figure 38).

Table 2: Products of halon 1301 interactions at τ=6 milliseconds.

Major products		Minor products		Detectable products	
Species	Mole fraction	Species	Mole fraction	Species	Mole fraction
HF	2.94E-2	FO	5.82E-5	CHF_3	9.17E-6
Br	1.66E-2	CH_3Br	2.83E-5	CF_3	5.42E-6
COF_2	1.18E-2	CF_3Br	2.30E-5	HOF	4.43E-6
HBr	1.06E-3	Br_2	2.03E-5	F	1.41E-6

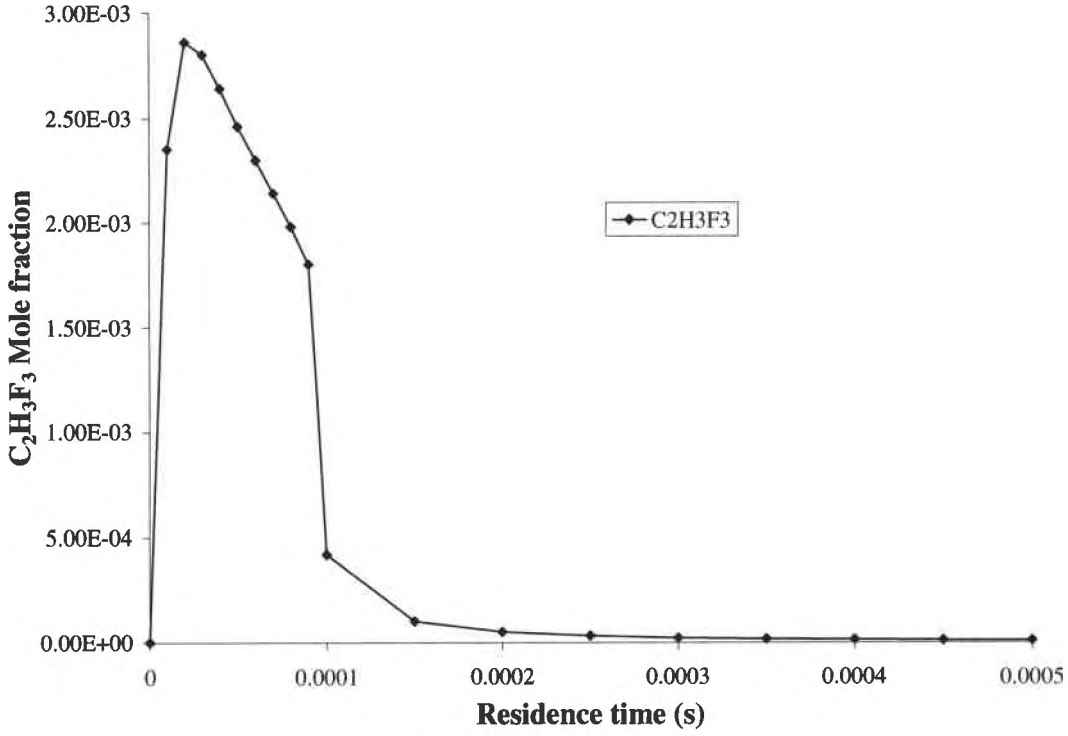

Fig. 38: Profile of $C_2H_3F_3$.

CHAPTER VII

CONCLUSIONS AND FUTURE DIRECTION

The measurements of the WSR combustion environment have improved, with a 90% recovery of CO and the prevention of total consumption of THC. This is achieved with a new probe design, a small-bore stainless steel design that is water-cooled. In addition to the new probe design, a PSR-in-series modeling procedure allows for any probe design to be modeled with the WSR to predict the experimental measurements.

Halon 1301 has been shown to act as both an initiator and inhibitor of methane combustion at equivalence ratios of 0.7 and 1.2. It initiates the consumption of methane as it dissociates into the CF_3 and Br radicals, which abstract a hydrogen atom from methane to form the intermediates CHF_3 and HBr. Halon 1301 impedes the consumption of methane by increasing the delay in radical pool accumulation (O, H, and OH radicals). This is achieved by the consumption of the H radical by HBr to produce H_2.

Additional simulation studies may be useful. The probe limitations on the measurement of product species of halon 1301 can be investigated. Also, halon 1301 can be modeled at concentrations other than 2 percent to investigate its behavior at lower concentrations. This is especially interesting since the temperature was experimentally observed to increase with the addition of halon 1301 at low concentrations.

This project will continue with data from the past experiments in the WSR with pulses of halon 1301 (1996). The PSR-in-series estimation of the quartz probe will be modified to accept a transient input, and comparisons will be made to the experimental data. The ultimate goals of this experiment are to gain some insight into the phenomena involved in flame inhibition with halon 1301 and to apply this knowledge to the experimentation with other fire-suppressants. Additional experiments were conducted with CF_3I and C_2HF_5 for comparison to CF_3Br (1996), and investigation into their inhibition mechanisms is possible.

Appendix A: Listing of complete reaction mechanism.

ELEMENTS

H O C F Br HE

END

SPECIES

CH4 CH3 CH2 CH H HE O OH HO2 H2O O2 CH2OH CH3O CO2 CO
CH2O C2H2 C3H2 C2H3 C2H4 H2 H2O2 C C2H C2H6 C2H5
HCCO CH2CO HCCOH C4H2 CH2(S) C3H3 C4H3 HCO
C3H8 C3H6 N*C3H7 I*C3H7 Br Br2 HBr CH3Br CBrF3
CHF3 CF3 COF2 COF F2 F FO C4H4 CH3OH C2H5Br C2H3Br C2HBr
C2H3F3 C2H2F2 HF HOF

END

REACTIONS	A_i**(cm-mol-s-K)**	β_i	E_i**(cal/mole)**
CH4 + O = CH3 + OH	1.02E9	1.5	8604.
CH4 + O2 = CH3 + HO2	7.90E13	0.0	56000.
2CH3(+M) = C2H6(+M)	9.03E16	-1.2	654.
LOW /1.7E38 -6.05 1292./			
TROE /0.604 6927. 132./			
H2/2/ CO/2/ CO2/3/ H2O/5/			
CH3 + H(+M) = CH4(+M)	6.0E16	-1.0	0.0
LOW /8.00E26 -3.0 0.0/			
SRI /0.45 797. 979./			
H2/2/ CO/2/ CO2/3/ H2O/5/			
CH4 + H = CH3 + H2	2.20E4	3.00	8750.
CH4 + OH = CH3 + H2O	1.60E6	2.1	2460.
CH4 + HO2 = CH3 + H2O2	1.80E11	0.0	18700.
CH3 + HO2 = CH3O + OH	2.00E13	0.0	0.0
CH3 + O2 = CH3O + O	2.05E19	-1.57	29229.
CH3 + O = CH2O + H	8.00E13	0.0	0.0
CH2OH + H = CH3 + OH	1.00E14	0.0	0.0
CH3O + H = CH3 + OH	1.00E14	0.0	0.0
CH3 + OH = CH2 + H2O	7.50E6	2.0	5000.
CH3 + H = CH2 + H2	9.00E13	0.0	15100.
CH3O + M = CH2O + H + M	1.00E14	0.0	25000.
CH2OH + M = CH2O + H + M	1.00E14	0.0	25000.
CH3O + H = CH2O + H2	2.00E13	0.0	0.0
CH2OH + H = CH2O + H2	2.00E13	0.0	0.0
CH3O + OH = CH2O + H2O	1.00E13	0.0	0.0
CH2OH + OH = CH2O + H2O	1.00E13	0.0	0.0
CH3O + O = CH2O + OH	1.00E13	0.0	0.0
CH2OH + O = CH2O + OH	1.00E13	0.0	0.0
CH3O + O2 = CH2O + HO2	6.30E10	0.0	2600.
CH2OH + O2 = CH2O + HO2	1.48E13	0.0	1500.
CH2 + H = CH + H2	1.00E18	-1.56	0.0
CH2 + OH = CH + H2O	1.13E7	2.0	3000.
CH2 + OH = CH2O + H	2.50E13	0.0	0.0
CH + O2 = HCO + O	3.30E13	0.0	0.0
CH + O = CO + H	5.70E13	0.0	0.0
CH + OH = HCO + H	3.00E13	0.0	0.0
CH + CO2 = HCO + CO	3.40E12	0.0	690.
CH + H = C + H2	1.50E14	0.0	0.0
CH + H2O = CH2O + H	5.72E12	0.0	-755.0
CH + CH2O = CH2CO + H	9.46E13	0.0	-515.
CH + C2H2 = C3H2 + H	1.00E14	0.0	0.0
CH + CH2 = C2H2 + H	4.00E13	0.0	0.0
CH + CH3 = C2H3 + H	3.00E13	0.0	0.0
CH + CH4 = C2H4 + H	6.00E13	0.0	0.0
C + O2 = CO + O	2.00E13	0.0	0.0

```
C + OH = CO + H                          5.00E13      0.0   0.0
C + CH3 = C2H2 + H                       5.00E13      0.0   0.0
C + CH2 = C2H + H                        5.00E13      0.0   0.0
CH2 + CO2 = CH2O + CO                    1.10E11      0.0   1000.
CH2 + O = CO + 2H                        5.00E13      0.0   0.0
CH2 + O = CO + H2                        3.00E13      0.0   0.0
CH2 + O2 = CO2 + 2H                      1.60E12      0.0   1000.
CH2 + O2 = CH2O + O                      5.00E13      0.0   9000.
CH2 + O2 = CO2 + H2                      6.90E11      0.0   500.
CH2 + O2 = CO + H2O                      1.90E10      0.0   -1000.
CH2 + O2 = CO + OH + H                   8.60E10      0.0   -500.
CH2 + O2 = HCO + OH                      4.30E10      0.0   -500.
CH2O + OH = HCO + H2O                    3.43E9       1.18  -447.
CH2O + H = HCO + H2                      2.19E8       1.77  3000.
CH2O + M = HCO + H + M                   3.31E16      0.0   81000
CH2O + O = HCO + OH                      1.80E13      0.0   3080.
HCO + OH = H2O + CO                      1.00E14      0.0   0.0
HCO + M = H + CO + M                     2.50E14      0.0   16802.
 CO/1.9/ H2/1.9/ CH4/2.8/ CO2/3.0/ H2O/5.0/
HCO + H = CO + H2                        1.19E13      0.25  0.0
HCO + O = CO + OH                        3.00E13      0.0   0.0
HCO + O = CO2 + H                        3.00E13      0.0   0.0
HCO + O2 = HO2 + CO                      3.30E13     -0.40  0.0
CO + O + M = CO2 + M                     6.17E14      0.0   3000.
CO + OH = CO2 + H                        1.51E7       1.30  -758.
CO + O2 = CO2 + O                        1.60E13      0.0   41000.
HO2 + CO = CO2 + OH                      5.80E13      0.0   22934.
C2H6 + CH3 = C2H5 + CH4                  5.50E-1      4.00  8300.
C2H6 + H = C2H5 + H2                     5.40E2       3.5   5210.
C2H6 + O = C2H5 + OH                     3.00E7       2.00  5115.
C2H6 + OH = C2H5 + H2O                   8.70E9       1.05  1810.
C2H4 + H = C2H3 + H2                     1.10E14      0.0   8500.
C2H4 + O = CH3 + HCO                     1.60E9       1.20  746.
C2H4 + OH = C2H3 + H2O                   2.02E13      0.0   5955.
CH2 + CH3 = C2H4 + H                     3.00E13      0.0   0.0
H + C2H4(+M) = C2H5(+M)                  2.21E13      0.0   2066.
LOW /6.37E27 -2.8 -54./
H2/2/ CO/2/ CO2/3/ H2O/5/
C2H5 + H = 2CH3                          1.00E14      0.0   0.0
C2H5 + O2 = C2H4 + HO2                   8.43E11      0.0   3875.
C2H2 + O = CH2 + CO                      1.02E7       2.00  1900.
C2H2 + O = HCCO + H                      1.02E7       2.00  1900.
H2 + C2H = C2H2 + H                      4.09E5       2.39  864.
H + C2H2(+M) = C2H3(+M)                  5.54E12      0.0   2410.
LOW /2.67E27 -3.5 2410./
H2/2/ CO/2/ CO2/3/ H2O/5/
C2H3 + H = C2H2 + H2                     4.00E13      0.0   0.0
C2H3 + O = CH2CO + H                     3.00E13      0.0   0.0
C2H3 + O2 = CH2O + HCO                   4.00E12      0.0   -250.
C2H3 + OH = C2H2 + H2O                   5.00E12      0.0   0.0
C2H3 + CH2 = C2H2 + CH3                  3.00E13      0.0   0.0
C2H3 + C2H = 2C2H2                       3.00E13      0.0   0.0
C2H3 + CH = CH2 + C2H2                   5.00E13      0.0   0.0
OH + C2H2 = C2H + H2O                    3.37E7       2.00  14000.
OH + C2H2 = HCCOH + H                    5.04E5       2.30  13500.
OH + C2H2 = CH2CO + H                    2.18E-4      4.50  -1000.
OH + C2H2 = CH3 + CO                     4.83E-4      4.00  -2000.
```

```
HCCOH + H = CH2CO + H                 1.00E13      0.0   0.0
C2H2 + O = C2H + OH                   3.16E15     -0.6   15000.
CH2CO + O = CO2 + CH2                 1.75E12      0.0   1350.
CH2CO + H = CH3 + CO                  1.13E13      0.0   3428.
CH2CO + H = HCCO + H2                 5.00E13      0.0   8000.
CH2CO + O = HCCO + OH                 1.00E13      0.0   8000.
CH2CO + OH = HCCO + H2O               7.50E12      0.0   2000.
CH2CO(+M) = CH2 + CO(+M)              3.00E14      0.0   70980.
LOW /3.60E15 0.0 59270./
C2H + O2 = 2CO + H                    5.00E13      0.0   1500.
C2H + C2H2 = C4H2 + H                 3.00E13      0.0   0.0
H + HCCO = CH2(S) + CO                1.00E14      0.0   0.0
O + HCCO = H + 2CO                    1.00E14      0.0   0.0
HCCO + O2 = 2CO + OH                  1.60E12      0.0   854.
CH + HCCO = C2H2 + CO                 5.00E13      0.0   0.0
2HCCO = C2H2 + 2CO                    1.00E13      0.0   0.0
CH2(S) + M = CH2 + M                  1.00E13      0.0   0.0
 H/0.0/
CH2(S) + CH4 = 2CH3                   4.00E13      0.0   0.0
CH2(S) + C2H6 = CH3 + C2H5            1.20E14      0.0   0.0
CH2(S) + O2 = CO + OH + H             3.00E13      0.0   0.0
CH2(S) + H2 = CH3 + H                 7.00E13      0.0   0.0
CH2(S) + H = CH2 + H                  2.00E14      0.0   0.0
C2H + O = CH + CO                     5.00E13      0.0   0.0
C2H + OH = HCCO + H                   2.00E13      0.0   0.0
2CH2 = C2H2 + H2                      4.00E13      0.0   0.0
CH2 + HCCO = C2H3 + CO                3.00E13      0.0   0.0
CH2 + C2H2 = C3H3 + H                 1.20E13      0.0   6600.
C4H2 + OH = C3H2 + HCO                6.66E12      0.0   -410.
C3H2 + O2 = HCO + HCCO                1.00E13      0.0   0.0
C3H3 + O2 = CH2CO + HCO               3.00E10      0.0   2868.
C3H3 + O = CH2O + C2H                 2.00E13      0.0   0.0
C3H3 + OH = C3H2 + H2O                2.00E13      0.0   0.0
2C2H2 = C4H3 + H                      2.00E12      0.0   45900.
C4H3 + M = C4H2 + H + M               1.00E16      0.0   59700.
CH2(S) + C2H2 = C3H3 + H              3.00E13      0.0   0.0
C4H2 + O = C3H2 + CO                  1.20E12      0.0   0.0
C2H2 + O2 = HCCO + OH                 2.00E8       1.50  30100.
C2H2 + M = C2H + H + M                4.20E16      0.0   107000.
C2H4 + M = C2H2 + H2 + M              1.50E15      0.0   55800.
C2H4 + M = C2H3 + H + M               1.40E15      0.0   82360.
H2 + O2 = 2OH                         1.70E13      0.0   47780.
OH + H2 = H2O + H                     1.17E9       1.3   3626.
O + OH = O2 + H                       4.00E14     -0.5   0.0
O + H2 = OH + H                       5.06E4       2.67  6290.
H + O2 + M = HO2 + M                  3.61E17     -0.72  0.0
 H2O/18.6/ CO2/4.2/ H2/2.9/ CO/2.1/
OH + HO2 = H2O + O2                   7.50E12      0.0   0.0
H + HO2 = 2OH                         1.40E14      0.0   1073.
O + HO2 = O2 + OH                     1.40E13      0.0   1073.
2OH = O + H2O                         6.00E8       1.3   0.0
2H + M = H2 + M                       1.00E18     -1.00  0.0
 H2/0.0/ H2O/0.0/ CO2/0.0/
2H + H2 = 2H2                         9.20E16     -0.60  0.0
2H + H2O = H2 + H2O                   6.00E19     -1.25  0.0
2H + CO2 = H2 + CO2                   5.49E20     -2.00  0.0
H + OH + M = H2O + M                  1.60E22     -2.00  0.0
```

```
 H2O/5.0/
H + O + M = OH + M                    6.20E16     -0.60  0.0
 H2O/5.0/
2O + M = O2 + M                       1.89E13      0.0   -1788.
H + HO2 = H2 + O2                     1.25E13      0.0   0.0
2HO2 = H2O2 + O2                      2.00E12      0.0   0.0
H2O2 + M = 2OH + M                    1.30E17      0.0   45500.
H2O2 + H = HO2 + H2                   1.60E12      0.0   3800.
H2O2 + OH = H2O + HO2                 1.00E13      0.0   1800.
C3H8 + H = N*C3H7 + H2                1.30E14      0.0   9699
C3H8 + H = I*C3H7 + H2                1.00E14      0.0   8337
C3H8 + O = N*C3H7 + OH                3.00E13      0.0   5757
C3H8 + O = I*C3H7 + OH                2.60E13      0.0   4467
C3H8 + OH = N*C3H7 + H2O              3.70E12      0.0   1648
C3H8 + OH = I*C3H7 + H2O              2.80E13      0.0   860
N*C3H7 + H = C3H8                     2.00E13      0.0   0.0
I*C3H7 + H = C3H8                     2.00E13      0.0   0.0
N*C3H7 + O2 = C3H6 + HO2              1.00E12      0.0   4992
I*C3H7 + O2 = C3H6 + HO2              1.00E12      0.0   2986
N*C3H7 = C2H4 + CH3                   3.00E14      0.0   32991
N*C3H7 = C3H6 + H                     1.00E14      0.0   37291
I*C3H7 = C3H6 + H                     2.00E14      0.0   38677
C3H6 + O = CH3 + CH3 + CO             5.00E12      0.0   454
C2H5 + CH3 = C3H8                     7.00E12      0.0   0
HBr + M = H + Br + M                  3.50E21     -2.0   87670
  REV/6.00E20     -1.9    0/
HBr + O2 = Br + HO2                   1.2E12       0.0   41530
  REV/1.50E12       0.0    1168/
HBr + CH3 = CH3Br + H                 3.00E12      0.0   22600
  REV/1.50E14       0.0    5239/
HBr + CH3 = CH4 + Br                  5.37E12      0.0   1604
  REV/4.70E13       0.0    18180/
HBr + C2H5 = C2H5Br + H               9.61E10      0.0   21420
  REV/1.36E13       0.0    5000/
HBr + C2H5 = C2H6 + Br                6.03E11      0.0   809
  REV/7.47E13       0.0    12940/
HBr + C2H3 = C2H3Br + H               3.87E12      0.0   16310
  REV/0.28E14       0.0    5000/
HBr + C2H3 = C2H4 + Br                6.00E11      0.0   500
  REV/7.00E13       0.0    21050/
HBr + C2H = C2H2 + Br                 6.00E11      0.0   500
  REV/3.70E13       0.0    38050/
HBr + HCO = CH2O + Br                 2.84E11      0.0   244
  REV/1.02E13       0.0    1584/
HBr + H = H2 + Br                     6.25E13      0.0   2396
  REV/1.70E14       0.0    19090/
HBr + O = Br + OH                     2.40E12      0.0   2693
  REV/2.75E12       0.0    17320/
HBr + OH = H2O + Br                   2.09E12      0.0   0
  REV/1.97E13       0.0    31840/
HBr + HO2 = Br + H2O2                 6.89E11      0.0   3770
  REV/6.03E12       0.0    5940/
HBr + Br = Br2 + H                    2.72E14      0.0   43540
  REV/2.27E11       1.0    435/
Br + Br + M = Br2 + M                 7.48E13      0.0   -1695
  REV/1.15E14       0.0    42830/
Br + CH3 = CH3Br                      1.55E12      0.0   0
```

```
  REV/7.65E13       0.0   70307/
Br + C2H5 = C2H5 + Br                 2.40E11       0.0   0
  REV/6.55E12       0.0   67208/
Br + C2H3 = C2H3Br                    2.45E11       0.0   0
  REV/1.30E13       0.0   78804/
Br + C2H = C2HBr                      2.50E11       0.0   0
  REV/2.65E13       0.0   105173/
CH3Br + Br = Br2 + CH3                1.26E09       0.0   17700
  REV/1.00E13       0.0   1000/
CBrF3 = CF3 + Br                      2.00E13       0.0   64500
  REV/3.80E11       0.0   500/
CBrF3 + CH3 = CH3Br + CF3             5.75E12       0.0   5200
  REV/4.70E11       0.0   4260/
CBrF3 + H = CF3 + HBr                 2.20E14       0.0   9306
  REV/2.46E11       0.0   25720/
CBrF3 + Br = Br2 + CF3                9.37E09       0.0   26060
  REV/5.80E12       0.0   1000/
CHF3 + M = CF3 + H + M                3.26E15       0.0   107800
  REV/5.48E13       0.0   0/
CHF3 + CH3 = CF3 + CH4                5.97E15       0.0   13930
  REV/2.00E12       0.0   11000/
CHF3 + C2H5 = CF3 + C2H6              2.85E11       0.0   10980
  REV/8.70E11       0.0   8019/
CHF3 + C2H3 = CF3 + C2H4              7.32E10       0.0   2100
  REV/2.00E11       0.0   2600/
CHF3 + H = CF3 + H2                   5.00E12       0.0   5000
  REV/2.95E11       0.0   8600/
CHF3 + OH = CF3 + H2O                 6.76E06       1.8   4270
  REV/2.90E11       0.0   15770/
CHF3 + O = CF3 + OH                   5.00E12       0.0   10800
  REV/1.32E11       0.0   5300/
CHF3 + Br = CF3 + HBr                 2.00E13       0.0   23000
  REV/4.67E11       0.0   2660/
CF3 + O2 = COF2 + FO                  1.20E13       0.0   12500
  REV/7.85E12       0.0   27100/
CF3 + CH3 = C2H3F3                    6.76E13       0.0   0
  REV/3.90E17       0.0   91680/
C2H3F3 = C2H2F2 + HF                  3.60E13       0.0   70000
  REV/2.12E11       0.0   102450/
CF3 + OH = COF2 + HF                  3.98E12       0.0   0
  REV/4.90E13       0.0   115650/
CF3 + O = COF2 + F                    1.28E14       0.0   2000
  REV/5.00E14       0.0   83420/
COF2 + CH3 = C2H2F2 + OH              6.60E12       0.0   53950
  REV/2.00E12       0.0   1000/
COF2 + H = COF + HF                   7.72E10       0.0   2300
  REV/2.34E09       0.0   8500/
COF2 + OH = COF + HOF                 1.58E12       0.0   71380
  REV/6.20E10       0.0   1000/
COF2 + O = COF + FO                   3.00E13       0.0   77100
  REV/9.60E10       0.0   1000/
COF + M = F + CO + M                  2.10E16       0.0   33490
  REV/1.20E16       0.0   0/
COF + H = HF + CO                     2.00E14       0.0   0
  REV/3.63E14       0.0   105000/
COF + OH = CO + HOF                   1.00E14       0.0   0
  REV/4.67E14       0.0   19180/
```

```
COF + OH = CO2 + HF                     3.47E11      0.0   750
  REV/1.00E14      0.0   12800/
F2 + M = F + F                          2.12E13      0.0   33600
  REV/3.25E08      1.0   -6136/
F2 + H = HF + F                         8.80E13      0.0   2396
  REV/1.33E13      0.0   100300/
F2 + OH = HF + F + O                    7.00E13      0.0   18000
  REV/1.15E13      0.0   13690/
F2 + O = FO + F                         9.77E12      0.0   11290
  REV/2.43E12      0.0   25900/
F + CH4 = HF + CH3                      1.80E14      0.0   800
  REV/5.25E12      0.0   32880/
F + C2H6 = HF + C2H5                    6.03E13      0.0   280
  REV/1.30E10      0.0   37880/
F + C2H4 = HF + C2H3                    1.51E07      2.0   6000
  REV/3.60E05      2.0   31800/
F + H2 = HF + H                         2.70E12      0.5   631
  REV/1.65E12      0.6   32400/
F + H + M = HF + M                      9.55E17     -1.0   0
  REV/2.50E22     -2.0   134000/
F + H2O = HF + OH                       2.53E13      0.0   800
  REV/7.50E12      0.0   17300/
F + HO2 = HF + O2                       5.00E13      0.0   0
  REV/1.13E14      0.0   88700/
F + HBr = HF + Br                       3.30E13      0.0   1000
  REV/9.20E13      0.0   49340/
F + CHF3 = HF + CF3                     1.00E14      0.0   1000
  REV/4.47E11      0.0   29000/
FO + FO = F + F + O2                    1.26E13      0.0   0
  REV/3.30E11      0.0   14190/
END
```

Appendix B: Sample output with energy conservation.

PSR: Perfectly Stirred Reactor Code
CHEMKIN-II Version 1.1, March 1989
DOUBLE PRECISION

WORKING SPACE REQUIREMENTS

	PROVIDED	REQUIRED
LOGICAL	245	239
INTEGER	10000	8128
REAL	17500	17009
CHARACTER	200	170

CKLIB: Chemical Kinetics Library
CHEMKIN-II Version 1.9, October 1989
DOUBLE PRECISION

KEYWORD INPUT

```
ENRG
TINL  300
TEMP  1740
PRES  0.9989
TAU   0.006
VOL   250
QLOS  100
REAC  CH4     0.06816
REAC  O2      0.1956865
REAC  N2      0.7361535
REAC  CBrF3   0.00
XEST  N2      0.74
XEST  CO2     0.06
XEST  H2O     0.14
XEST  O2      0.06
PRNT 0
END
```

RESIDENCE TIME	6.00E-03	SEC
MASS FLOW RATE	8.09E+00	GM/SEC
PRESSURE	9.99E-01	ATM
MASS DENSITY	1.94E-04	GM/CM3
VOLUME	2.50E+02	CM3
TEMPERATURE (INLET)	**300.00**	**K**
TEMPERATURE	**1746.55**	**K**
HEAT LOSS	**1.00E+02**	**CAL/SEC**

INLET MOLE FRACTIONS

CH4	= 6.82E-02	CH3	= .00E+00	CH2	= .00E+00
CH	= .00E+00	H	= .00E+00	O	= .00E+00
N	= .00E+00	OH	= .00E+00	HO2	= .00E+00
H2O	= .00E+00	O2	= 1.96E-01	CH2OH	= .00E+00
CH3O	= .00E+00	CO2	= .00E+00	CO	= .00E+00
CH2O	= .00E+00	C2H2	= .00E+00	C3H2	= .00E+00
C2H3	= .00E+00	C2H4	= .00E+00	H2	= .00E+00
H2O2	= .00E+00	C	= .00E+00	C2H	= .00E+00
C2H6	= .00E+00	C2H5	= .00E+00	HCCO	= .00E+00
CH2CO	= .00E+00	HCCOH	= .00E+00	C4H2	= .00E+00
CH2(S)	= .00E+00	C3H3	= .00E+00	C4H3	= .00E+00
HCO	= .00E+00	H2CN	= .00E+00	HCN	= .00E+00
HCNO	= .00E+00	NO	= .00E+00	NO2	= .00E+00
HOCN	= .00E+00	HNCO	= .00E+00	NH2	= .00E+00
NH	= .00E+00	NCO	= .00E+00	C2N2	= .00E+00
N2O	= .00E+00	HNO	= .00E+00	NNH	= .00E+00
NH3	= .00E+00	N2	= 7.36E-01	CN	= .00E+00
HONO	= .00E+00	HNO3	= .00E+00	NO3	= .00E+00
C3H8	= .00E+00	C3H6	= .00E+00	N*C3H7	= .00E+00
I*C3H7	= .00E+00	Br	= .00E+00	Br2	= .00E+00
HBr	= .00E+00	CH3Br	= .00E+00	CBrF3	= .00E+00
CHF3	= .00E+00	CF3	= .00E+00	COF2	= .00E+00
COF	= .00E+00	F2	= .00E+00	F	= .00E+00
FO	= .00E+00	C4H4	= .00E+00	CH3OH	= .00E+00
C2H5Br	= .00E+00	C2H3Br	= .00E+00	C2HBr	= .00E+00
C2H3F3	= .00E+00	C2H2F2	= .00E+00	HF	= .00E+00
HOF	= .00E+00				

EXIT MOLE FRACTIONS

CH4	= 5.88E-05	CH3	= 1.21E-05	CH2	= 3.69E-07
CH	= 5.73E-09	H	= 4.82E-04	O	= 1.09E-03
N	= 3.68E-10	OH	= 3.34E-03	HO2	= 1.66E-05
H2O	= 1.33E-01	O2	= 6.03E-02	CH2OH	= 4.74E-07
CH3O	= 4.36E-08	CO2	= 6.44E-02	CO	= 3.41E-03
CH2O	= 1.26E-05	C2H2	= 4.12E-09	C3H2	= 8.97E-15
C2H3	= 5.66E-10	C2H4	= 1.97E-08	H2	= 1.16E-03
H2O2	= 1.33E-06	C	= 3.02E-10	C2H	= 3.87E-12
C2H6	= 4.30E-09	C2H5	= 1.97E-11	HCCO	= 5.40E-10
CH2CO	= 2.14E-09	HCCOH	= 1.56E-10	C4H2	= 1.78E-17
CH2(S)	= 1.10E-08	C3H3	= 4.57E-14	C4H3	= 1.52E-19
HCO	= 4.00E-07	H2CN	= 5.51E-13	HCN	= 1.13E-08
HCNO	= 2.76E-09	NO	= 8.93E-06	NO2	= 3.43E-09
HOCN	= 3.16E-10	HNCO	= 5.24E-10	NH2	= 4.29E-11
NH	= 2.34E-10	NCO	= 3.84E-10	C2N2	= 1.99E-16
N2O	= 4.72E-07	HNO	= 9.77E-10	NNH	= 3.02E-11
NH3	= 3.54E-11	N2	= 7.33E-01	CN	= 3.06E-11
HONO	= 8.39E-10	HNO3	= 9.71E-14	NO3	= 1.41E-16
C3H8	= 8.25E-15	C3H6	= 3.61E-13	N*C3H7	= 9.54E-18
I*C3H7	= 4.66E-18	Br	= .00E+00	Br2	= .00E+00
HBr	= .00E+00	CH3Br	= .00E+00	CBrF3	= .00E+00
CHF3	= .00E+00	CF3	= .00E+00	COF2	= .00E+00
COF	= .00E+00	F2	= .00E+00	F	= .00E+00
FO	= .00E+00	C4H4	= .00E+00	CH3OH	= .00E+00
C2H5Br	= .00E+00	C2H3Br	= .00E+00	C2HBr	= .00E+00
C2H3F3	= .00E+00	C2H2F2	= .00E+00	HF	= .00E+00
HOF	= .00E+00				

Appendix C: Sample output without the energy equation.

```
PSR:  Perfectly Stirred Reactor Code
      CHEMKIN-II Version 1.1, March 1989
      DOUBLE PRECISION

               WORKING SPACE REQUIREMENTS

                 PROVIDED        REQUIRED
LOGICAL               245             239
INTEGER             10000            8128
REAL                17500           17009
CHARACTER             200             170


CKLIB:  Chemical Kinetics Library
        CHEMKIN-II Version 1.9, October 1989
        DOUBLE PRECISION

          KEYWORD INPUT

          TGIV
          TEMP  2020.2
          PRES  0.9986
          TAU   0.00001
          VOL   250
          REAC   CH4       0.0669131
          REAC   O2        0.1921061
          REAC   N2        0.722685
          REAC   CBrF3     0.0182958
          AROP
          PRNT 0
          END
  STANJAN:  Version 3.8C, May 1988
            W. C. Reynolds, Stanford Univ.

        EQINIT: WORKING SPACE REQUIREMENTS
                  PROVIDED        REQUIRED
INTEGER             1690            1690
REAL                2154            2154


FIRST SOLUTION ESTIMATE IS EQUILIBRIUM

               RESIDENCE TIME                1.00E-05  SEC
               MASS FLOW RATE                4.30E+03  GM/SEC
               PRESSURE                      9.99E-01  ATM
               MASS DENSITY                  1.72E-04  GM/CM3
               VOLUME                        2.50E+02  CM3
               TEMPERATURE (FIXED)            2020.20  K
```

INLET MOLE FRACTIONS

CH4	6.69E-02	CH3	.00E+00	CH2	.00E+00
CH	.00E+00	H	.00E+00	O	.00E+00
N	.00E+00	OH	.00E+00	HO2	.00E+00
H2O	.00E+00	O2	1.92E-01	CH2OH	.00E+00
CH3O	.00E+00	CO2	.00E+00	CO	.00E+00
CH2O	.00E+00	C2H2	.00E+00	C3H2	.00E+00
C2H3	.00E+00	C2H4	.00E+00	H2	.00E+00
H2O2	.00E+00	C	.00E+00	C2H	.00E+00
C2H6	.00E+00	C2H5	.00E+00	HCCO	.00E+00
CH2CO	.00E+00	HCCOH	.00E+00	C4H2	.00E+00
CH2(S)	.00E+00	C3H3	.00E+00	C4H3	.00E+00
HCO	.00E+00	H2CN	.00E+00	HCN	.00E+00
HCNO	.00E+00	NO	.00E+00	NO2	.00E+00
HOCN	.00E+00	HNCO	.00E+00	NH2	.00E+00
NH	.00E+00	NCO	.00E+00	C2N2	.00E+00
N2O	.00E+00	HNO	.00E+00	NNH	.00E+00
NH3	.00E+00	N2	7.23E-01	CN	.00E+00
HONO	.00E+00	HNO3	.00E+00	NO3	.00E+00
C3H8	.00E+00	C3H6	.00E+00	N*C3H7	.00E+00
I*C3H7	.00E+00	Br	.00E+00	Br2	.00E+00
HBr	.00E+00	CH3Br	.00E+00	CBrF3	1.83E-02
CHF3	.00E+00	CF3	.00E+00	COF2	.00E+00
COF	.00E+00	F2	.00E+00	F	.00E+00
FO	.00E+00	C4H4	.00E+00	CH3OH	.00E+00
C2H5Br	.00E+00	C2H3Br	.00E+00	C2HBr	.00E+00
C2H3F3	.00E+00	C2H2F2	.00E+00	HF	.00E+00
HOF	.00E+00				

EXIT MOLE FRACTIONS

CH4	7.56E-03	CH3	4.67E-03	CH2	1.39E-04
CH	2.00E-06	H	3.05E-03	O	1.11E-03
N	2.96E-08	OH	2.84E-03	HO2	2.37E-04
H2O	6.01E-02	O2	1.16E-01	CH2OH	8.54E-05
CH3O	6.75E-05	CO2	4.74E-03	CO	4.17E-02
CH2O	1.69E-03	C2H2	2.46E-04	C3H2	1.13E-07
C2H3	2.51E-05	C2H4	5.99E-04	H2	2.62E-02
H2O2	4.93E-07	C	3.30E-07	C2H	4.08E-07
C2H6	6.24E-05	C2H5	4.49E-07	HCCO	1.43E-05
CH2CO	2.37E-05	HCCOH	1.93E-06	C4H2	6.55E-08
CH2(S)	8.88E-06	C3H3	1.45E-06	C4H3	2.42E-10
HCO	1.15E-04	H2CN	3.29E-09	HCN	8.27E-07
HCNO	1.17E-08	NO	9.08E-07	NO2	6.34E-10
HOCN	4.55E-09	HNCO	1.26E-08	NH2	3.65E-09
NH	9.58E-09	NCO	1.74E-08	C2N2	1.70E-13
N2O	4.15E-07	HNO	2.83E-09	NNH	5.11E-10
NH3	3.34E-09	N2	6.83E-01	CN	2.95E-09
HONO	1.15E-11	HNO3	2.36E-15	NO3	-2.89E-18
C3H8	5.12E-09	C3H6	1.14E-06	N*C3H7	4.59E-11
I*C3H7	1.25E-11	Br	1.04E-02	Br2	2.02E-06
HBr	6.01E-03	CH3Br	2.42E-04	CBrF3	6.65E-04
CHF3	3.49E-03	CF3	8.95E-04	COF2	1.18E-02
COF	2.81E-07	F2	5.46E-10	F	2.14E-05
FO	1.19E-03	C4H4	.00E+00	CH3OH	.00E+00
C2H5Br	5.44E-11	C2H3Br	4.45E-06	C2HBr	6.36E-08
C2H3F3	3.42E-04	C2H2F2	9.31E-20	HF	1.09E-02
HOF	4.33E-07				

Appendix D: AIAA Paper 97-0907.

AIAA 97-0907

Probe Design Optimization for the Well Stirred Reactor

J. W. Blust, M. G. Getz,
and S. Zabarnick
University of Dayton
Dayton, OH

35th Aerospace Sciences Meeting & Exhibit
January 6-9, 1997/Reno NV

PROBE DESIGN OPTIMIZATION FOR THE WELL STIRRED REACTOR

J. W. Blust*, M. G. Getz and S. Zabarnick
University of Dayton, Dayton, OH

Abstract

To correctly analyze emissions from a combustion experiment, efforts must be made to guarantee that the sample gas composition is not altered as it is extracted from the process. A sampling probe must terminate reactions as it draws the sample gas to the emissions analyzers. It is on this basis that a probe was designed for the analysis of the combustion of methane in air in a toroidal well stirred reactor (WSR). The WSR provides a laboratory idealization of an efficient, highly compact primary zone of a gas turbine combustor. During previous experiments, it was undetermined if this probe terminated reactions of CO and UHC species. With the use of the PSR code using the CHEMKIN-II formalism, a simulation of four probe designs was conducted to determine the optimum probe for quenching CO and UHC reactions. The probes were simulated as a series of PSR volume elements with temperature defined by a temperature profile measured with a 0.508 mm O.D. type K thermocouple. A water-cooled small-bore stainless steel probe was proven to be the most efficient quenching probe. Experimental data was collected illustrating a recovery of 99 percent of the CO and 43 percent of the THC that was simulated as the WSR products. The probe also proved to be robust and compatible with the analyzers with the aid of a sampling pump. Future work with the WSR will be conducted using this small-bore design.

Nomenclature

atm = pressure in atmospheres
CO = carbon monoxide
I.D. = inside diameter
LP = loading parameter (gm/sec-L-atm)
M = Mach number
N.D. = nominal diameter
NO_X = oxides of nitrogen
O.D. = outside diameter
PFR = plug flow reactor
ppmC = parts per million carbon
ppmV = parts per million by volume
PSR = perfectly stirred reactor
slpm = standard liters per minute
t = time
T = temperature
THC = total hydrocarbons
UHC = unburned hydrocarbons
WSR = well stirred reactor
ϕ = equivalence ratio
τ = residence time

Subscripts

eb = eddy breakup
f = flame
tm = turbulent mixing

1. Introduction

Experiments which require the analysis of emissions data, particularly combustion experiments, often rely on the use of a probe to withdraw a gas sample from the process. Gas samples are typically pumped to an infrared spectrometer, flame ionization detector, paramagnetic analyzer, or a chemiluminescent analyzer to provide near real-time analysis of the emissions composition. This data can inform experimenters whether an aircraft engine meets emissions standards or provide insight to the fundamental combustion process.

Often, however, a probe may fail to terminate the chemical reactions associated with the combustion process in the sample. The data is no longer indicative of the combustion emissions. This "probe effect," if unchecked, may lead to an incorrect analysis of the chemical process in a flame, or the misevaluation of an engine's performance on the test stand. Thus, the design of a sampling probe is fundamental to any emissions test.

The use of a probe is often associated with emissions testing from both a model gas turbine combustor or a combustion kinetics experiment with large flame volume. In such tests, the combustion process is uniform over a relatively large volume, and the small-scale spatial resolution of the emissions is not essential. Therefore, a probe drawing a large volume of sample gas as compared to the typical laser diagnostic technique is justified. Many large flame volume combustion experiments have been performed with numerous probe designs (Brezinski et al[1], Dagaut et al.[2], Horning et al.[3], Lam et al.[4], Prado et al.[5], Thornton et al.[6], Zelina and Ballal[7]). Additionally, model gas turbine combustor tests with various probe designs have been performed (Drennan et al.[8], Shouse et al.[9]). The

---

* Ph.D. Student, Member AIAA.

toroidal well stirred reactor (WSR) (Zelina and Ballal[10], Nenniger et al.[11]) represents both a model gas turbine combustor and typical combustion kinetics experiment with large flame volume, and provides a laboratory idealization of an efficient, highly compact primary zone of a gas turbine combustor to facilitate the study of combustion and emissions. For this reason, the WSR was selected for the study of probe design.

2. Motivation

Previous emissions studies were made with a variety of fuels and test conditions in the WSR using an air-cooled quartz probe. This probe was constructed of three concentric tubes with an I.D. of 0.267 cm for the sample gas flow. The outer two tubes provided a passageway for cooling air. This design is illustrated in Fig. 1. Quartz was chosen because of the concern for high temperature catalytic reactions occurring on the surface of a metal probe. During these experiments, concentrations of O_2, CO_2, NO_X, CO and UHC were measured. The flow rate of the cooling air was 50 slpm.

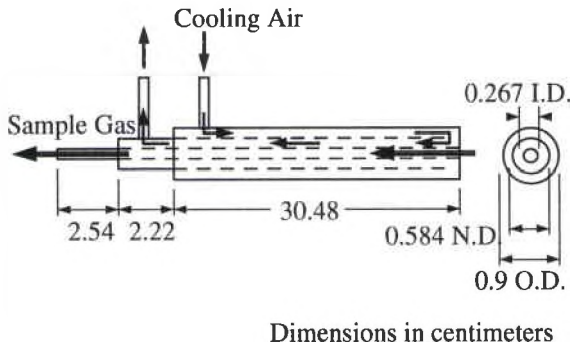

Fig. 1: Design of quartz probe.

Zabarnick and Zelina[12] previously compared WSR measured emissions from methane-air combustion to predicted values calculated by the PSR code (Glarborg et al.[13,14]) using the CHEMKIN-II kinetics formalism. PSR and WSR results were comparable for the concentration profiles of O_2 and CO_2 varying with ϕ, and also for temperature vs. ϕ data. This indicated that the probe had no effect on these profiles. However, no comparison was drawn for the concentration profiles of CO and UHC. It was unknown whether a probe effect was occurring with these species.

Subsequently, Zelina[15] compared WSR measured CO data to the calculated data of the 28-Step Allied-Signal Engines PSR code and the equilibrium compositions from the Gordon-McBride code[16] in addition to the PSR code using CHEMKIN-II. This comparison was made for a setting of $\tau = 6$ ms and varying ϕ. These results are shown in Fig. 2. Not surprisingly, for $\phi < 0.8$, the measured CO values are much higher than equilibrium because a short residence time does not provide sufficient time to complete oxidation of CO. However, for $\phi \geq 0.8$, the measured CO concentration closely resembles equilibrium data despite the non-equilibrium conditions of the WSR. This indicates that the probe was providing a long enough residence time to allow the species to reach an equilibrium state. Further, the measured CO is not even the same order of magnitude as the predicted values from PSR/CHEMKIN-II and AE PSR, whereas both models agree closely. (100 cal/sec heat loss was utilized by the models because this loss was previously shown to give closest agreement of reactor temperature to model temperature at a given ϕ. This corresponds to a 3-5 percent heat loss from the reactor.) Thus, it was proven necessary to design a probe that provided better quenching, reducing the amount of probe effect on CO.

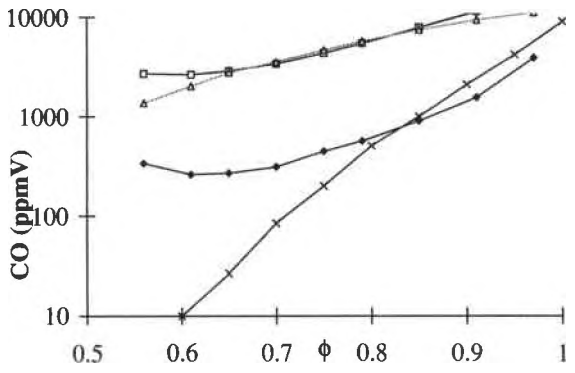

Fig. 2: Measured CO versus equivalence ratio for methane using quartz probe (diamond). Simulated CO versus equivalence ratio using PSR/CHEMKIN-II (square) and AE PSR (triangle). Residence time is 6 ms. Also shown are equilibrium values for methane (X).

3. Experimental Setup

1. WSR Test Facility

The 250-ml toroidal WSR test facility and instrumentation is shown in Fig. 3. The Horiba Emissions Analyzers were comprised of the following units: model MPA-510 oxygen analyzer (0 to 50 percent), model FIA-510 total hydrocarbon analyzer (0 to 10,000 ppm carbon), model VIA-510 CO (0 to 20 percent) and CO_2 (0 to 100 percent) analyzer, and model CLA-510 SS NO and NO_X analyzer (0 to 2000 ppmV). These units were calibrated with gases of the following concentrations: THC = 404 ppmV propane, NO = 92.0 ppmV, NO_2 = 1.6 ppmV, CO = 0.4 percent, O_2 = 4.03 percent and CO_2 = 11.06 percent. Emissions readings were delivered on dry basis. The units required a total of 2 slpm gas sample, with a pressure within $\pm$10 cm of water of ambient. A gas sample was drawn from the WSR by a probe design and pumped into

each unit through a heated sampling line to be analyzed for the various product species. To measure combustion temperature, T_f, a type B thermocouple (platinum-6% rhodium, platinum-30% rhodium) coated with an alumina ceramic glue was used. This coating served two purposes: (i) it reduced catalytic activity on the thermocouple surface, and (ii) it protected the thermocouple from its environment, because platinum-rhodium alloys are subject to high-temperature contamination that can embrittle the alloy. Temperature measurements were corrected for radiation heat loss.

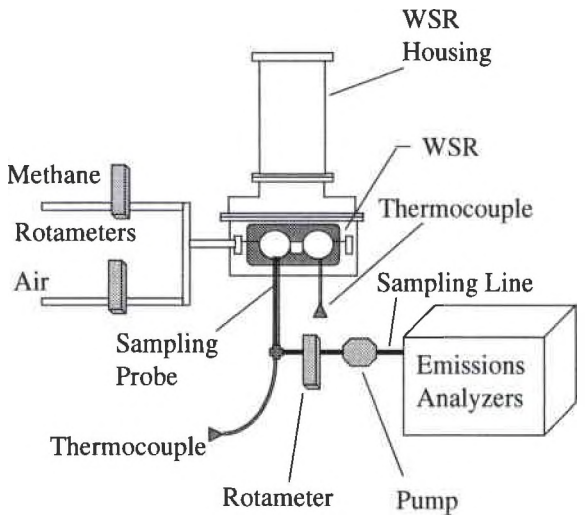

Fig. 3: WSR test facility and associated instrumentation.

The WSR test facility was operated at atmospheric pressure. Air and methane flow rates to the WSR were measured via rotameters. In this facility, the air rotameter was rated at 0 to 493 slpm and fuel rotameter at 0 to 57 slpm range. Gas sample temperature within a probe was measured using a 0.508 mm O.D. type K thermocouple connected to an Omega HH82 handheld digital thermometer. Sample flow rate was measured using a rotameter rated 0 to 25 slpm. An additional single speed corrosion resistant pump rated 12 slpm was connected to the sampling line for some experiments.

The reactor was typically operated over a range of equivalence ratios $0.56 < \phi < 0.97$, residence times $\tau = 6$ or 7 ms, loading parameter LP ~ 1 gm/sec-L-atm, and reactor temperatures $T_f = 1559$ to 2043 K. Hot mixture velocity in the torus was calculated to be 58 m/s, with calculated turbulent mixing time $t_{tm} = 0.0196$ ms, and eddy breakup time $t_{eb} = 1.01$ ms when the reactor residence time $\tau = 6$ ms at $T_f = 1834$ K, and methane was burning in air at $\phi = 0.7$. These represent typical operating conditions.

2. Error Analysis

Methane flow was monitored to within 4 percent using a Gilmont rotameter. Air flow was monitored to within 5.5 percent using a Brooks rotameter. The combined error produced an uncertainty of 7 percent in ϕ. The T_f measurements, after correcting for heat loss, were accurate to within 50 K. The thermocouple inserted into the probe was accurate to within 3 K after correction for heat loss. The Horiba emissions analyzers quote an accuracy to within 1 percent of full scale. For these WSR experiments, this represented an error of: 2 ppmV NO_X, 50 ppmV CO, 10 ppmV carbon for THC, 0.25 percent O_2, and 0.5 percent CO_2.

3. PSR Code

The PSR code of Glarborg et al. incorporates the CHEMKIN-II formalism to predict steady-state temperature and species composition. The PSR theory assumes that the reactor temperature and species concentrations are spatially uniform, and that mixing occurs infinitely fast. Other key assumptions in the PSR code include: (i) non-catalytic reactor walls; (ii) a reactor flow characterized by a nominal residence time; and (iii) a constant reactor heat loss controlled by the user. For this work, the PSR output was used as a simulation of methane in air combustion for both the WSR and the probe designs.

4. Probe Design Principles

Ultimately, for a probe to be successfully implemented in an emissions test, it must meet three criteria:

1. The probe must be robust enough for repeat use.
2. The probe must be compatible with the emissions analyzers.
3. The probe must successfully quench the gas sample to terminate chemical reactions.

These criteria are discussed below:

1. Robustness

A literature search (see Introduction) suggested that most probes in current use feature three concentric tubes, the outer two of which provide a passageway for a cooling fluid, while the innermost carries the sample gas. Operation with an air-cooled quartz probe showed no weakness in this basic design.

However, quartz is fragile and requires careful considerations in its installation. Also, devitrification[17], or recrystallization of the probe due to high combustion temperatures, was observed to occur at the probe tip where the three concentric tubes were fused. This led to

weakening and rupture of the tip following several hours of operation. For this reason, numerous quartz probes must be constructed at a time, and treated as expendable items. Due to these inherent difficulties, the quartz probe did not pass criterion (1.).

2. Compatibility with Analyzers

The Horiba analyzers required that sample gas be delivered to the pumping units within ±10 cm of water in pressure (±0.00966 atm) from ambient. Failure to work within this pressure limitation caused erroneous emissions readings. This sensitivity to vacuum is common among real-time instrumentation. This condition limited the allowable pressure drop in the sample line, thereby limiting the inner diameter of the probe or causing the need for a pump to overcome a large probe pressure drop. Thus, this is not so much a criterion placed on the probe itself as it is on the entire sampling system.

3. Quenching

Since the quartz probe was shown to fail in quenching CO reactions (Fig. 2), it was of interest to prevent the continued oxidation of CO in the probe during lean methane-air combustion. In lean, premixed combustion CO is consumed in the following reaction steps at high temperatures (>500 K)[18]:

$$CO + O_2 \rightarrow CO_2 + O \quad (1)$$

$$O + H_2O \rightarrow 2\,OH \quad (2)$$

$$CO + OH \rightarrow CO_2 + H \quad (3)$$

$$H + O_2 \rightarrow OH + O \quad (4)$$

To prevent CO consumption it becomes necessary to reduce the time the gas sample remains hot. This can be accomplished by the combination of rapid removal of heat from the gas sample, and minimizing time the sample spends in the hottest section of the probe. Thus, a high overall heat transfer between the hot sample and probe cooling fluid and a high probe gas velocity are required for excellent quenching of the sample.

Additionally, the concentration of UHC is proportional to CO[19]. Any method utilized to prevent CO oxidation will also reduce UHC oxidation.

5. Results and Discussion

For quenching of the CO reaction in the probe to be successful, it was essential that: (i) emissions data acquired from the WSR for given combustion conditions be as close as possible to the values determined by the reactor simulation created using PSR/CHEMKIN-II; and (ii) that if a discrepancy existed, a PSR/CHEMKIN-II probe simulation be able to account for the difference between WSR and reactor simulation.

Four probe designs, including the quartz probe, were constructed for use in the WSR to test quenching. The three additional probes are illustrated in Fig. 4 and are described below:

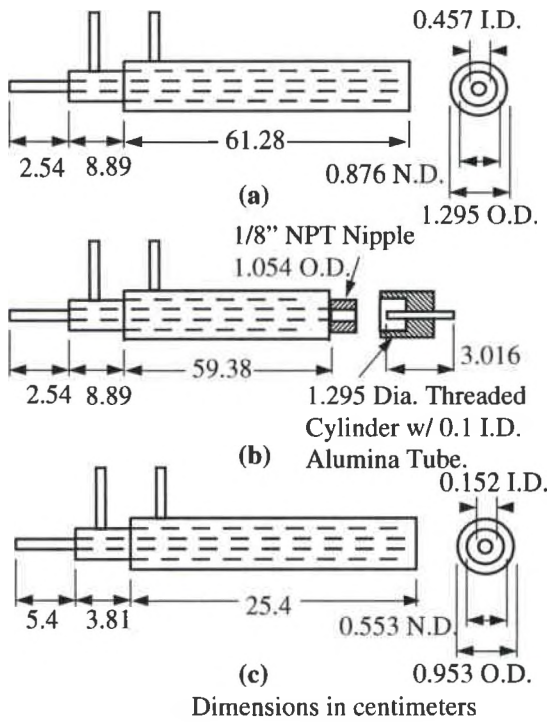

Fig. 4: Stainless steel probe designs.

(a) Stainless Steel Probe: This probe was constructed of three concentric tubes, with I.D. of the sample tube 0.457 cm, and O.D. 1.295 cm. The three tubes were welded at the tip to create a passageway for cooling fluid. Heated water (70 C) demineralized by reverse osmosis was used as cooling fluid, with typical flow rate 0.2 lpm. This probe was designed to rapidly remove heat from the sample through conductive metal walls.

(b) Stainless Steel Probe with Alumina Tip: This probe was constructed similarly to the previous model, except that an 1/8" NPT nipple was welded to the tip. A replaceable 1.295 cm outside diameter stainless steel cylinder was screwed onto the nipple. A 1 mm I.D., 3.02 cm long alumina tube was glued along the axis of the cylinder to serve as the sample gas pathway. Approximately 0.5 cm of the tube protruded from the cylinder. The probe was cooled by the heated, demineralized water. However, the alumina tip received no cooling. This probe was designed to provide high sample velocity, and hence short residence time, at the tip where temperature was highest. This was accomplished in the narrow bore of the alumina tube.

(c) Small-Bore Stainless Steel Probe: This probe was essentially a miniature of the first stainless steel probe, with I.D. of the sample tube 0.152 cm, and O.D. 0.953 cm. It was similarly cooled by heated, demineralized water. This probe was designed to rapidly remove heat through the walls, as in the first probe, and have high sample velocity to minimize sample residence time, as in the second probe.

For each probe design, a temperature profile was measured during methane combustion at $\phi = 0.6$ using a 0.508 mm O.D. type K thermocouple. The thermocouple was inserted into the sample gas flow so that the tip of the thermocouple was located along the centerline of the tube at all times. This ensured a temperature measurement of the sample gas rather than the temperature of the walls of the probe. The thermocouple was advanced to the tip of the probe through a 1/4-inch tube tee, sealed with a septum and nut, and the perpendicular port was used for drawing the sample gas. The length of the thermocouple wire external to the tube tee was recorded to determine the position of the thermocouple down the probe. It was extracted down the probe until the temperature readings approached a single reading, and a temperature profile of the probe was created. The flow rate of the sample gas was recorded via rotameter for each temperature profile. These temperature profiles are depicted in Fig. 5(a) as a function of the distance down the probe and in Fig. 5(b) versus cumulative residence time in the probe.

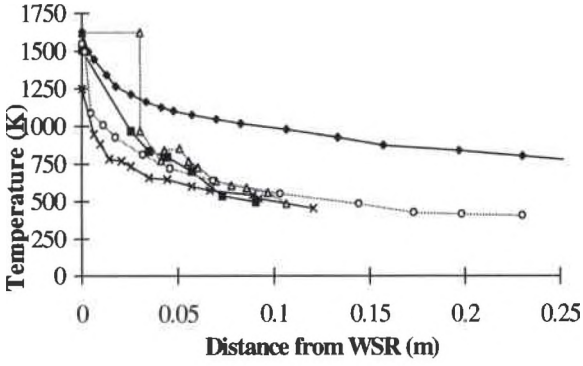

(a)

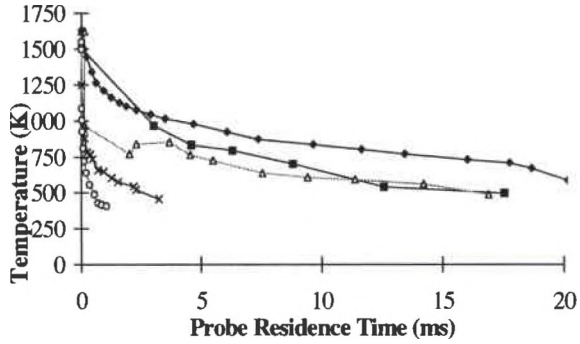

(b)

Fig. 5: (a) Temperature profile in probe versus distance from WSR. (b) Temperature profile in probe versus cumulative probe residence time for stainless steel probe (square), stainless steel probe with alumina tip (triangle), small-bore stainless steel probe (X), quartz probe (diamond), and small-bore stainless steel probe with pump (circle).

The temperature profiles facilitated creation of a PSR simulation of the probes. In particular, probes were modeled as a series of small PSRs in series, each element of which was characterized by a temperature and volume, while the mass flow rate through each PSR remained constant. This tanks-in-series simulation, illustrated in Fig. 6, was believed to be an accurate model of the probe. The probe would be best approximated as a plug flow reactor (PFR) with varying temperature, since the sample flow in general was turbulent, and turbulent flow approaches the PFR residence time distribution. However, a long series of PSRs approaches the PFR residence time distribution. Further, incrementing this simulation with a series of PSRs at varying temperature is computationally simple.

For each pair of temperature readings, average temperature and reactor volume for each PSR was defined. The PSR-simulated products of the WSR were

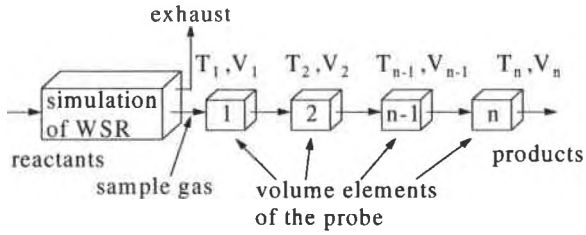

Fig. 6: PSR tanks-in-series simulation of a probe design.

used as inputs for the first probe PSR. The products from this PSR were then used as the inputs for the next element, and this was continued until emissions concentrations within an element were unchanged. The output of the final PSR was then the simulated analyzer readings corresponding to the given WSR conditions using the simulated probe design. The modeled profiles of CO versus distance down the probe and cumulative residence time are depicted in Figs. 7 (a) and (b), respectively. Similarly, modeled profiles of THC versus distance down the probe and cumulative residence time are shown in Figs. 8 (a) and (b). The THC concentration includes species such as methane, ethane, and the C-H-O compounds exceeding the 0.1 ppm threshold.

The results of these simulations were informative. The simulations showed that three probe designs were incapable of allowing the analyzers to read concentrations indicative of the WSR products. The small-bore stainless steel probe proved to be the only capable design (Table 1); this probe was capable of retaining approximately 99 percent of the CO concentration simulated to be the WSR product concentration. The next best quenching occurred in the quartz probe with nearly 66 percent recovery, followed by the stainless steel probe with the alumina tip at 41 percent, and then the worst being the 24 percent recovery using the stainless steel probe. The THC recovery was also the greatest for the small-bore stainless steel probe. These results indicate that an

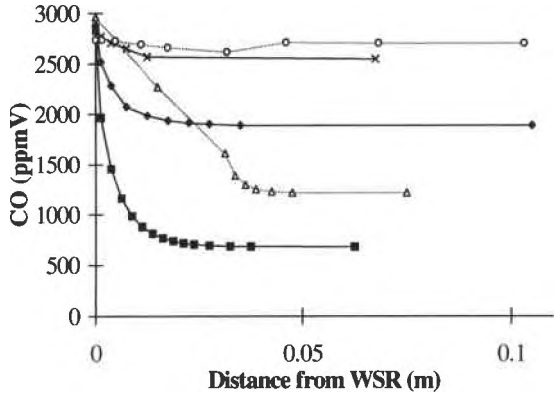

(a)

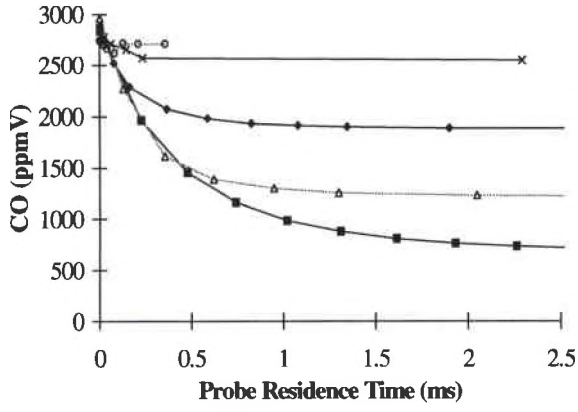

(b)

Fig. 7: (a) Simulated CO versus distance from WSR. (b) Simulated CO versus cumulative probe residence time for stainless steel probe (square), stainless steel probe with alumina tip (triangle), small-bore stainless steel probe (X), quartz probe (diamond), and small-bore stainless steel probe with pump (circle).

Table 1: CO and THC Recovery for Each Probe Design

Probe	$[CO]_{out}$ (ppmV)	$[CO]_{in}$ (ppmV)	Recovery (Percent)	$[THC]_{out}$ (ppmC)	$[THC]_{in}$ (ppmC)	Recovery (Percent)
Stainless steel	683	2836	24	0	126	0
Stainless steel w/ alumina tip	1218	2961	41	0.2	131	0.2
Quartz	1889	2880	66	3.1	138	2.2
Small-bore stainless steel	2548	2863	89	64	131	49
Small-bore stainless steel w/ pump	2706	2738	99	48	112	43

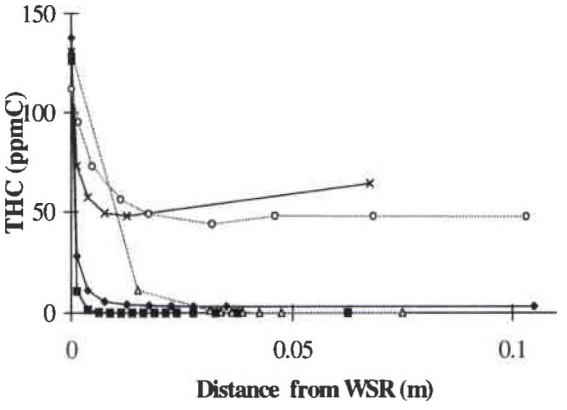

(a)

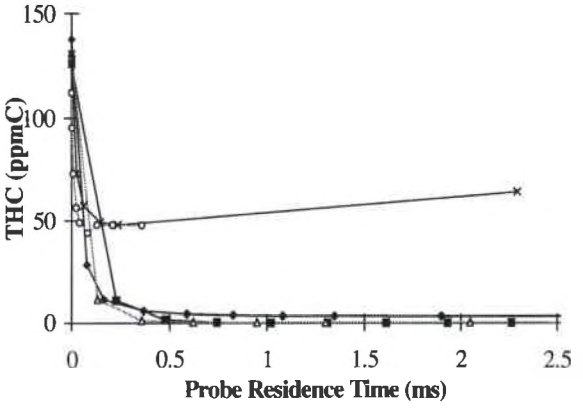

(b)

Fig. 8: (a) Simulated THC versus distance from WSR. (b) Simulated THC versus cumulative probe residence time for (square) stainless steel probe, (triangle) stainless steel probe with alumina tip, (X) small-bore stainless steel probe, (diamond) quartz probe, and (circle) small-bore stainless steel probe with pump.

optimal probe should have short probe residence time with effective temperature reduction. Both of these characteristics are illustrated for the small-bore stainless steel probe in Figs. 5 (a) and (b).

Directed by the results of the probe simulations, the small-bore stainless steel probe was implemented to collect data. Initially, the probe caused the sampling system to be incompatible with the Horiba analyzers. Pressure in the sample line was too low (-0.029 atm from ambient) and the analyzers did not respond to changes in the WSR combustion conditions.

As suggested in the probe design principles, the small diameter of the probe was causing too large of a pressure drop, so a pump was used to return the sample gas pressure to near ambient. Once this was done, the analyzers responded to the changing conditions, and data was collected over a range of ϕ with $\tau = 6$ ms. This data closely resembled the modeled data from both the AE PSR and the CHEMKIN-II PSR codes, as shown in Fig. 9. The order of magnitude of the CO concentrations are all the same, therefore the logarithmic scale is no longer necessary for comparison. The experiment succeeded in producing data that best represented the true WSR product concentration of CO.

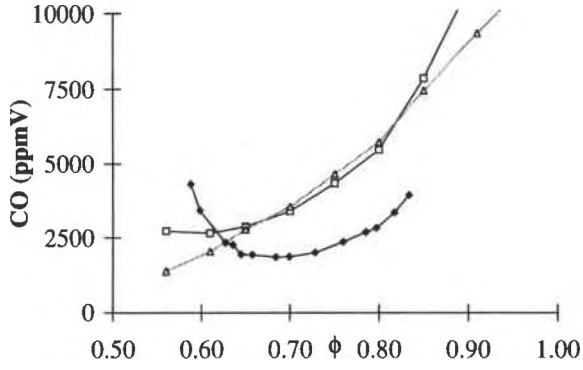

Fig. 9: Measured CO versus equivalence ratio for methane using small-bore stainless steel probe with pump (diamond). Simulated CO versus equivalence ratio using PSR/CHEMKIN-II (square) and AE PSR (triangle). Residence time is 6 ms.

6. Summary and Conclusions

A study of the probe effect on CO and UHC in four probe designs was completed. It was shown that

the small-bore stainless steel probe provided excellent quenching of CO and UHC reactions when connected in series with a pump. Using a pump permitted this probe to be compatible with the analyzers. Further, because this probe was constructed of stainless steel, it was more robust than similar designs using quartz.

A few points need to be addressed concerning the above analysis:

1. Mach number (M) through the small-bore stainless steel probe was estimated using the measured mass flow rate and temperature profile. At the entrance, M = 0.78, which implies that the sample gas was compressible. Thus, gas density, velocity and residence time in each modeled PSR were not exact. Error in the residence time in the highest temperature region was estimated to be 33 percent. Compressibility was ignored because of difficulty in accurately determining the actual velocity in the probe.

2. Emissions of UHC are difficult to measure because UHC concentrations from methane drop off an order of magnitude between ϕ = 0.58 and 0.62. Thus, modeling UHC to within 50 percent is fortunate.

3. The effects of surface catalysis of CO reactions with the metal probe have not been investigated. Certainly, this effect is minor compared to the effect of poor quenching. Gouldin and Tacke[20] claimed that catalytic effects did not appear to be important in temperature measurement using a platinum, platinum-10% rhodium thermocouple in several burner types. If no catalysis effect on temperature were detected, perhaps catalysis effect on CO reactions is similarly negligible.

To investigate this possibility, two small-bore stainless steel probes will be constructed, and one will be passivated with phosphoric acid while the other will be untreated. Differences between emissions from each probe will be monitored.

4. Additionally, the effect of the equivalence ratio upon the performance of the probe will be determined. All the current temperature profiles and PSR probe simulations were run for methane in air at an equivalence ratio of 0.6.

7. Acknowledgment

This work is supported by the Air Force Wright Laboratory, Aeropropulsion and Power Directorate, Wright Patterson Air Force Base, OH, under contract F33615-92-C-2207, with Mr. Charles W. Frayne serving as technical monitor. The authors are grateful to Mr. Rich Striebich for providing assistance with the Horiba analyzers, and Dr. Joseph Zelina at Allied-Signal Engines for his simulation of probe effect using the Allied-Signal Engines PSR code.

8. References

1. Brezinsky, K., Litzinger, T. A., and Glassman, I., "The High Temperature Oxidation of the Methyl Side Chain of Toluene," *International Journal of Chemical Kinetics*, Vol. 16, pp. 1053-1074, 1984.

2. Dagaut, P., Reuillon, M., and Cathonnet, M., "Experimental Study of the Oxidation of *n*-Heptane in a Jet Stirred Reactor from Low to High Temperature and Pressures up to 40 Atm," *Combustion and Flame*, Vol. 101, pp. 132-140, 1995.

3. Horning, D. C., Steele, R. C., and Malte, P. C., "Formation of NO_X and N_2O in a Lean-Premixed, High-Pressure, Jet-Stirred Reactor," 95F-210, Western States Section, The Combustion Institute, 1995.

4. Lam, F. W., Howard, J. B., and Longwell, J. P., "The Behavior of Polycyclic Aromatic Hydrocarbons During the Early Stages of Soot Formation," *Twenty-Second Symposium (International) on Combustion*, pp. 323-332, The Combustion Institute, Pittsburgh, 1988.

5. Prado, G. P., Lee, M. L., Hites, R. A., Hoult, D. P., and Howard, J. B., "Soot and Hydrocarbon Formation in a Turbulent Diffusion Flame," *Sixteenth Symposium (International) on Combustion*, pp. 649-661, The Combustion Institute, Pittsburgh, 1976.

6. Thornton, M. M., Malte, P. C., and Crittenden, A. L., "A Well-Stirred Reactor Study of Pyrolysis and Oxidation Kinetics: Carbon Monoxide and *n*-Pentane Oxidation," *Combustion Science and Technology*, Vol. 54, pp. 275-297, 1987.

7. Zelina, J., and Ballal, D. R., "Combustion and Emissions Studies Using a Well Stirred Reactor," AIAA Paper No. 94-2903, 1994.

8. Drennan, S. A., Peterson, C. O., Khatib, F. M., Sowa, W. A., and Samuelsen, G. S., "Pollutant Emissions from and within a Model Gas Turbine Combustor at Elevated Pressures and Temperatures," AGARD Paper No. CP-536, 1993.

9. Shouse, D. T., Frayne, C., Stutrud, J., Gogineni, S., and Sturgess, G. J., "The Role of Transverse Air Jets in the Formation of Gas

Turbine Emissions," AIAA Paper No. 96-0705, 1996.

10. Zelina, J., and Ballal, D. R., "Combustion Studies in a Well-Stirred Reactor," AIAA Paper No. 94-0114, 1994.

11. Nenniger, J. E., Kridiotis, A., Chomiak, J., Longwell, J. P., and Sarofim, A. F., "Characterization of a Toroidal Well Stirred Reactor," *Twentieth Symposium (International) on Combustion*, pp. 473-479, The Combustion Institute, Pittsburgh, 1984.

12. Zabarnick, S. and Zelina, J., "Chemical Kinetics of NO_X Production in a Well Stirred Reactor," AIAA Paper No. 94-3828-CP, 1994.

13. Glarborg, P., Kee, R. J., Grcar, J. F., and Miller, J. A., "PSR: A Fortran Program for Modeling Well-Stirred Reactors," *Sandia Report SAND86-8209 UC-4*, Sandia National Laboratories, Livemore, CA, 1988.

14. Glarborg, P., Miller, J. A., and Kee, R. J., "Kinetic Modeling and Sensitivity Analysis of Nitrogen Oxide Formation in Well-Stirred Reactors," *Combustion and Flame*, Vol. 65, pp. 177-202, 1986.

15. Zelina, J. Internal communication.

16. Gordon S., and McBride, B. J., "Computer Program for Calculation of Complex Chemical Equilibrium Compositions, Rocket Performance, Incident and Reflected Shocks, and Chapman-Jouget Detonations" (NASA, Washington D. C.), *SP-273 Interim Revision*, 1976.

17. Ainslie, N. G., Morelock, C. R., and Turnbull, D., "Devitrification Kinetics of Fused Silica," *Symposium of Nucleation and Crystallization in Glasses and Melts*, pp. 97-107, 1962.

18. Glassman, Irvin. Combustion. Second edition. Academic Press, Inc. pp. 63-67, 1987.

19. Zelina, J., "Combustion Studies in a Well-Stirred Reactor," *Doctor of Philosophy Thesis*, University of Dayton, 1995.

20. Gouldin, F. C., and Tacke, M. M., "Evaluation of Compensated Thermocouple Measurements in Premixed Flames," AIAA Paper No. 95-0142, 1995.

Appendix E: Excel spreadsheet used to define probe PSR elements.

PFRTIME.xls		6/10/1996										
Data used comes from AV0AFVF1.xls												
Methane-air combustion in the all-ceramic WSR. Residence time was held ~ constant while phi was changed.												
Air and fuel are preheated to ~ 60 C. Methane was **technical grade**.												
Data for the reaction at phi = 0.59 was interpolated to create smaller PSR sections between the readings (11.125 and 12)												
The **quartz probe** is simulated as 18 PSR's in series												
The probe residence time is unaffected by the equivalence ratio / temperature of the reactor and is approximately 7 ms.												
Simple averaging of the endpoint characteristics is used for the calculations												
Phi = 0.59, Treactor = 1605 K												
x (in)	**temp (K)**	**avg. temp**	**dens (g/l)**	**vel (in/s)**	**tau (ms)**	**dist (m)**	**V (m^3)**	**Re**	**avg. temp**	**tau (ms)**	**Q (m^3/s)**	
11.125	1581		0.217116	1266.561		0						
11.3	1143	1362	0.300316	915.673	0.160386	0.004445	2.44E-08	367.5574	1362	0.160386	0.045635	
11.475	1017	1080	0.337523	814.7327	0.202265	0.00889	2.44E-08	412.0883	1080	0.202265	0.04067	
11.65	937	977	0.36634	750.6436	0.223588	0.013335	2.44E-08	411.3756	977	0.223588	0.039932	
11.825	897	917	0.382677	718.599	0.238218	0.01778	2.44E-08	463.5322	917	0.238218	0.039151	
12	852	874.5	0.402889	682.5489	0.249795	0.022225	2.44E-08	463.6186	874.5	0.249795	0.039309	
12.5	822	837	0.417592	658.5155	0.745676	0.034925	6.96E-08	480.3575	837	0.745676	0.038996	
13.1875	782	802	0.438953	626.471	1.07005	0.052388	9.57E-08	498.6832	802	1.07005	0.039277	
13.75	764	773	0.449295	612.0509	0.908341	0.066675	7.83E-08	519.5016	773	0.908341	0.038749	
14.125	733	748.5	0.468296	587.2164	0.625382	0.0762	5.22E-08	519.654	748.5	0.625382	0.039107	
14.5	702	717.5	0.488976	562.3819	0.652402	0.085725	5.22E-08	544.201	717.5	0.652402	0.039143	
15.125	679	690.5	0.505539	543.9562	1.129854	0.1016	8.7E-08	544.098	690.5	1.129854	0.038946	
15.4375	644	661.5	0.533014	515.9173	0.589693	0.109538	4.35E-08	571.2916	661.5	0.589693	0.039338	
15.875	636	640	0.539719	509.5084	0.853304	0.12065	6.09E-08	570.9141	640	0.853304	0.038538	
16.25	587	611.5	0.584772	470.2538	0.765492	0.130175	5.22E-08	603.5769	611.5	0.765492	0.039896	
16.8125	558	572.5	0.615163	447.0215	1.226458	0.144463	7.83E-08	640.682	572.5	1.226458	0.039293	
17.25	334	446	1.027728	267.572	1.224472	0.155575	6.09E-08	784.1004	446	1.224472	0.05114	
17.75	586.15	460.075	0.58562	469.5728	1.356586	0.168275	6.96E-08	794.3002	460.075	1.356586	0.03006	
18.375	544.15	565.15	0.630821	435.9261	1.380454	0.18415	8.7E-08	641.1563	565.15	1.380454	0.039776	**Q (avg)**
19.125	519.15	531.65	0.661198	415.8982	1.760927	0.2032	1.04E-07	640.6252	531.65	1.760927	0.03922	0.039799
					total residence time (ms)							
					15.36334							

Appendix F: Manual to the modified Chemkin PSR code.

Chemkin is modified to model the WSR and sampling probe sequentially with a single input file. This leads to better modeling of the WSR measurements taken by analyzers. The modified code is used to evaluated new probe designs (Blust et al., 1997a) and to predict measurements taken with any probe (halon 1301 studies with a quartz probe). The temperature profile of the probe is measured and used to define the probe as a series of PSR elements (pp. 17-20). The information is assembled into a single input file and a single output file records the output from the WSR and each probe PSR element. These files are described in detail next.

The modifications to the Chemkin code cause the simulated species concentrations to be written to additional files (matt.dat and matt3.dat) in a format to be used as an input file. A counter variable designates which file is to be used as input for the next run, and another indicates when the last element is simulated. The output for each simulation is written to the Chemkin default output file (psrout.dat).

However, due to the formats used in writing the next input files, the modified algorithm is limited in its applications. The input for the first PSR is defined by a residence time, and the ensuing PSR elements are defined by a single flow rate. This applies well to the WSR and its sampling probe, but may model other systems well. However, research done with the WSR will always require the use of a probe and this strict modeling format. Therefore, this modified algorithm should prove very useful modeling studies of the WSR.

The input file "psrin.dat" is retained as the primary input file. However, additional information must be supplied in this file. The format of this file can be seen in the example supplied with this explanation. The input file has no new requirements from "TGIV" to "END," and should contain very similar information as the example file. However, prior to the "TGIV" keyword, an integer input must be supplied to indicate the number of WSR approximations that will be used for the probe. This number will coincide with the first entry for the number of probe approximation explained next. After the "END" statement, the following five numbers are repeated:

description	units	format
temperature of the next probe PSR approximation	(K)	I4
pressure of the next probe PSR approximation	(atm)	F5.4
flowrate of the gas sample through the probe	(gpm)	F6.5
volume of the next probe PSR approximation	(cm^3)	F7.6
the number of the probe PSR approximation		I2
(0 means the information given was for the last probe PSR approximation)		
(the number equals the number of PSR approximations that are to follow)		

NOTICE: Despite giving information for (n) PSR elements for the probe, the algorithm will only calculate the output for (n-1) PSR elements. The last set of PSR parameters is written in one of the output files without being simulated.

Once again, the output file "psrout.dat" has been retained as the primary output file. This file will contain the output from each and every simulation from the WSR and the probe. Trends can be followed and plotted as the gas sample travels through the probe. The amount of each set of output is defaulted as "PRNT 0" and can only be changed if the Fortran code is changed. However, this is very trivial and can be requested. There exists two more output files, "matt.dat" and "matt3.dat." These files are the input files created for the current simulation and the next one. When the algorithm is done with a simulation, one of these files will contain the input for the (n)th PSR approximation while the other will contain the (n-1) PSR approximation information that was used to compute the last set of output. The (n)th PSR information is in a format ready for use with the unmodified algorithm, and can be cut and pasted as it is for such a purpose. However, this file would require manipulation prior to use with this modified algorithm. It would have to be accompanied by another set of data for the (n+1) PSR approximation. SUGGESTION: A probe simulation generally does not need to extend past 500K, therefore supplying an (n)th PSR approximation of 500K or less should give sufficient confidence that the composition calculated as coming out of the (n-1) PSR is in fact the effluent composition of the probe. This also generally corresponds to 75% of the distance down the probe, so that there should be no concern for finding an (n) number of data sets.

PSRIN.DAT

```
2
TGIV
TEMP  1822
PRES  0.9989
TAU   0.007
VOL   250
REAC   CH4       0.0666666666
REAC   O2        0.1960784314
REAC   N2        0.737254902
PRNT 0
END
1705
0.9886
0.03893
0.013709
2
1500
0.9886
0.03893
0.013709
1
1250
0.9886
0.03893
0.02
0
```

```
PSR:  Perfectly Stirred Reactor Code
       CHEMKIN-II Version 1.1, March 1989
       DOUBLE PRECISION

               WORKING SPACE REQUIREMENTS

                 PROVIDED        REQUIRED
LOGICAL               245             239
INTEGER             10000            8128
REAL                17500           17009
CHARACTER             200             170


 CKLIB:  Chemical Kinetics Library
         CHEMKIN-II Version 1.9, October 1989
         DOUBLE PRECISION

           KEYWORD INPUT

          TGIV
          TEMP  1822
          PRES  0.9989
          TAU   0.007
          VOL   250
          REAC   CH4       0.0666666666
          REAC   O2        0.1960784314
          REAC   N2        0.737254902
          PRNT 0
          END
   STANJAN:  Version 3.8C, May 1988
             W. C. Reynolds, Stanford Univ.

         EQINIT: WORKING SPACE REQUIREMENTS
                  PROVIDED        REQUIRED
INTEGER             1690            1690
REAL                2154            2154


 FIRST SOLUTION ESTIMATE IS EQUILIBRIUM

 I KNOW THERE ARE NO MORE INPUT FILES

                RESIDENCE TIME                 7.00E-03  SEC
                MASS FLOW RATE                 6.65E+00  GM/SEC
                PRESSURE                       9.99E-01  ATM
                MASS DENSITY                   1.86E-04  GM/CM3
                VOLUME                         2.50E+02  CM3
                TEMP (FIXED)                    1822.00  K
```

INLET MOLE FRACTIONS

CH4	= 6.67E-02	CH3	= .00E+00	CH2	= .00E+00
CH	= .00E+00	H	= .00E+00	O	= .00E+00
N	= .00E+00	OH	= .00E+00	HO2	= .00E+00
H2O	= .00E+00	O2	= 1.96E-01	CH2OH	= .00E+00
CH3O	= .00E+00	CO2	= .00E+00	CO	= .00E+00
CH2O	= .00E+00	C2H2	= .00E+00	C3H2	= .00E+00
C2H3	= .00E+00	C2H4	= .00E+00	H2	= .00E+00
H2O2	= .00E+00	C	= .00E+00	C2H	= .00E+00
C2H6	= .00E+00	C2H5	= .00E+00	HCCO	= .00E+00
CH2CO	= .00E+00	HCCOH	= .00E+00	C4H2	= .00E+00
CH2(S)	= .00E+00	C3H3	= .00E+00	C4H3	= .00E+00
HCO	= .00E+00	H2CN	= .00E+00	HCN	= .00E+00
HCNO	= .00E+00	NO	= .00E+00	NO2	= .00E+00
HOCN	= .00E+00	HNCO	= .00E+00	NH2	= .00E+00
NH	= .00E+00	NCO	= .00E+00	C2N2	= .00E+00
N2O	= .00E+00	HNO	= .00E+00	NNH	= .00E+00
NH3	= .00E+00	N2	= 7.37E-01	CN	= .00E+00
HONO	= .00E+00	HNO3	= .00E+00	NO3	= .00E+00
C3H8	= .00E+00	C3H6	= .00E+00	N*C3H7	= .00E+00
I*C3H7	= .00E+00	Br	= .00E+00	Br2	= .00E+00
HBr	= .00E+00	CH3Br	= .00E+00	CBrF3	= .00E+00
CHF3	= .00E+00	CF3	= .00E+00	COF2	= .00E+00
COF	= .00E+00	F2	= .00E+00	F	= .00E+00
FO	= .00E+00	C4H4	= .00E+00	CH3OH	= .00E+00
C2H5Br	= .00E+00	C2H3Br	= .00E+00	C2HBr	= .00E+00
C2H3F3	= .00E+00	C2H2F2	= .00E+00	HF	= .00E+00
HOF	= .00E+00				

EXIT MOLE FRACTIONS

CH4	= 4.04E-05	CH3	= 9.14E-06	CH2	= 3.18E-07
CH	= 6.04E-09	H	= 4.66E-04	O	= 1.19E-03
N	= 6.36E-10	OH	= 3.81E-03	HO2	= 1.43E-05
H2O	= 1.29E-01	O2	= 6.33E-02	CH2OH	= 4.07E-07
CH3O	= 4.16E-08	CO2	= 6.32E-02	CO	= 3.17E-03
CH2O	= 9.40E-06	C2H2	= 2.04E-09	C3H2	= 4.20E-15
C2H3	= 2.48E-10	C2H4	= 8.79E-09	H2	= 1.14E-03
H2O2	= 9.61E-07	C	= 2.90E-10	C2H	= 2.56E-12
C2H6	= 1.55E-09	C2H5	= 5.69E-12	HCCO	= 3.29E-10
CH2CO	= 1.15E-09	HCCOH	= 1.07E-10	C4H2	= 5.13E-18
CH2(S)	= 1.03E-08	C3H3	= 1.87E-14	C4H3	= 3.98E-20
HCO	= 2.92E-07	H2CN	= 6.79E-13	HCN	= 1.29E-08
HCNO	= 4.31E-09	NO	= 1.91E-05	NO2	= 6.66E-09
HOCN	= 4.58E-10	HNCO	= 8.25E-10	NH2	= 5.95E-11
NH	= 3.00E-10	NCO	= 5.34E-10	C2N2	= -7.20E-17
N2O	= 4.79E-07	HNO	= 1.54E-09	NNH	= 4.40E-11
NH3	= 4.85E-11	N2	= 7.34E-01	CN	= 4.30E-11
HONO	= 1.15E-09	HNO3	= 1.22E-13	NO3	= 8.19E-11
C3H8	= 9.34E-16	C3H6	= 1.22E-13	N*C3H7	= 2.42E-18
I*C3H7	= 7.32E-19	Br	= .00E+00	Br2	= .00E+00
HBr	= .00E+00	CH3Br	= .00E+00	CBrF3	= .00E+00
CHF3	= .00E+00	CF3	= .00E+00	COF2	= .00E+00
COF	= .00E+00	F2	= .00E+00	F	= .00E+00
FO	= .00E+00	C4H4	= .00E+00	CH3OH	= 2.70-120
C2H5Br	= .00E+00	C2H3Br	= .00E+00	C2HBr	= .00E+00
C2H3F3	= .00E+00	C2H2F2	= .00E+00	HF	= .00E+00
HOF	= .00E+00				

```
PSR:  Perfectly Stirred Reactor Code
      CHEMKIN-II Version 1.1, March 1989
      DOUBLE PRECISION

              WORKING SPACE REQUIREMENTS

                PROVIDED        REQUIRED
LOGICAL              245             239
INTEGER            10000            8128
REAL               17500           17009
CHARACTER            200             170


CKLIB:  Chemical Kinetics Library
        CHEMKIN-II Version 1.9, October 1989
        DOUBLE PRECISION

          KEYWORD INPUT

        TGIV
        TEMP    1705
        PRES    .9886
        FLRT    .03893
        VOL     .01371
        REAC     CH4         4.04E-05
        REAC     CH3         9.14E-06
        REAC     CH2         3.18E-07
        REAC     CH          6.04E-09
        REAC     H           4.66E-04
        REAC     O           1.19E-03
        REAC     N           6.36E-10
        REAC     OH          3.81E-03
        REAC     HO2         1.43E-05
        REAC     H2O         1.29E-01
        REAC     O2          6.33E-02
        REAC     CH2OH       4.07E-07
        REAC     CH3O        4.16E-08
        REAC     CO2         6.32E-02
        REAC     CO          3.17E-03
        REAC     CH2O        9.40E-06
        REAC     C2H2        2.04E-09
        REAC     C3H2        4.20E-15
        REAC     C2H3        2.48E-10
        REAC     C2H4        8.79E-09
        REAC     H2          1.14E-03
        REAC     H2O2        9.61E-07
        REAC     C           2.90E-10
        REAC     C2H         2.56E-12
        REAC     C2H6        1.55E-09
        REAC     C2H5        5.69E-12
        REAC     HCCO        3.29E-10
        REAC     CH2CO       1.15E-09
        REAC     HCCOH       1.07E-10
        REAC     C4H2        5.13E-18
        REAC     CH2(S)      1.03E-08
        REAC     C3H3        1.87E-14
```

```
REAC      C4H3        3.98E-20
REAC      HCO         2.92E-07
REAC      H2CN        6.79E-13
REAC      HCN         1.29E-08
REAC      HCNO        4.31E-09
REAC      NO          1.91E-05
REAC      NO2         6.66E-09
REAC      HOCN        4.58E-10
REAC      HNCO        8.25E-10
REAC      NH2         5.95E-11
REAC      NH          3.00E-10
REAC      NCO         5.34E-10
REAC      C2N2       -7.20E-17
REAC      N2O         4.79E-07
REAC      HNO         1.54E-09
REAC      NNH         4.40E-11
REAC      NH3         4.85E-11
REAC      N2          7.34E-01
REAC      CN          4.30E-11
REAC      HONO        1.15E-09
REAC      HNO3        1.22E-13
REAC      NO3         8.19E-11
REAC      C3H8        9.34E-16
REAC      C3H6        1.22E-13
REAC      N*C3H7      2.42E-18
REAC      I*C3H7      7.32E-19
REAC      Br           .00E+00
REAC      Br2          .00E+00
REAC      HBr          .00E+00
REAC      CH3Br        .00E+00
REAC      CBrF3        .00E+00
REAC      CHF3         .00E+00
REAC      CF3          .00E+00
REAC      COF2         .00E+00
REAC      COF          .00E+00
REAC      F2           .00E+00
REAC      F            .00E+00
REAC      FO           .00E+00
REAC      C4H4         .00E+00
REAC      CH3OH      2.70-120
REAC      C2H5Br       .00E+00
REAC      C2H3Br       .00E+00
REAC      C2HBr        .00E+00
REAC      C2H3F3       .00E+00
REAC      C2H2F2       .00E+00
REAC      HF           .00E+00
REAC      HOF          .00E+00
PRNT    0
END
CAUTION...REACTANT MOLE FRACTIONS SUM TO  .9993708990430969
```

STANJAN: Version 3.8C, May 1988
W. C. Reynolds, Stanford Univ.

EQINIT: WORKING SPACE REQUIREMENTS

	PROVIDED	REQUIRED
INTEGER	1690	1690
REAL	2154	2154

FIRST SOLUTION ESTIMATE IS EQUILIBRIUM

I KNOW THERE ARE NO MORE INPUT FILES

RESIDENCE TIME	6.94E-05	SEC
MASS FLOW RATE	3.89E-02	GM/SEC
PRESSURE	9.89E-01	ATM
MASS DENSITY	1.97E-04	GM/CM3
VOLUME	1.37E-02	CM3
TEMP (FIXED)	1705.00	K

INLET MOLE FRACTIONS

CH4	= 4.04E-05	CH3	= 9.15E-06	CH2	= 3.18E-07
CH	= 6.04E-09	H	= 4.66E-04	O	= 1.19E-03
N	= 6.36E-10	OH	= 3.81E-03	HO2	= 1.43E-05
H2O	= 1.29E-01	O2	= 6.33E-02	CH2OH	= 4.07E-07
CH3O	= 4.16E-08	CO2	= 6.32E-02	CO	= 3.17E-03
CH2O	= 9.41E-06	C2H2	= 2.04E-09	C3H2	= 4.20E-15
C2H3	= 2.48E-10	C2H4	= 8.80E-09	H2	= 1.14E-03
H2O2	= 9.62E-07	C	= 2.90E-10	C2H	= 2.56E-12
C2H6	= 1.55E-09	C2H5	= 5.69E-12	HCCO	= 3.29E-10
CH2CO	= 1.15E-09	HCCOH	= 1.07E-10	C4H2	= 5.13E-18
CH2(S)	= 1.03E-08	C3H3	= 1.87E-14	C4H3	= 3.98E-20
HCO	= 2.92E-07	H2CN	= 6.79E-13	HCN	= 1.29E-08
HCNO	= 4.31E-09	NO	= 1.91E-05	NO2	= 6.66E-09
HOCN	= 4.58E-10	HNCO	= 8.26E-10	NH2	= 5.95E-11
NH	= 3.00E-10	NCO	= 5.34E-10	C2N2	= -7.20E-17
N2O	= 4.79E-07	HNO	= 1.54E-09	NNH	= 4.40E-11
NH3	= 4.85E-11	N2	= 7.34E-01	CN	= 4.30E-11
HONO	= 1.15E-09	HNO3	= 1.22E-13	NO3	= 8.20E-11
C3H8	= 9.35E-16	C3H6	= 1.22E-13	N*C3H7	= 2.42E-18
I*C3H7	= 7.32E-19	Br	= .00E+00	Br2	= .00E+00
HBr	= .00E+00	CH3Br	= .00E+00	CBrF3	= .00E+00
CHF3	= .00E+00	CF3	= .00E+00	COF2	= .00E+00
COF	= .00E+00	F2	= .00E+00	F	= .00E+00
FO	= .00E+00	C4H4	= .00E+00	CH3OH	= 2.70-120
C2H5Br	= .00E+00	C2H3Br	= .00E+00	C2HBr	= .00E+00
C2H3F3	= .00E+00	C2H2F2	= .00E+00	HF	= .00E+00
HOF	= .00E+00				

EXIT MOLE FRACTIONS

CH4	= 3.22E-06	CH3	= 7.38E-07	CH2	= 2.07E-08
CH	= 2.79E-10	H	= 4.30E-04	O	= 1.06E-03
N	= 1.83E-10	OH	= 3.09E-03	HO2	= 1.45E-05
H2O	= 1.30E-01	O2	= 6.32E-02	CH2OH	= 2.67E-08
CH3O	= 2.50E-09	CO2	= 6.38E-02	CO	= 2.72E-03
CH2O	= 9.90E-07	C2H2	= 2.49E-10	C3H2	= 8.36E-17
C2H3	= 2.36E-11	C2H4	= 8.45E-10	H2	= 9.88E-04
H2O2	= 1.57E-06	C	= 1.31E-11	C2H	= 1.98E-13
C2H6	= 5.95E-11	C2H5	= 4.25E-13	HCCO	= 3.68E-11
CH2CO	= 1.95E-10	HCCOH	= 1.73E-11	C4H2	= 4.42E-19
CH2(S)	= 5.75E-10	C3H3	= 5.94E-16	C4H3	= 1.92E-20
HCO	= 3.21E-08	H2CN	= 6.69E-14	HCN	= 6.43E-09
HCNO	= 2.46E-09	NO	= 1.92E-05	NO2	= 7.67E-09
HOCN	= 2.20E-10	HNCO	= 5.11E-10	NH2	= 3.85E-11
NH	= 1.84E-10	NCO	= 2.17E-10	C2N2	= 5.54E-17
N2O	= 4.82E-07	HNO	= 1.91E-09	NNH	= 2.25E-11
NH3	= 3.26E-11	N2	= 7.35E-01	CN	= 1.52E-11
HONO	= 2.31E-09	HNO3	= 2.53E-13	NO3	= 8.12E-11
C3H8	= 1.08E-17	C3H6	= 2.33E-14	N*C3H7	= 5.31E-20
I*C3H7	= 2.28E-19	Br	= .00E+00	Br2	= .00E+00
HBr	= .00E+00	CH3Br	= .00E+00	CBrF3	= .00E+00
CHF3	= .00E+00	CF3	= .00E+00	COF2	= .00E+00
COF	= .00E+00	F2	= .00E+00	F	= .00E+00
FO	= .00E+00	C4H4	= .00E+00	CH3OH	= -3.87E-35
C2H5Br	= .00E+00	C2H3Br	= .00E+00	C2HBr	= .00E+00
C2H3F3	= .00E+00	C2H2F2	= .00E+00	HF	= .00E+00
HOF	= .00E+00				

PSR: Perfectly Stirred Reactor Code
CHEMKIN-II Version 1.1, March 1989
DOUBLE PRECISION

WORKING SPACE REQUIREMENTS

	PROVIDED	REQUIRED
LOGICAL	245	239
INTEGER	10000	8128
REAL	17500	17009
CHARACTER	200	170

CKLIB: Chemical Kinetics Library
CHEMKIN-II Version 1.9, October 1989
DOUBLE PRECISION

KEYWORD INPUT

```
TGIV
TEMP    1500
PRES    .9886
FLRT    .03893
VOL     .01371
REAC     CH4        3.22E-06
REAC     CH3        7.38E-07
REAC     CH2        2.07E-08
```

```
REAC      CH          2.79E-10
REAC      H           4.30E-04
REAC      O           1.06E-03
REAC      N           1.83E-10
REAC      OH          3.09E-03
REAC      HO2         1.45E-05
REAC      H2O         1.30E-01
REAC      O2          6.32E-02
REAC      CH2OH       2.67E-08
REAC      CH3O        2.50E-09
REAC      CO2         6.38E-02
REAC      CO          2.72E-03
REAC      CH2O        9.90E-07
REAC      C2H2        2.49E-10
REAC      C3H2        8.36E-17
REAC      C2H3        2.36E-11
REAC      C2H4        8.45E-10
REAC      H2          9.88E-04
REAC      H2O2        1.57E-06
REAC      C           1.31E-11
REAC      C2H         1.98E-13
REAC      C2H6        5.95E-11
REAC      C2H5        4.25E-13
REAC      HCCO        3.68E-11
REAC      CH2CO       1.95E-10
REAC      HCCOH       1.73E-11
REAC      C4H2        4.42E-19
REAC      CH2(S)      5.75E-10
REAC      C3H3        5.94E-16
REAC      C4H3        1.92E-20
REAC      HCO         3.21E-08
REAC      H2CN        6.69E-14
REAC      HCN         6.43E-09
REAC      HCNO        2.46E-09
REAC      NO          1.92E-05
REAC      NO2         7.67E-09
REAC      HOCN        2.20E-10
REAC      HNCO        5.11E-10
REAC      NH2         3.85E-11
REAC      NH          1.84E-10
REAC      NCO         2.17E-10
REAC      C2N2        5.54E-17
REAC      N2O         4.82E-07
REAC      HNO         1.91E-09
REAC      NNH         2.25E-11
REAC      NH3         3.26E-11
REAC      N2          7.35E-01
REAC      CN          1.52E-11
REAC      HONO        2.31E-09
REAC      HNO3        2.53E-13
REAC      NO3         8.12E-11
REAC      C3H8        1.08E-17
REAC      C3H6        2.33E-14
REAC      N*C3H7      5.31E-20
REAC      I*C3H7      2.28E-19
REAC      Br           .00E+00
REAC      Br2          .00E+00
```

```
         REAC     HBr          .00E+00
         REAC     CH3Br        .00E+00
         REAC     CBrF3        .00E+00
         REAC     CHF3         .00E+00
         REAC     CF3          .00E+00
         REAC     COF2         .00E+00
         REAC     COF          .00E+00
         REAC     F2           .00E+00
         REAC     F            .00E+00
         REAC     FO           .00E+00
         REAC     C4H4         .00E+00
         REAC     CH3OH     -3.87E-35
         REAC     C2H5Br       .00E+00
         REAC     C2H3Br       .00E+00
         REAC     C2HBr        .00E+00
         REAC     C2H3F3       .00E+00
         REAC     C2H2F2       .00E+00
         REAC     HF           .00E+00
         REAC     HOF          .00E+00
         PRNT    0
         END
 CAUTION...REACTANT MOLE FRACTIONS SUM TO  1.00032880657927
  STANJAN:  Version 3.8C, May 1988
            W. C. Reynolds, Stanford Univ.

        EQINIT: WORKING SPACE REQUIREMENTS
                  PROVIDED        REQUIRED
INTEGER             1690            1690
REAL                2154            2154


FIRST SOLUTION ESTIMATE IS EQUILIBRIUM

I KNOW THERE ARE NO MORE INPUT FILES

                RESIDENCE TIME              7.90E-05  SEC
                MASS FLOW RATE              3.89E-02  GM/SEC
                PRESSURE                    9.89E-01  ATM
                MASS DENSITY                2.24E-04  GM/CM3
                VOLUME                      1.37E-02  CM3
                TEMP (FIXED)                 1500.00  K


                      INLET MOLE FRACTIONS

  CH4       =  3.22E-06      CH3       =  7.38E-07      CH2       =  2.07E-08
  CH        =  2.79E-10      H         =  4.30E-04      O         =  1.06E-03
  N         =  1.83E-10      OH        =  3.09E-03      HO2       =  1.45E-05
  H2O       =  1.30E-01      O2        =  6.32E-02      CH2OH     =  2.67E-08
  CH3O      =  2.50E-09      CO2       =  6.38E-02      CO        =  2.72E-03
  CH2O      =  9.90E-07      C2H2      =  2.49E-10      C3H2      =  8.36E-17
  C2H3      =  2.36E-11      C2H4      =  8.45E-10      H2        =  9.88E-04
  H2O2      =  1.57E-06      C         =  1.31E-11      C2H       =  1.98E-13
  C2H6      =  5.95E-11      C2H5      =  4.25E-13      HCCO      =  3.68E-11
  CH2CO     =  1.95E-10      HCCOH     =  1.73E-11      C4H2      =  4.42E-19
  CH2(S)    =  5.75E-10      C3H3      =  5.94E-16      C4H3      =  1.92E-20
  HCO       =  3.21E-08      H2CN      =  6.69E-14      HCN       =  6.43E-09
```

HCNO	=	2.46E-09	NO	=	1.92E-05	NO2	=	7.67E-09
HOCN	=	2.20E-10	HNCO	=	5.11E-10	NH2	=	3.85E-11
NH	=	1.84E-10	NCO	=	2.17E-10	C2N2	=	5.54E-17
N2O	=	4.82E-07	HNO	=	1.91E-09	NNH	=	2.25E-11
NH3	=	3.26E-11	N2	=	7.35E-01	CN	=	1.52E-11
HONO	=	2.31E-09	HNO3	=	2.53E-13	NO3	=	8.12E-11
C3H8	=	1.08E-17	C3H6	=	2.33E-14	N*C3H7	=	5.31E-20
I*C3H7	=	2.28E-19	Br	=	.00E+00	Br2	=	.00E+00
HBr	=	.00E+00	CH3Br	=	.00E+00	CBrF3	=	.00E+00
CHF3	=	.00E+00	CF3	=	.00E+00	COF2	=	.00E+00
COF	=	.00E+00	F2	=	.00E+00	F	=	.00E+00
FO	=	.00E+00	C4H4	=	.00E+00	CH3OH	=	-3.87E-35
C2H5Br	=	.00E+00	C2H3Br	=	.00E+00	C2HBr	=	.00E+00
C2H3F3	=	.00E+00	C2H2F2	=	.00E+00	HF	=	.00E+00
HOF	=	.00E+00						

EXIT MOLE FRACTIONS

CH4	=	4.42E-07	CH3	=	6.78E-08	CH2	=	1.07E-09
CH	=	6.89E-12	H	=	3.50E-04	O	=	7.72E-04
N	=	3.94E-11	OH	=	1.90E-03	HO2	=	2.08E-05
H2O	=	1.31E-01	O2	=	6.33E-02	CH2OH	=	1.35E-09
CH3O	=	1.39E-10	CO2	=	6.43E-02	CO	=	2.28E-03
CH2O	=	1.13E-07	C2H2	=	2.70E-11	C3H2	=	1.30E-18
C2H3	=	1.93E-12	C2H4	=	9.48E-11	H2	=	7.53E-04
H2O2	=	3.78E-06	C	=	2.80E-13	C2H	=	7.80E-15
C2H6	=	3.28E-12	C2H5	=	1.17E-13	HCCO	=	3.24E-12
CH2CO	=	3.38E-11	HCCOH	=	2.26E-12	C4H2	=	4.10E-20
CH2(S)	=	2.12E-11	C3H3	=	1.78E-17	C4H3	=	8.36E-21
HCO	=	4.59E-09	H2CN	=	3.41E-14	HCN	=	4.08E-09
HCNO	=	1.61E-09	NO	=	1.92E-05	NO2	=	1.30E-08
HOCN	=	8.05E-11	HNCO	=	2.73E-10	NH2	=	2.19E-11
NH	=	8.63E-11	NCO	=	8.27E-11	C2N2	=	2.26E-17
N2O	=	4.89E-07	HNO	=	2.61E-09	NNH	=	7.16E-12
NH3	=	1.99E-11	N2	=	7.35E-01	CN	=	4.52E-12
HONO	=	9.88E-09	HNO3	=	1.94E-12	NO3	=	8.01E-11
C3H8	=	1.27E-18	C3H6	=	4.73E-15	N*C3H7	=	2.43E-20
I*C3H7	=	1.89E-19	Br	=	.00E+00	Br2	=	.00E+00
HBr	=	.00E+00	CH3Br	=	.00E+00	CBrF3	=	.00E+00
CHF3	=	.00E+00	CF3	=	.00E+00	COF2	=	.00E+00
COF	=	.00E+00	F2	=	.00E+00	F	=	.00E+00
FO	=	.00E+00	C4H4	=	.00E+00	CH3OH	=	-8.42E-35
C2H5Br	=	.00E+00	C2H3Br	=	.00E+00	C2HBr	=	.00E+00
C2H3F3	=	.00E+00	C2H2F2	=	.00E+00	HF	=	.00E+00
HOF	=	.00E+00						

```
TGIV
TEMP    1250
PRES    .9886
FLRT    .03893
VOL     .02000
REAC     CH4          4.42E-07
REAC     CH3          6.78E-08
REAC     CH2          1.07E-09
REAC     CH           6.89E-12
REAC     H            3.50E-04
REAC     O            7.72E-04
REAC     N            3.94E-11
REAC     OH           1.90E-03
REAC     HO2          2.08E-05
REAC     H2O          1.31E-01
REAC     O2           6.33E-02
REAC     CH2OH        1.35E-09
REAC     CH3O         1.39E-10
REAC     CO2          6.43E-02
REAC     CO           2.28E-03
REAC     CH2O         1.13E-07
REAC     C2H2         2.70E-11
REAC     C3H2         1.30E-18
REAC     C2H3         1.93E-12
REAC     C2H4         9.48E-11
REAC     H2           7.53E-04
REAC     H2O2         3.78E-06
REAC     C            2.80E-13
REAC     C2H          7.80E-15
REAC     C2H6         3.28E-12
REAC     C2H5         1.17E-13
REAC     HCCO         3.24E-12
REAC     CH2CO        3.38E-11
REAC     HCCOH        2.26E-12
REAC     C4H2         4.10E-20
REAC     CH2(S)       2.12E-11
REAC     C3H3         1.78E-17
REAC     C4H3         8.36E-21
REAC     HCO          4.59E-09
REAC     H2CN         3.41E-14
REAC     HCN          4.08E-09
REAC     HCNO         1.61E-09
REAC     NO           1.92E-05
REAC     NO2          1.30E-08
REAC     HOCN         8.05E-11
REAC     HNCO         2.73E-10
REAC     NH2          2.19E-11
REAC     NH           8.63E-11
REAC     NCO          8.27E-11
REAC     C2N2         2.26E-17
REAC     N2O          4.89E-07
REAC     HNO          2.61E-09
REAC     NNH          7.16E-12
REAC     NH3          1.99E-11
```

```
REAC     N2          7.35E-01
REAC     CN          4.52E-12
REAC     HONO        9.88E-09
REAC     HNO3        1.94E-12
REAC     NO3         8.01E-11
REAC     C3H8        1.27E-18
REAC     C3H6        4.73E-15
REAC     N*C3H7      2.43E-20
REAC     I*C3H7      1.89E-19
REAC     Br           .00E+00
REAC     Br2          .00E+00
REAC     HBr          .00E+00
REAC     CH3Br        .00E+00
REAC     CBrF3        .00E+00
REAC     CHF3         .00E+00
REAC     CF3          .00E+00
REAC     COF2         .00E+00
REAC     COF          .00E+00
REAC     F2           .00E+00
REAC     F            .00E+00
REAC     FO           .00E+00
REAC     C4H4         .00E+00
REAC     CH3OH      -8.42E-35
REAC     C2H5Br       .00E+00
REAC     C2H3Br       .00E+00
REAC     C2HBr        .00E+00
REAC     C2H3F3       .00E+00
REAC     C2H2F2       .00E+00
REAC     HF           .00E+00
REAC     HOF          .00E+00
PRNT    0
END
```

```
TGIV
TEMP    1500
PRES    .9886
FLRT    .03893
VOL     .01371
REAC     CH4         3.22E-06
REAC     CH3         7.38E-07
REAC     CH2         2.07E-08
REAC     CH          2.79E-10
REAC     H           4.30E-04
REAC     O           1.06E-03
REAC     N           1.83E-10
REAC     OH          3.09E-03
REAC     HO2         1.45E-05
REAC     H2O         1.30E-01
REAC     O2          6.32E-02
REAC     CH2OH       2.67E-08
REAC     CH3O        2.50E-09
REAC     CO2         6.38E-02
REAC     CO          2.72E-03
REAC     CH2O        9.90E-07
REAC     C2H2        2.49E-10
REAC     C3H2        8.36E-17
REAC     C2H3        2.36E-11
REAC     C2H4        8.45E-10
REAC     H2          9.88E-04
REAC     H2O2        1.57E-06
REAC     C           1.31E-11
REAC     C2H         1.98E-13
REAC     C2H6        5.95E-11
REAC     C2H5        4.25E-13
REAC     HCCO        3.68E-11
REAC     CH2CO       1.95E-10
REAC     HCCOH       1.73E-11
REAC     C4H2        4.42E-19
REAC     CH2(S)      5.75E-10
REAC     C3H3        5.94E-16
REAC     C4H3        1.92E-20
REAC     HCO         3.21E-08
REAC     H2CN        6.69E-14
REAC     HCN         6.43E-09
REAC     HCNO        2.46E-09
REAC     NO          1.92E-05
REAC     NO2         7.67E-09
REAC     HOCN        2.20E-10
REAC     HNCO        5.11E-10
REAC     NH2         3.85E-11
REAC     NH          1.84E-10
REAC     NCO         2.17E-10
REAC     C2N2        5.54E-17
REAC     N2O         4.82E-07
REAC     HNO         1.91E-09
REAC     NNH         2.25E-11
REAC     NH3         3.26E-11
```

```
REAC      N2          7.35E-01
REAC      CN          1.52E-11
REAC      HONO        2.31E-09
REAC      HNO3        2.53E-13
REAC      NO3         8.12E-11
REAC      C3H8        1.08E-17
REAC      C3H6        2.33E-14
REAC      N*C3H7      5.31E-20
REAC      I*C3H7      2.28E-19
REAC      Br           .00E+00
REAC      Br2          .00E+00
REAC      HBr          .00E+00
REAC      CH3Br        .00E+00
REAC      CBrF3        .00E+00
REAC      CHF3         .00E+00
REAC      CF3          .00E+00
REAC      COF2         .00E+00
REAC      COF          .00E+00
REAC      F2           .00E+00
REAC      F            .00E+00
REAC      FO           .00E+00
REAC      C4H4         .00E+00
REAC      CH3OH      -3.87E-35
REAC      C2H5Br       .00E+00
REAC      C2H3Br       .00E+00
REAC      C2HBr        .00E+00
REAC      C2H3F3       .00E+00
REAC      C2H2F2       .00E+00
REAC      HF           .00E+00
REAC      HOF          .00E+00
PRNT    0
END
1250
.9886
.03893
.020000
 0
```

Appendix G: Partial ROP analysis output from Appendix C.

NORMALIZED AND ABSOLUTE RATE-OF-PRODUCTION COEFFICIENTS

1. CH4

		NORMALIZED	(MOLES/CC-SEC)
1.	CH4+O<=>CH3+OH	-.093	(-3.16E-03)
2.	CH4+O2<=>CH3+HO2	.086	(2.88E-05)
4.	CH3+H(+M)<=>CH4(+M)	.877	(2.92E-04)
5.	CH4+H<=>CH3+H2	-.398	(-1.35E-02)
6.	CH4+OH<=>CH3+H2O	-.165	(-5.58E-03)
66.	C2H6+CH3<=>C2H5+CH4	.037	(1.22E-05)
271.	HBr+CH3<=>CH4+Br	-.213	(-7.20E-03)
294.	CHF3+CH3<=>CF3+CH4	-.105	(-3.55E-03)
318.	F+CH4<=>HF+CH3	-.025	(-8.63E-04)
	NET RATE-OF-PRODUCTION (MOLES/CC-SEC) =		3.33E-04
	NET RATE-OF-CONSUMPTION (MOLES/CC-SEC) =		3.39E-02

2. CH3

		NORMALIZED	(MOLES/CC-SEC)
1.	CH4+O<=>CH3+OH	.085	(3.16E-03)
3.	2CH3(+M)<=>C2H6(+M)	-.041	(-1.43E-03)
5.	CH4+H<=>CH3+H2	.360	(1.35E-02)
6.	CH4+OH<=>CH3+H2O	.149	(5.58E-03)
8.	CH3+HO2<=>CH3O+OH	-.023	(-8.03E-04)
9.	CH3+O2<=>CH3O+O	-.020	(-6.81E-04)
10.	CH3+O<=>CH2O+H	-.436	(-1.51E-02)
11.	CH2OH+H<=>CH3+OH	-.134	(-4.64E-03)
12.	CH3O+H<=>CH3+OH	.019	(7.04E-04)
13.	CH3+OH<=>CH2+H2O	-.118	(-4.08E-03)
14.	CH3+H<=>CH2+H2	-.027	(-9.20E-04)
73.	CH2+CH3<=>C2H4+H	-.020	(-7.05E-04)
75.	C2H5+H<=>2CH3	-.026	(-8.93E-04)
111.	CH2(S)+H2<=>CH3+H	-.060	(-2.09E-03)
270.	HBr+CH3<=>CH3Br+H	.015	(5.68E-04)
271.	HBr+CH3<=>CH4+Br	.193	(7.20E-03)
284.	Br+CH3<=>CH3Br	-.016	(-5.40E-04)
294.	CHF3+CH3<=>CF3+CH4	.095	(3.55E-03)
302.	CF3+CH3<=>C2H3F3	-.063	(-2.19E-03)
306.	COF2+CH3<=>C2H2F2+OH	.053	(1.98E-03)
318.	F+CH4<=>HF+CH3	.023	(8.63E-04)
	NET RATE-OF-PRODUCTION (MOLES/CC-SEC) =		3.74E-02
	NET RATE-OF-CONSUMPTION (MOLES/CC-SEC) =		3.46E-02

6. O

		NORMALIZED	(MOLES/CC-SEC)
1.	CH4+O<=>CH3+OH	-.104	(-3.16E-03)
9.	CH3+O2<=>CH3O+O	.022	(6.81E-04)
10.	CH3+O<=>CH2O+H	-.494	(-1.51E-02)
47.	CH2+O2<=>CH2O+O	.099	(3.11E-03)
55.	CH2O+O<=>HCO+OH	-.019	(-5.69E-04)
133.	O+OH<=>O2+H	.866	(2.70E-02)
134.	O+H2<=>OH+H	-.193	(-5.91E-03)
139.	2OH<=>O+H2O	-.027	(-8.16E-04)
305.	CF3+O<=>COF2+F	-.092	(-2.81E-03)
	NET RATE-OF-PRODUCTION (MOLES/CC-SEC) =		3.12E-02
	NET RATE-OF-CONSUMPTION (MOLES/CC-SEC) =		3.05E-02

5. H

		NORMALIZED	(MOLES/CC-SEC)
5.	CH4+H<=>CH3+H2	-.179	(-1.35E-02)
10.	CH3+O<=>CH2O+H	.195	(1.51E-02)
11.	CH2OH+H<=>CH3+OH	.060	(4.64E-03)
14.	CH3+H<=>CH2+H2	-.012	(-9.20E-04)
46.	CH2+O2<=>CO2+2H	.019	(1.46E-03)
53.	CH2O+H<=>HCO+H2	-.182	(-1.37E-02)
57.	HCO+M<=>H+CO+M	.273	(2.11E-02)
58.	HCO+H<=>CO+H2	-.014	(-1.02E-03)
63.	CO+OH<=>CO2+H	.019	(1.46E-03)
70.	C2H4+H<=>C2H3+H2	-.011	(-8.43E-04)
74.	H+C2H4(+M)<=>C2H5(+M)	.015	(1.13E-03)
110.	CH2(S)+O2<=>CO+OH+H	.015	(1.12E-03)
111.	CH2(S)+H2<=>CH3+H	-.028	(-2.09E-03)
132.	OH+H2<=>H2O+H	.244	(1.88E-02)
133.	O+OH<=>O2+H	-.359	(-2.70E-02)
134.	O+H2<=>OH+H	.076	(5.91E-03)
137.	H+HO2<=>2OH	-.037	(-2.81E-03)
278.	HBr+H<=>H2+Br	-.109	(-8.25E-03)
291.	CBrF3+H<=>CF3+HBr	-.021	(-1.59E-03)
321.	F+H2<=>HF+H	.027	(2.06E-03)
	NET RATE-OF-PRODUCTION (MOLES/CC-SEC) =		7.72E-02
	NET RATE-OF-CONSUMPTION (MOLES/CC-SEC) =		7.54E-02

8. OH

		NORMALIZED	(MOLES/CC-SEC)
1.	CH4+O<=>CH3+OH	.065	(3.16E-03)
6.	CH4+OH<=>CH3+H2O	-.119	(-5.58E-03)
8.	CH3+HO2<=>CH3O+OH	.017	(8.03E-04)
11.	CH2OH+H<=>CH3+OH	-.099	(-4.64E-03)
12.	CH3O+H<=>CH3+OH	.015	(7.04E-04)
13.	CH3+OH<=>CH2+H2O	-.087	(-4.08E-03)
52.	CH2O+OH<=>HCO+H2O	-.114	(-5.30E-03)
55.	CH2O+O<=>HCO+OH	.012	(5.69E-04)
56.	HCO+OH<=>H2O+CO	-.025	(-1.19E-03)
63.	CO+OH<=>CO2+H	-.031	(-1.46E-03)
110.	CH2(S)+O2<=>CO+OH+H	.023	(1.12E-03)
132.	OH+H2<=>H2O+H	-.403	(-1.88E-02)
133.	O+OH<=>O2+H	.558	(2.70E-02)
134.	O+H2<=>OH+H	.122	(5.91E-03)
137.	H+HO2<=>2OH	.116	(5.63E-03)
139.	2OH<=>O+H2O	.034	(1.63E-03)
280.	HBr+OH<=>H2O+Br	-.023	(-1.08E-03)
298.	CHF3+OH<=>CF3+H2O	-.015	(-7.04E-04)
306.	COF2+CH3<=>C2H2F2+OH	-.042	(-1.98E-03)
323.	F+H2O<=>HF+OH	.018	(8.68E-04)
	NET RATE-OF-PRODUCTION (MOLES/CC-SEC) =		4.84E-02
	NET RATE-OF-CONSUMPTION (MOLES/CC-SEC) =		4.67E-02

14. CO2

		NORMALIZED	(MOLES/CC-SEC)
31.	CH+CO2<=>HCO+CO	-.325	(-9.84E-07)
43.	CH2+CO2<=>CH2O+CO	-.675	(-2.05E-06)
46.	CH2+O2<=>CO2+2H	.255	(7.29E-04)
48.	CH2+O2<=>CO2+H2	.124	(3.56E-04)
60.	HCO+O<=>CO2+H	.049	(1.40E-04)
63.	CO+OH<=>CO2+H	.511	(1.46E-03)
64.	CO+O2<=>CO2+O	.036	(1.03E-04)
65.	HO2+CO<=>CO2+OH	.024	(6.87E-05)
	NET RATE-OF-PRODUCTION (MOLES/CC-SEC) =		2.86E-03
	NET RATE-OF-CONSUMPTION (MOLES/CC-SEC) =		3.03E-06

15. CO

		NORMALIZED	(MOLES/CC-SEC)
44.	CH2+O<=>CO+2H	.010	(2.80E-04)
56.	HCO+OH<=>H2O+CO	.045	(1.19E-03)
57.	HCO+M<=>H+CO+M	.788	(2.11E-02)
58.	HCO+H<=>CO+H2	.038	(1.02E-03)
61.	HCO+O2<=>HO2+CO	.029	(7.64E-04)
63.	CO+OH<=>CO2+H	-.893	(-1.46E-03)
64.	CO+O2<=>CO2+O	-.063	(-1.03E-04)
65.	HO2+CO<=>CO2+OH	-.042	(-6.87E-05)
110.	CH2(S)+O2<=>CO+OH+H	.042	(1.12E-03)
	NET RATE-OF-PRODUCTION (MOLES/CC-SEC) =		2.67E-02
	NET RATE-OF-CONSUMPTION (MOLES/CC-SEC) =		1.64E-03

34. HCO

		NORMALIZED	(MOLES/CC-SEC)
28.	CH+O2<=>HCO+O	.011	(2.78E-04)
52.	CH2O+OH<=>HCO+H2O	.217	(5.30E-03)
53.	CH2O+H<=>HCO+H2	.562	(1.37E-02)
55.	CH2O+O<=>HCO+OH	.023	(5.69E-04)
56.	HCO+OH<=>H2O+CO	-.049	(-1.19E-03)
57.	HCO+M<=>H+CO+M	-.866	(-2.11E-02)
58.	HCO+H<=>CO+H2	-.042	(-1.02E-03)
61.	HCO+O2<=>HO2+CO	-.031	(-7.64E-04)
71.	C2H4+O<=>CH3+HCO	.012	(2.97E-04)
83.	C2H3+O2<=>CH2O+HCO	.018	(4.51E-04)
277.	HBr+HCO<=>CH2O+Br	.153	(3.73E-03)
	NET RATE-OF-PRODUCTION (MOLES/CC-SEC) =		2.44E-02
	NET RATE-OF-CONSUMPTION (MOLES/CC-SEC) =		2.43E-02

59. Br

		NORMALIZED	(MOLES/CC-SEC)
271.	HBr+CH3<=>CH4+Br	-.615	(-7.20E-03)
277.	HBr+HCO<=>CH2O+Br	-.319	(-3.73E-03)
278.	HBr+H<=>H2+Br	.459	(8.25E-03)
279.	HBr+O<=>Br+OH	.014	(2.58E-04)
280.	HBr+OH<=>H2O+Br	.060	(1.08E-03)
284.	Br+CH3<=>CH3Br	-.046	(-5.40E-04)
289.	CBrF3<=>CF3+Br	.459	(8.24E-03)
	NET RATE-OF-PRODUCTION (MOLES/CC-SEC) =		1.80E-02
	NET RATE-OF-CONSUMPTION (MOLES/CC-SEC) =		1.17E-02

```
61. HBr                                          NORMALIZED  (MOLES/CC-SEC)
          270. HBr+CH3<=>CH3Br+H                      .043     ( 5.68E-04)
          271. HBr+CH3<=>CH4+Br                       .540     ( 7.20E-03)
          277. HBr+HCO<=>CH2O+Br                      .280     ( 3.73E-03)
          278. HBr+H<=>H2+Br                         -.849     (-8.25E-03)
          279. HBr+O<=>Br+OH                         -.026     (-2.58E-04)
          280. HBr+OH<=>H2O+Br                       -.111     (-1.08E-03)
          291. CBrF3+H<=>CF3+HBr                      .120     ( 1.59E-03)
          325. F+HBr<=>HF+Br                         -.012     (-1.18E-04)
               NET RATE-OF-PRODUCTION (MOLES/CC-SEC)  =  1.33E-02
               NET RATE-OF-CONSUMPTION (MOLES/CC-SEC) =  9.72E-03
62. CH3Br                                        NORMALIZED  (MOLES/CC-SEC)
          270. HBr+CH3<=>CH3Br+H                    -1.000     (-5.68E-04)
          284. Br+CH3<=>CH3Br                         .756     ( 5.40E-04)
          290. CBrF3+CH3<=>CH3Br+CF3                  .244     ( 1.74E-04)
               NET RATE-OF-PRODUCTION (MOLES/CC-SEC)  =  7.14E-04
               NET RATE-OF-CONSUMPTION (MOLES/CC-SEC) =  5.68E-04
63. CBrF3                                        NORMALIZED  (MOLES/CC-SEC)
          289. CBrF3<=>CF3+Br                        -.823     (-8.24E-03)
          290. CBrF3+CH3<=>CH3Br+CF3                 -.017     (-1.74E-04)
          291. CBrF3+H<=>CF3+HBr                     -.159     (-1.59E-03)
               NET RATE-OF-PRODUCTION (MOLES/CC-SEC)  =   .00E+00
               NET RATE-OF-CONSUMPTION (MOLES/CC-SEC) =  1.00E-02
64. CHF3                                         NORMALIZED  (MOLES/CC-SEC)
          294. CHF3+CH3<=>CF3+CH4                     1.000     ( 3.55E-03)
          297. CHF3+H<=>CF3+H2                       -.298     (-4.32E-04)
          298. CHF3+OH<=>CF3+H2O                     -.487     (-7.04E-04)
          299. CHF3+O<=>CF3+OH                       -.031     (-4.55E-05)
          300. CHF3+Br<=>CF3+HBr                     -.038     (-5.55E-05)
          326. F+CHF3<=>HF+CF3                       -.145     (-2.10E-04)
               NET RATE-OF-PRODUCTION (MOLES/CC-SEC)  =  3.55E-03
               NET RATE-OF-CONSUMPTION (MOLES/CC-SEC) =  1.45E-03
65. CF3                                          NORMALIZED  (MOLES/CC-SEC)
          289. CBrF3<=>CF3+Br                         .719     ( 8.24E-03)
          290. CBrF3+CH3<=>CH3Br+CF3                  .015     ( 1.74E-04)
          291. CBrF3+H<=>CF3+HBr                      .139     ( 1.59E-03)
          294. CHF3+CH3<=>CF3+CH4                    -.325     (-3.55E-03)
          297. CHF3+H<=>CF3+H2                        .038     ( 4.32E-04)
          298. CHF3+OH<=>CF3+H2O                      .061     ( 7.04E-04)
          301. CF3+O2<=>COF2+FO                      -.184     (-2.01E-03)
          302. CF3+CH3<=>C2H3F3                      -.200     (-2.19E-03)
          304. CF3+OH<=>COF2+HF                      -.034     (-3.67E-04)
          305. CF3+O<=>COF2+F                        -.257     (-2.81E-03)
          326. F+CHF3<=>HF+CF3                        .018     ( 2.10E-04)
               NET RATE-OF-PRODUCTION (MOLES/CC-SEC)  =  1.15E-02
               NET RATE-OF-CONSUMPTION (MOLES/CC-SEC) =  1.09E-02
78. HF                                           NORMALIZED  (MOLES/CC-SEC)
          303. C2H3F3<=>C2H2F2+HF                     .303     ( 1.98E-03)
          304. CF3+OH<=>COF2+HF                       .056     ( 3.67E-04)
          318. F+CH4<=>HF+CH3                         .132     ( 8.63E-04)
          321. F+H2<=>HF+H                            .314     ( 2.06E-03)
          323. F+H2O<=>HF+OH                          .133     ( 8.68E-04)
          325. F+HBr<=>HF+Br                          .018     ( 1.18E-04)
          326. F+CHF3<=>HF+CF3                        .032     ( 2.10E-04)
               NET RATE-OF-PRODUCTION (MOLES/CC-SEC)  =  6.55E-03
               NET RATE-OF-CONSUMPTION (MOLES/CC-SEC) =   .00E+00
```

BIBLIOGRAPHY

Anderson, S. O., Metchis, K. L., Rubenstein, R., "The History of the Halon Phaseout and Regulation of Halon Alternatives," in Halon Replacements: Technology and Science, Miziolek, A. W., Tsang, W., eds., pp. 8-15, 1995.

Babushok, V., Noto, T., Burgess, D. R. F., Hamins, A., and Tsang, W., "Influence of CF_3I, CF_3Br, and CF_3H on the High-Temperature Combustion of Methane," *Combustion and Flame*, Vol. 102, pp. 351-366, 1996.

Ballenthin, J. O., Miller, T., Calo, J. M., Blust, J., and Getz, M., "Free-Jet, Molecular Beam Mass Spectrometer System for Monitoring the Gas-Phase Composition in a Well-Stirred Combustor," presented at the *Fifth International Congress on Toxic Combustion Products*, Dayton, Ohio, June 25-27, 1997.

Battin-Leclerc, F., Comé, G. M., and Baronnet, F., "The Inhibiting Effect of CF_3Br on the Reaction $CH_4 + O_2$ at 1070 K," *Combustion and Flame*, Vol. 99, pp. 644-652, 1994.

Benson, S., Thermochemical Kinetics, "Methods for the Estimation of Thermochemical Data and Rate Parameters," second edition, John Wiley & Sons, NY, 1976.

Biordi, J. C., Lazarra, C. P., and Papp, J. F., "Flame-Structure Studies of CF_3Br-Inhibited Methane Flames," *Fourteenth (International) Symposium on Combustion*, *The Combustion Institute*, Pittsburg, PA, p. 367, 1974.

Biordi, J. C., Lazarra, C. P., and Papp, J. F., "Flame-Structure Studies of CF_3Br-Inhibited Methane Flames. 2. Kinetics and Mechanisms," *Fifteenth (International) Symposium on Combustion*, *The Combustion Institute*, Pittsburg, PA, pp. 917-932, 1975.

Biordi, J. C., Lazarra, C. P., and Papp, J. F., "The Effect of CF_3Br on Radical Concentration Profiles in Methane Flames," in Halogenated Fire Suppressants, Gann, R. G., ed., pp. 256-294, 1975.

Biordi, J. C., Lazarra, C. P., and Papp, J. F., "Flame-Structure Studies of CF_3Br-Inhibited Methane Flames. 3. Effect of 1-Percent CF_3Br on Composition, Rate Constants, and Net Reaction-Rates," *Journal of Physical Chemistry*, Vol. 81, Number 12, pp. 1139-1145, 1977.

Biordi, J. C., Lazarra, C. P., and Papp, J. F., "Flame-Structure Studies for CF_3Br-Inhibited Methane Flames. 4. Reactions of Inhibitor-Related Species in Flames Containing Initially 1.1-Percent Bromo-Triflouro-Methane," *Journal of Physical Chemstry*, Vol. 82, No. 2, pp. 125-132, 1978.

Blust, J. W., Getz, M. G., and Zabarnick, S., "Probe Design Optimization for the Well Stirred Reactor," *AIAA Paper no. 97-0907*, presented at the 25th Aerospace Sciences Meeting & Exhibit in Reno, NV, January 6-10, 1997.

Blust, J., Ballal, D. R., Sturgess, G. J., "Emissions Characteristics of Liquid Hydrocarbons in a Well-Stirred Reactor," *AIAA Paper no. 97-2710*, presented at Joint Propulsion Conference, Seattle, WA, July 6-9, 1997.

Burgess, D. R. F., Jr., Zachariah, M. R., Tsang, W., and Westmoreland, P. R., "Thermochemical and Chemical Kinetic Data for Fluorinated Hydrocarbons," *NIST Technical Note 1412*, U. S. Department of Commerce, Washington, D. C., 1995.

Ford, C. L., "An Overview of Halon 1301 Systems," in Halogenated Fire Suppressants, Gann, R. G., ed., pp. 1-63, 1975.

Freemantle, M., "Search for Halon Replacements Stymied by Complexities of Fires," *Chemical and Engineering News*, pp. 25-31, January 30, 1995.

Gann, R. G., editor, Halogenated Fire Suppressants, *ACS Symposium Series 16*, hosted by Southwest Research Institute, San Antonio, Texas, April 23-24, 1975, American Chemical Society, Washington, D. C., pp. vii-ix, 1975.

Gann, R. G., "Initial Reactions in Flame Inhibition by Halogenated Hydrocarbons," in Halogenated Fire Suppressants, Gann, R. G., ed., pp. 318-340, 1975.

Glarborg, P., Kee, R. J., Grcar, J. F., and Miller, J. A., "PSR: A Fortran Program for Modeling Well-Stirred Reactors," *Sandia Report SAND 86-8209 UC-4*, Sandia National Laboratories, Livermore,CA, October 1988.

Glassman, I., Combustion, second edition, Academic Press, NY, 1987.

Gordon, S., and McBride, B. J., "Computer Program for Calculation of Complex Chemical Equilibrium Compositions, Rocket Performance, Incident and Reflected Shocks, and Chapman-Jouget Detonations," NASA Lewis Research Center, *NASA SP-273*, March, 1976.

Grosshandler, W. L., Gann, R. G., and Pitts, W. M., editors, "Evaluation of Alternative In-Flight Fire Suppressants for Full-Scale Testing in Simulated Aircraft Engine Nacelles and Dry Bays," U. S. Department of Commerce, *NIST SP 861*, April, 1994.

Hamins, A., Trees, D., Seshadri, K., and Chelliah, H. K., "Extinction of Nonpremixed Flames with Halogenated Fire Suppressants," *Twenty-fifth Symposium (International) on Combustion*, *The Combustion Institute*, Pittsburg, PA, pp. 221-230, 1994.

Incropera, F. P., DeWitt, D. P., Introduction to Heat Transfer, second edition, John Wiley & Sons, NY, p. A15, 1990.

Kee, R. J., Rupley, F. M., and Miller, J. A., "Chemkin II: A FORTRAN Chemical Kinetics Package for the Analysis of Gas-Phase Chemical Kinetics," *Sandia Report SAND 89-8009B*, Sandia National Laboratories, Livermore, CA, September 1989.

Kee, R. J., Grcar, J. F., Smooke, M. D., and Miller, J. A., "A Fortran Program for Modeling Steady Laminar One-Dimensional Premixed Flames," *Sandia Report SAND 85-8240 UC-4*, Sandia National Laboratories, Livermore, CA, August 1989.

Lide, D., ed., CRC Handbook of Chemistry and Physics, 71st edition, 1990-1991.

Lutz, A. E., Kee, R. J., and Miller, J. A., "SENKIN: A Fortran Program for Predicting Homogeneous Gas Phase Chemical Kinetics with Sensitivity Analysis," *Sandia Report SAND 87-8248 UC-4*, Sandia National Laboratories, Livermore, CA, October 1988.

Masri, A. R., "Chemical Inhibition of Nonpremixed Flames of Hydrocarbon Fuels with CF_3Br," *Combustion Science and Technology*, Vol. 96, pp. 189-212, 1994.

Miller, J. A., and Bowman, C. T., "Mechanism and Modeling of Nitrogen Chemistry in Combustion," *Prog. Energy Combust. Sci.*, Vol. 15, pp. 287-338, 1989.

Nenniger, J. E., Kridiotis, A. C., Chomiak, J., Longwell, J. P., Sarafim, A. F., "Characterization of a Toroidal Well-Stirred Reactor," *Twentieth Symposium (International) on Combustion, The Combustion Institute*, Pittsburg, PA, pp. 473-479, 1984.

Pitts, W. M., Nyden, M. R., Gann, R. G., Mallard, W. G., and Tsang, W., "Construction of an Exploratory List of Chemicals to Initiate the Search for Halon Alternatives," *NIST Technical Note 1279*, U. S. Department of Commerce, August, 1990.

Trees, D., Grudno, A., Ilincic, N., Weibweiler, T., and Seshadri, K., "Experimental and Numerical Studies on Chemical Inhibition of Methane-Air Diffusion Flames by CF_3Br and CF_3H," *The Combustion Institute*, Joint Technical Meeting, April 23-26, 1995.

Tsang, W., and Hampson, R. F., "Chemical Kinetics Data Base for Combustion Chemistry. Part I. Methane and Related Compounds," *Journal of Physical Chemistry Reference Data*, Vol. 15, No. 3, 1986.

Warnatz, J., "The Mechanism of High Temperature Combustion of Propane and Butane," *Combustion Science and Technology*, Vol. 34, pp. 177-200, 1983.

Westbrook, C. K., "Numerical Modeling of Flame Inhibition by CF_3Br," *Combustion Science and Technology*, Vol. 34, pp. 201-235, 1983.

Zabarnick, S., "Laser-Induced Flourescence Diagnostics and Chemical Kinetic Modeling of a $CH_4/NO_2/O_2$ Flame at 55 Torr," *Combustion and Flame*, Vol. 85, pp. 27-50, 1991.

Zabarnick, S., and Zelina, J., "Chemical Kinetics of NO_x Production in a Well Stirred Reactor," *AIAA Paper no. 94-3828-CP*, 1994.

Zelina, J., and Ballal, D. R., "Combustion Studies in a Well Stirred Reactor," *AIAA Paper No. 94-0114*, 1994.

Zelina, J., and Ballal, D. R., "Emissions Studies in a Well-Stirred Reactor and Applications to Combustion Modeling," *presented at the 1996 International Joint Power Generation Conference*, Houston, Texas, October 14-17, 1996.

RELATED WORKS FROM THIS PROJECT

Ballenthin, J. O., Miller, T., Calo, J. M., Blust, J., and Getz, M., "Free-Jet, Molecular Beam Mass Spectrometer System for Monitoring the Gas-Phase Composition in a Well-Stirred Combustor," presented at the *Fifth International Congress on Toxic Combustion Products*, Dayton, Ohio, June 25-27, 1997.

Blust, J. W., Getz, M. G., and Zabarnick, S., "Probe Design Optimization for the Well Stirred Reactor," *AIAA Paper no. 97-0907*, presented in Reno, NV, January 6-10, 1997.

Calo, J. M., Miller, T. Ballenthin, J. O., Striebich, R, Blust, J. and Getz, M., "The Residence Time Distribution (RTD) of the Well-Stirred Reactor (WSR)," to be published as USAF technical paper.

Calo, J. M., Miller, T. Ballenthin, J. O., Striebich, R, Blust, J. and Getz, M., "Fast Pulse Injections of Fire Suppressants into a Well-Stirred Combustor," presented at the *Fifth International Congress on Toxic Combustion Byproducts*, Dayton, Ohio, June 25-27, 1997.

Getz, M., Blust, J., Calo, J. M., Miller, T., and Ballenthin, J. O., "Modeling of the Response of a Well-Stirred Combustor to the Injection of Fire Suppressants," presented at the *Fifth International Congress on Toxic Combustion Products*, Dayton, Ohio, June 25-27, 1997.